Dissertation

Microbiota alterations during epithelial tumor evolution and their functional consequences

submitted by

Nandhitha MADHUSUDHAN

for the Academic Degree of

Doctor of Philosophy

(PhD)

at the

Medical University of Graz

Institute of Pathology

under the Supervision of

Prof. Dr. Gregor GORKIEWICZ

2020

Statutory Declaration

I hereby declare that this thesis is my own original work and that I have fully acknowledged by name all of those individuals and organizations that have contributed to the research for this thesis. Due acknowledgement has been made in the text to all other material used. Throughout this thesis and in all related publications, I followed the "Standards of Good Scientific Practice and Ombuds Committee at the Medical University of Graz."

Date: 25 -09-2020 *Nandhitha Madhusudhan*

Disclosures

Parts of my dissertation have been published and I acknowledge all the authors below who have contributed to this thesis. I confirm that all co-authors have agreed to use their data in my thesis. Both the manuscripts below are open access articles distributed under the Creative Commons Attribution License which permits unrestricted use, distribution and reproduction in any medium, provided the original work is properly cited.

1. Madhusudhan N, Pausan MR, Halwachs B, Durdevic M, Windisch M, Kehrmann J, et al. Molecular Profiling of Keratinocyte Skin Tumors Links Staphylococcus aureus Overabundance and Increased Human beta-Defensin-2 Expression to Growth Promotion of Squamous Cell Carcinoma. Cancers (Basel). 2020; 12(3). (1) https://doi.org/10.3390/cancers12030541

2. Halwachs B, Madhusudhan N, Krause R, Nilsson RH, Moissl-Eichinger C, Hogenauer C, et al. Critical Issues in Mycobiota Analysis. Front Microbiol. 2017;8:180 (2). https://doi.org/10.3389/fmicb.2017.00180

The following authors have actively contributed to the results reported in this thesis:

Manuela-Raluca Pausan, Department of Internal Medicine, Medical University of Graz, Graz, Austria

Bettina Halwachs, Institute of Pathology, Medical University of Graz, Graz, Austria

Marija Durdević, Institute of Pathology, Medical University of Graz, Graz, Austria

Markus Windisch, Institute of Pathology, Medical University of Graz, Graz, Austria

Jan Kehrmann, Institute of Medical Microbiology, University Hospital Essen, University of Duisburg-Essen, Essen, Germany

Vijaykumar Patra, Department of Dermatology, Medical University of Graz, Graz, Austria

Peter Wolf, Department of Dermatology, Medical University of Graz, Graz, Austria

Petra Boukamp, Leibniz Research Institute for Environmental Medicine, Düsseldorf, Germany

Christine Moissl-Eichinger, Department of Internal Medicine, Medical University of Graz, Graz, Austria

Lorenzo Cerroni, Department of Dermatology, Medical University of Graz, Graz, Austria

Jürgen C. Becker, Department of Translational Skin Cancer Research and Department of Dermatology, University Hospital Essen, Essen, Germany

Gregor Gorkiewicz, Institute of Pathology, Medical University of Graz, Graz, Austria

The above mentioned authors have explicitly agreed with the use of all data for the thesis. Permission to reproduce published figures have been obtained via RightsLink®.

Graz, *Nandhitha Madhusudhan*

Real passion is much more beautiful
than the pinnacle of one's accomplishments

-Sudha Murthy

Acknowledgements

Forever thankful to this adventurous journey of PhD that I embarked on a few years ago.

First, I would like to thank my PhD supervisor, Prof. Gregor Gorkiewicz for his continuous support and encouragement throughout. Thank you for always making me believe that there is light at the end of the tunnel. I will always be grateful for all the learnings, both professionally and personally that I imbibed from you during this journey. Most importantly, for always having an optimistic attitude and for giving the freedom to create and perform experiments independently.

My sincere thanks to Prof. Juergen Becker for supervising me in this project and for hosting me in his lab for 6 months in Essen during my research stay abroad. Thank you for all your valuable inputs and support in Graz and Essen.

Thank you DK-MOLIN, as I truly believe that this is one of the most amazing PhD programs, which gave me the opportunity to learn from some brilliant peers and for making life a lot easier being far away from home. I would like to sincerely thank Prof. Akos Heinemann for giving me the opportunity to be a part of this PhD program. I would also like to thank Austrian Science fund (FWF) for funding this project. I would like to thank my thesis committee members Prof. Peter Wolf and Prof. Christoph Högenauer for their valuable feed back and discussions.

This journey would not be the same if not for all my lab mates who were more of a family away from home. Thank you, Ana, Bettina, Philipp, Margit, Barbara, Marija, Sandra, Markus, Theresa and Lena for all the great times we have had inside and outside lab. Special thanks to Vishwanath who has been a part of my PhD journey from the program hearing till date. Thank you for being a great friend and more importantly a great listener. Thank you, Vicky for being my skin microbiome partner in crime and for all the discussions over *chai*. Meghana and Shironi, thank you guys for making me a part of all the fun and crazy times during and after lab hours. All the food and movies will not be forgotten. Thank you, Vinod, for all the help from Bangalore to Graz. I have had some of the best office room mates in ZMF. Thank you, guys, for making it so much fun and interesting always.

A big shout out to my best friends who always looked out for me despite the distance, time and situation Shwetha, Sunetra and Namita. Thanks for making my life easier by always being there.

None of this would be possible if not for the immense support I got from my family. I would like to thank my parents who made me believe that I could move out of my comfort zone and follow my ambitions. Thanks for giving me the confidence that I have you both to fall back upon irrespective of what happens. I owe this to you both. Thank you Nithin for being there and watching it all silently and letting me know you are always there when I needed you. Special thanks to my in-laws who always made sure to let me know how happy they are being a part of my journey and encouraging me to happily work on my PhD. Rishi thanks for being my partner in crime and helping me sail through.

Now to the person without whose support this whole journey would be impossible, thank you Chandu. Thank you for listening, being at receiving end of all my stress and tantrums and for always smiling and letting me know how much this means to you too. Thank you for making sure that the long-distance relationship was not impossible to deal with. You made 7000 kms seem very little. Your positive attitude and enthusiasm towards all my small achievements during this journey and your unconditional support for 6 full years was all I needed to be where I am today. Being equally crazy yet sane, being a great listener yet stopping me from over thinking and being the best travel partner for life, you made sure that this turns out to be some best days of my life.

Table of Contents

Abbreviations

AD: Atopic dermatitis

AK: Actinic keratosis

AMPs: Antimicrobial peptides

ANOSIM: Analysis of similarities

BCC: Basal cell carcinoma

bp: Base pair

CDT: Cytolethal distending toxin

CFU: Colony forming Unit

CHIPS: Chemotaxis inhibitory proteins

CI: Cell index

ClfA: Clumping factor A

CRC: Colorectal cancer

cSCC: Cutaneous squamous cell carcinoma

DMEM: Dulbecco's modified Eagle's medium

DNA: Deoxyribonucleic acid

EGFR: Epithelial growth factor receptor

FBS: Fetal bovine serum

FFPE: Formalin-fixed paraffin-embedded

GI: Gastro intestinal

GluSE: Glutamic acid-specific serine protease

HaCaT: Human immortal keratinocyte cell line

hBD: Human beta-defensin

H&E: Haematoxylin and Eosin

HPV: Human apilloma virus

HSC-1: Human cutaneous squamous cell carcinoma

IBD: Inflammatory bowel disease

IHC: Immunohistochemistry

IL: Interleukin

ITS: Internal transcribed spacer

Kb: kilo-base pairs

LDA: Linear discriminant analysis

LEfSe: Linear discriminant analysis effect size

LPS: Lipopolysaccharides

MOI: Multiplicity of infection

mRNA: Messenger ribonucleic acid

MUG: Medical University of Graz

NGS: Next generation sequencing

NK: Natural killer

NMSC: Non-melanoma skin cancer

nt: nucleotide

NTC: No template control

nuc A: Thermostable nuclease gene

OD: Optical density

OTU: Operational taxonomic unit

PAMPs: Pathogen-associated molecular pattern

PAS: Periodic acid Schiff

PCoA: Principal coordinate analysis

PCR: Polymerase chain reaction

PRRs: Pattern recognition receptors

QIIME: Quantitative insights into microbial ecology

qRT-PCR: Quantitative real time polymerase chain reaction

RDP: Ribosomal database project

RNA: Ribonucleic acid

rRNA: Ribosomal ribonucleic acid

ROS: Reactive oxygen species

RT: Room temperature

RTCA: Real-time cellular analysis

RT-qPCR: Real-time quantitative PCR

SEM: Standard error of mean

SCC: Squamous cell carcinoma

SCL-1: Human cutaneous squamous cell carcinoma

STAT: Signal transducer and activator of transcription

TLRs: Toll-like receptors

TNF- α: Tumor necrosis factor alpha

UV: Ultra violet

ZMF: Center for medical research

List of figures

List of tables

Abstract (English)

Malignant tumors develop from specific pre-invasive neoplastic lesions, which have been described for most epithelial organs, e.g. actinic keratosis (AK) for squamous cell carcinoma (SCC) of the skin and adenomatous polyps for colorectal cancer (CRC). They harbor genetic aberrations, immune and stromal cells as well as microbes. During tumor development, the host-microbiota equilibrium is altered leading to a pro-inflammatory resident microbiota which could drive cancer progression. Given the central importance of the microbiome in health and disease, elucidating the mechanisms that maintain the microbiome homeostasis at cutaneous (skin) and mucosal (GI) surfaces as well as the factors leading to microbiome disturbance (dysbiosis) and ultimately to chronic inflammation will improve our understanding of cancer initiation and progression.

Skin harbors a considerable number of microbes that play an important role in health and disease. Nevertheless, their contribution to skin tumorigenesis has not been well studied. Therefore, we comparatively assessed the microbial community compositions in human keratinocyte (non-melanoma) skin tumors, AK, SCC and basal cell carcinoma (BCC). Our study shows that skin tumors are characterized by markedly different microbial community structures. AK and SCC, unlike BCC exhibit a significantly increased bacterial biomass. Markedly, *Staphylococcus aureus*, a known skin pathogen was overabundant in the hyperkeratotic regions of SCC. Furthermore, skin tumors showed an altered expression of antimicrobial peptides (AMPs), which are important defense proteins of the skin, wherein human beta-defensin-2 (hBD-2) was elevated in SCC. Interestingly, this AMP is known to induce proliferation of squamous epithelia. To that end, we challenged SCC cells with *S. aureus* in vitro and observed specific induction of hBD-2 expression, which also promoted the growth of SCC cells. Thus, our studies demonstrate that a microbial community composition possibly favored due to the alteration of the microbial habitat (niche) perpetuates cancer development. In the case of SCC, increased *S. aureus* likely promotes tumor cell growth via specific induction of hBD-2, thus perpetuating the neoplastic process.

Another organ system wherein the microbiota possibly contributes to cancer development is the GI tract. The precursors of CRCs are adenomatous polyps. *Fusobacterium* species, anaerobes typically colonizing the oral cavity but also the GI tract, have shown to be increased in GI tumors and can promote their growth via (i) modulation of the E-cadherin/beta-catenin

signaling, (ii) modulation of the tumor-immune microenvironment and (iii) suppression of natural killer (NK) cell-mediated tumor destruction via modulation of the inhibitory TIGIT receptor. Part of this thesis validated an increased abundance of tumor- promoting *Fusobacterium* and *F. nucleatum* in adenomatous polyps and CRC compared to normal tissue. Interestingly we also observed a decreased expression of *FadA* from adenomas to carcinoma suggesting a possible down-regulation of this microbial colonization factor.

Additionally, another aspect of this thesis aimed at addressing critical issues in fungal compartment of the microbiota (i.e. mycobiota) which includes fungal DNA extraction and PCR amplification using the internal transcribed spacer (ITS) regions from human skin formalin-fixed and paraffin-embedded (FFPE) specimens. Fungi constitute an important part of human microbiota and contribute significantly to disease development. However, the tools used for microbial community analysis are typically developed for the bacterial component and they often fall short if applied to fungal data. We first wanted to achieve an ideal method to isolate fungal DNA from FFPE human skin, which represents the typical specimens for histopathology and is, therefore, widely available. Moreover, we sought to optimize PCR amplification of fungal ribosomal DNA using the ITS1 and -2 regions which are highly variable sequences and are used to distinguish fungal species. To that end, we showed that mechanical cell disruption during DNA isolation significantly lowered the DNA yield leading to a significant decrease in signal-to-noise ratio in ITS PCR. We also observed increased PCR performance using ITS2 primers in comparison to ITS1 in human skin samples.

In summary, this thesis points out that changes in microbiota emerging during carcinogenesis could promote tumor cell growth, modulated by diverse host and microbial factors such as alteration of AMP expression in cSCC progression or via regulation of microbial colonization factor such as in CRC.

Abstract (German)

Maligne Tumoren entwickeln sich aus präinvasiven neoplastischen Läsionen, die für die meisten Epithelorgane beschrieben wurden, z.B.: Aktinische Keratose (AK) bei Plattenepithelkarzinomen der Haut (SCC) und adenomatöse Polypen bei Darmkrebs (CRC). Sie beherbergen genetische Aberrationen, Immun- und Stromazellen sowie Mikroben. Während der Tumorentwicklung ändert sich das Gleichgewicht zwischen Wirt und Mikrobiota, was zu einer proinflammatorischen Mikrobiota führt, die das Fortschreiten des Krebses vorantreiben kann. Angesichts der zentralen Bedeutung des Mikrobioms für Gesundheit und Krankheit, wird die Aufklärung von Mechanismen der Mikrobiom Homöostase und Faktoren die zu mikrobiellem Ungleichgewicht und letztlich zu chronischen Entzündungen führen, unser Verständnis von Krebsentstehung und -progression verbessern.

Die Haut beherbergt eine beträchtliche Anzahl von Mikroben, die eine wichtige Rolle für Gesundheit und Krankheit spielen. Ihr Beitrag zur Hauttumorentstehung wurde jedoch nicht gut untersucht. Daher haben wir die Zusammensetzung der mikrobiellen Gemeinschaft bei menschlichen Keratinozyten-Hauttumoren, AK, SCC und Basalzellkarzinomen (BCC) vergleichend bewertet. Unsere Studie zeigt, dass Hauttumoren durch deutlich unterschiedliche mikrobielle Gemeinschaftsstrukturen gekennzeichnet sind. AK und SCC weisen im Gegensatz zu BCC eine signifikant erhöhte bakterielle Biomasse auf. *Staphylococcus aureus* war in den hyperkeratotischen Regionen von SCC deutlich häufiger. Ferner zeigten Hauttumoren eine veränderte Expression von antimikrobiellen Peptiden (AMPs), wobei menschliches ß-Defensin-2 (hBD-2) in SCC erhöht war. Interessanterweise ist bekannt, dass dieses AMP die Proliferation von Plattenepithelien induziert. Zu diesem Zweck infizierten wir SCC-Zellen *in vitro* mit *S. aureus* und beobachteten eine spezifische Induktion der hBD-2-Expression, die auch das Wachstum von SCC-Zellen förderte. Unsere Studien zeigen somit, dass eine Zusammensetzung der mikrobiellen Gemeinschaft, die möglicherweise aufgrund der Veränderung des mikrobiellen Lebensraums (Nische) bevorzugt wird, die Krebsentstehung fördert. Im Fall von SCC fördert ein erhöhter *S. aureus* wahrscheinlich das Tumorzellwachstum durch spezifische Induktion von hBD-2, wodurch der neoplastische Prozess vorangetrieben wird.

Ein weiteres Organsystem, bei dem die Mikrobiota zur Krebsentstehung beiträgt, ist der GI-Trakt. Es hat sich gezeigt, dass *Fusobacterium* Spezies, die typischerweise die Mundhöhle,

aber auch den GI-Trakt besiedeln, bei GI-Tumoren erhöht sind und deren Wachstum fördern können. Ein Teil dieser Arbeit bestätigte eine erhöhte Häufigkeit von tumorförderndem *Fusobacterium* und *F. nucleatum* in adenomatösen Polypen und CRC im Vergleich zu normalem Gewebe. Interessanterweise beobachteten wir auch eine verminderte Expression von FadA von Adenomen zu Karzinomen, was auf eine mögliche Herunterregulierung dieses mikrobiellen Kolonisationsfaktors hindeutet.

Ein weiterer Aspekt dieser Arbeit zielte darauf ab, kritische Probleme im Pilzkompartiment der Mikrobiota anzugehen, einschließlich der Pilz-DNA-Extraktion und PCR-Amplifikation unter Verwendung der internen transkribierten Spacer (ITS) -Regionen aus FFPE-Proben der menschlichen Haut. Die für die Analyse der mikrobiellen Gemeinschaft verwendeten Werkzeuge werden in der Regel für bakterielle Komponenten entwickelt und sind häufig unzureichend, wenn sie auf Pilzdaten angewendet werden. Daher wollten wir zunächst eine ideale Methode zur Isolierung von Pilz-DNA aus menschlichem Haut-FFPE erreichen, das die typischen Proben für die Histopathologie darstellt. Wir haben ferner versucht, die PCR-Amplifikation von ribosomaler Pilz-DNA unter Verwendung der ITS1- und -2-Regionen zu optimieren, bei denen es sich um hochvariable Sequenzen handelt, die zur Unterscheidung von Pilzarten verwendet werden. Wir haben gezeigt, dass eine mechanische Zellzerstörung während der DNA-Isolierung die DNA-Ausbeute signifikant senkte, was zu einer signifikanten Abnahme des Signal-Rausch-Verhältnisses bei der ITS-PCR führte. Wir beobachteten auch eine erhöhte PCR-Leistung unter Verwendung von ITS2-Primern im Vergleich zu ITS1.

Zusammenfassend weist diese Arbeit darauf hin, dass Veränderungen der Mikrobiota, die während der Karzinogenese auftreten, das Tumorzellwachstum fördern können, das durch verschiedene Wirts- und Mikrobenfaktoren wie die Veränderung der AMP-Expression in der cSCC-Progression oder durch die Regulierung des mikrobiellen Kolonisationsfaktors wie bei CRC moduliert wird.

I. Introduction

1. Human skin

Skin represents one of the largest organs of the body and serves as a physical and mechanical barrier against pathogens, UV radiations, chemicals and injuries. The skin (cutis) is composed of two layers, the epidermis and the dermis (Figure 1). The epidermis is the outermost layer of the skin and consists of layers of differentiated keratinocytes, melanocytes, Langerhans cells and Merkel cells (3-5) (Figure 2). Between the epidermis and the subcutaneous tissue lies the dermis which is further divided into the external papillary layer and the internal reticular layer. The dermis is comprised of connective tissue which is composed of collagen, elastin, blood vessels, nerves and sweat glands (4). Below the dermis is the hypodermis, or subcutaneous tissue, which consists mainly of adipose tissue and blood vessels (Figure 3) (4).

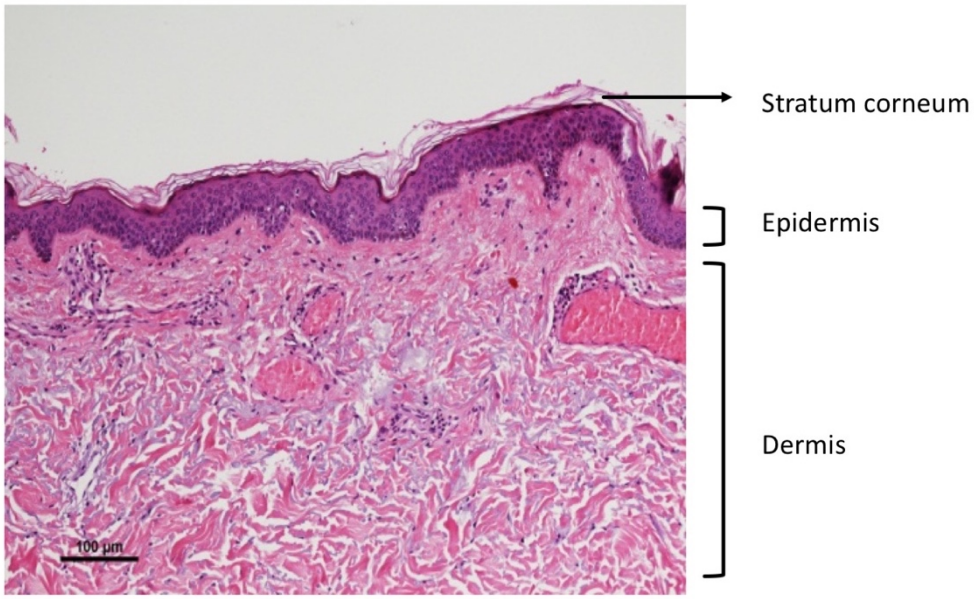

Figure 1. Microscopic anatomy of human healthy skin (i.e. cutis): shown are the two layers epidermis and dermis (H&E staining).

1.1. Layers of human skin

1.1.1. Epidermis

Epidermis being the top most layer of the skin acts as a protective barrier preventing the entry of bacteria, viruses and other foreign substances into the deeper layers. They are responsible for skin color, their texture and moisture content (4).

Keratinocytes are the primary cell type within epidermis (3, 4, 6). The 5 layers of epidermis (Figure 2) are as follows:

a. Stratum basale -The deepest germinal-layer containing basal cells which continuously divide. This layer is just above the dermis.
b. Stratum spinosum - Keratinocytes are interlinked via protruding cell processes that contain desmosomes.
c. Stratum granulosum - The keratinocytes in this layer contain keratohyalin granules (i.e. process of cell maturation) and are flatter with thick cell membranes and increased production of keratin.
d. Stratum lucidum - Thin layer of dead cells found in thick skin like, palm and sole. The cells harbor abundant eleiden, a lipid-rich protein, derived from keratohyalin.
e. Stratum corneum - The outermost layer of the skin is composed of squames (enucleated keratinocytes) which are cross-linked to act as skin barrier (7). This layer of dead cells prevents the entry of microbes. Cells in this layer are shed periodically and are replaced by cells pushed from the layers below.

The epithelial cells of the epidermis undergo a continuous process of maturation, also called keratinization, from bottom (i.e. stratum basale) to top (i.e. stratum corneum) (4).

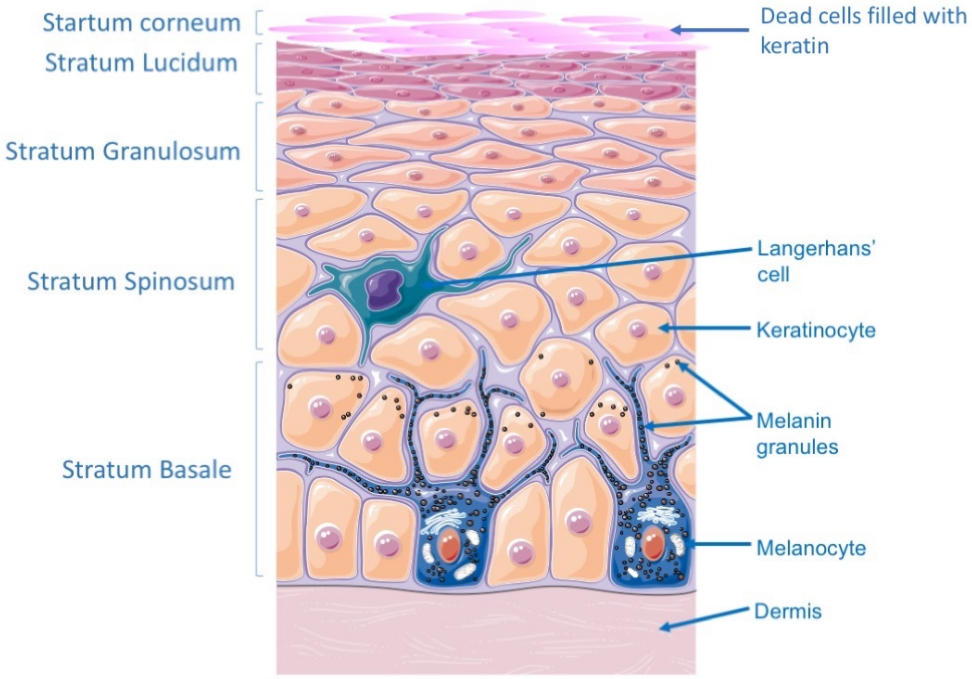

Figure 2. Layers of the epidermis and prevalent cell types (modified from Servier Medical Art, licensed under a Creative Common Attribution 3.0 Generic License)

1.1.2. Dermis

Dermis is the second layer below the epidermis which contains collagen as the primary constituent produced by fibroblasts. It consists of two connective tissue layers – 1) the outer papillary layer which contains fibrocytes, collagen and blood vessels and 2) the deeper reticular layer containing dense connective tissue with fewer fibrocytes. Dermis also contains the skin appendages, sensory neurons, hair follicles and sweat glands (3) (4) (Figure 3). Dermis is responsible for regional variation in skin thickness; for eg., their thickness within the head and neck region varies from 1 mm to 2.5mm (4).

1.1.3. Hypodermis

Hypodermis is the innermost, subcutaneous layer that connects skin to fibrous tissues of muscles and bones. It contains subcutaneous fat, neurons and blood vessels (4, 6) (Figure 3).

Notably, bacteria are mainly known to colonize the outmost stratum corneum, hair follicles and glands. However, studies have claimed the presence of bacteria also in the dermis and dermal adipose (8) (Figure 3).

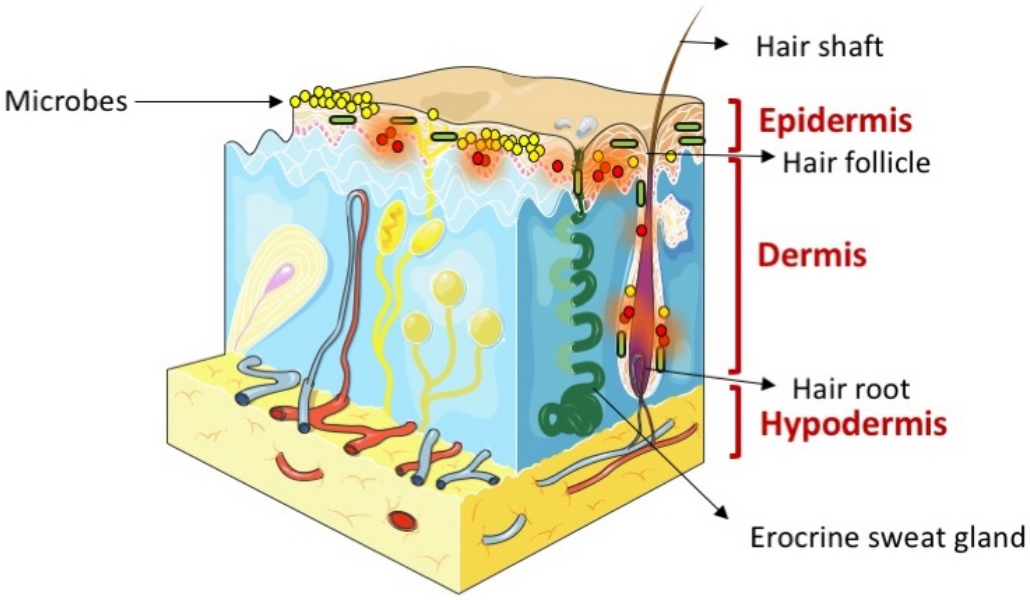

Figure 3. Layers of skin and appendages (modified from Servier Medical Art, licensed under a Creative Common Attribution 3.0 Generic License)

1.2. Skin physiology & microbiota

The different parts of the skin vary in their exposure to UV, pH, temperature, moisture and sebum content (9). Based on these physiological and topographical factors, skin sites have been divided into three main categories: moist, oily and dry (10). Microbial communities are known to vary between these skin sites as represented in figure 4 (11). For example, species of *Staphylococcus* and *Corynebacterium* are prevalent in moist areas whereas species of *Propionibacterium* are abundant in sebaceous sites (11, 12). Sweat glands, sebaceous glands and hair follicles influence the microenvironment of these different skin habitats (10). Also, the skin appendages play an important role in maintaining a stable physiology of the skin. For example, sweat glands aid in thermoregulation and also in acidifying the skin, thus, protecting the skin from ("wrong") microbial colonization (9). Additionally, constituents of sweat such as

free fatty acids and antimicrobial peptides (AMP) prevent colonization of certain microbes, (13) and sebaceous glands secreting sebum act as an antibacterial shield for the skin (10).

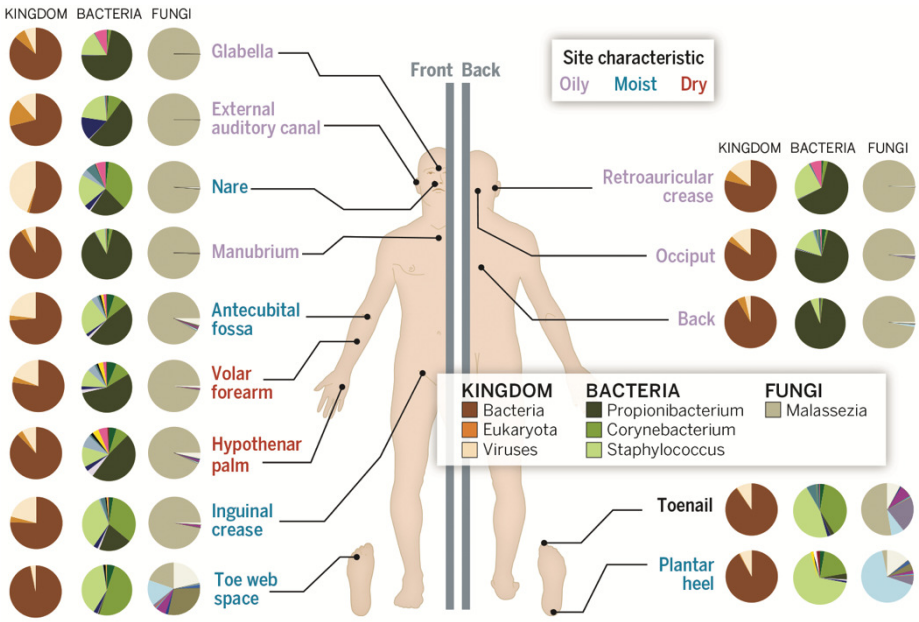

Figure 4. Skin microbiome including viruses, bacteria and fungal components in different skin sites. Reproduced from Belkaid Y, 2014 with permission of the publisher -The American Association for the Advancement of Science (License no 4381390878303).

2. Skin microbiome

Skin acts as a primary interface between the host and the environment. It is colonized by diverse commensal and pathogenic microorganisms which play a pivotal role in maintaining tissue homeostasis and immunity (14). The skin microbiome consists of bacteria, fungi , viruses and archaea but their role in skin tumor development is not well understood (15-17). An estimate of 1 million bacteria is known to inhabit a square centimeter of skin (18, 19). Skin commensals act as a barrier to prevent pathogen colonization, prime the immune system and enable break-down of natural products (11, 20, 21). Disturbance of the equilibrium between commensals and pathogens result in skin diseases (10). Notably, the skin immune system modulates the composition of the skin microbiota, which in turn also educates the immune system (11, 20).

In summary, keratinized skin cells, microbes and immune cells together cooperate to maintain physical and immune barrier of the skin during healthy and stressed conditions (11). A summary of important skin microbiome factors are listed in Table 1.

2.1. Skin bacteria

One million bacteria are estimated to be colonizing each square cm of the skin, which equates to a total of about 10^{10} bacterial cells prevalent on the $1.8m^2$ human skin (18). Quantitatively, bacteria dominate the skin microbiome. Skin bacteria are represented by 4 dominant phyla - Actinobacteria (52%), Firmicutes (24%), Proteobacteria (17%) and Bacteroidetes (7%) (9, 22, 23) (Figure 5). The proportions of the dominant phyla could vary greatly on the skin (24) (Figure 6). Notably, these 4 phyla are also dominant in the gastrointestinal tract, oral cavity and other mucosal surfaces (24-28) (Figure 6). Actinobacteria are the most abundant phylum on the skin (9, 24) (Figure 6). Importantly, specific bacteria are associated with the different moist, dry and sebaceous microenvironments of the skin (9, 11) (Figures 4 & 5). The dry areas of the skin such as forearm, buttock and different parts of the hand harbor the most diverse bacterial composition (24, 29, 30). The microbiome of the skin also shows a great variability over time which is more pronounced as in the gut and oral cavity (24).

In brief, the composition of the skin microbial communities is known to be dependent mainly on specific physiology of the respective skin site. The most abundant taxa (9, 10, 15, 24, 30) in these specific regions are:

1. Dry areas: *Propionibacterium acnes, Corynebacterium tuberculostearicum, Streptococcus mitis, Streptococcus oralis and Streptococcus pseudopneumoniae*
2. Moist areas: *Corynebacterium tuberculostearicum, Staphylococcus hominis, Propionibacterium acnes, Staphylococcus epidermidis and Staphylococcus capitis*
3. Sebaceous areas: *Propionibacterium acnes, Staphylococcus epidermidis, Corynebacterium tuberculostearicum, Staphylococcus capitis and Corynebacterium simulans.*

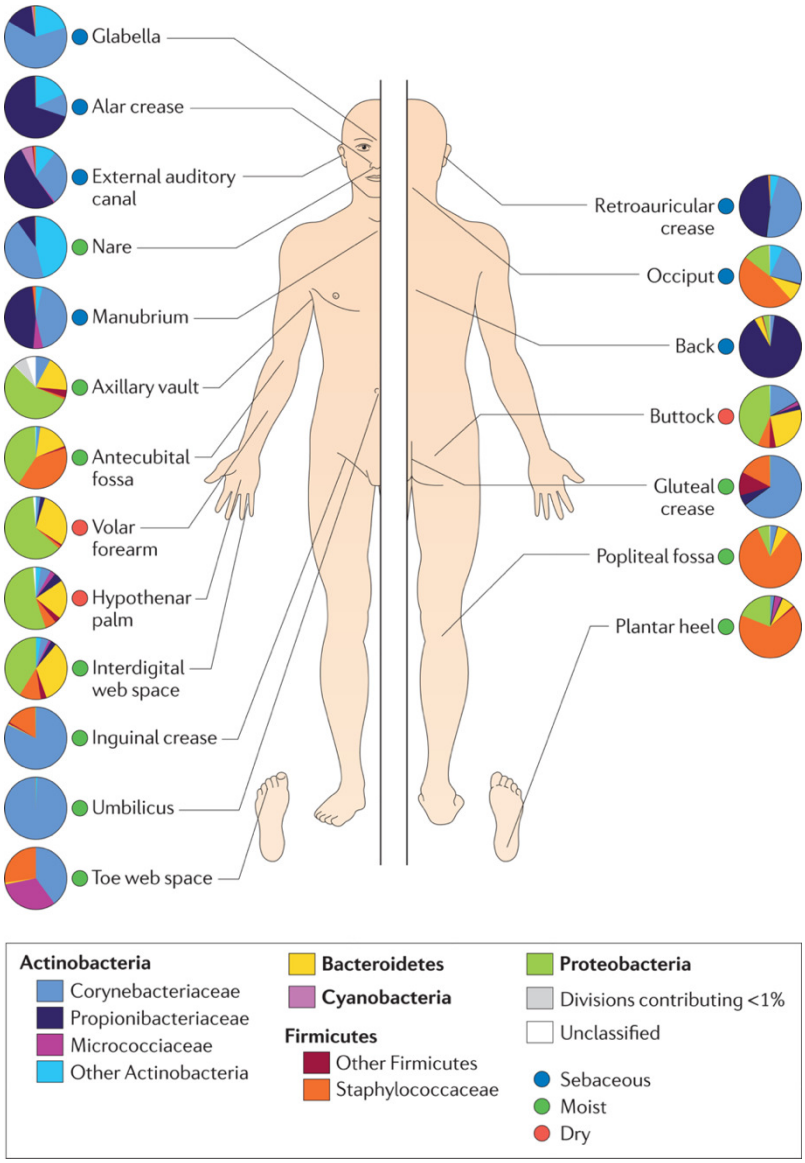

Figure 5. Topographical distribution of bacteria on different skin sites. Reproduced from Grice E A, 2011 with permission of the publisher -The American Association for the Advancement of Science (License no 4381420305811).

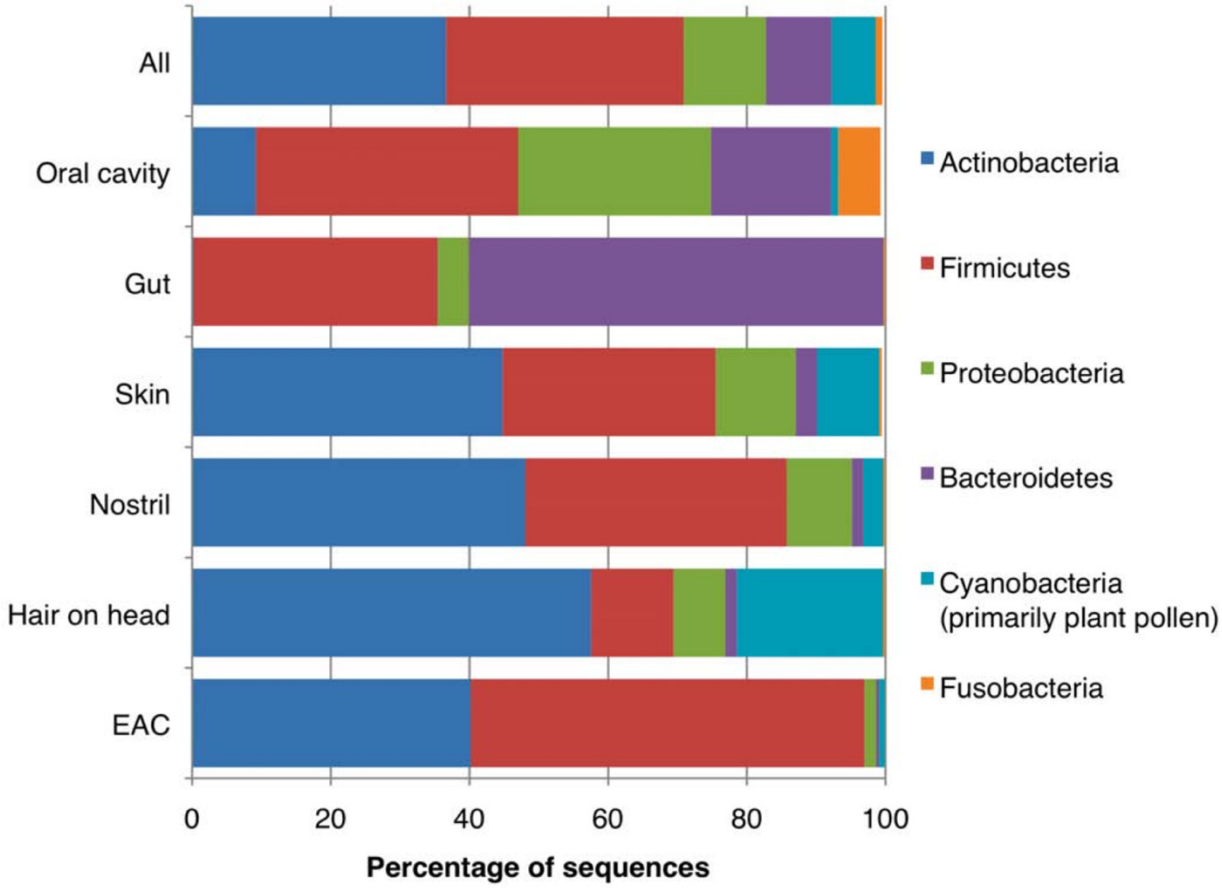

Figure 6. Relative abundance of the 6 most abundant phyla in different human body habitats. Reproduced from Costello E K, 2009 with permission of the publisher -The American Association for the Advancement of Science (License no 4381551414660).

2.2. Skin fungi

Skin is also colonized by a wide diversity of fungal species which contribute to its health and disease. Interestingly, unlike bacteria, the fungal microbiota shows a more equal distribution across core body sites regardless of physiology (12, 15). Approximately 390 fungal species have been described in humans (2). Further, the abundance of fungal cells differs from <0.1% in GI tract to up to 10% of microorganisms in skin, depending on the habitat (31). Notably, on an average, the fungal cell is about hundred fold larger than an average bacterial cell which results in significant fungal biomass. This provides ample bioactive molecules to the host thereby shaping its physiology (32). The genus *Malassezia* is the most dominant taxon (50-80% of the total skin fungi) across 11 core body and arm sites (back, occiput, external auditory canal, inguinal crease, retroauricular crease, glabella, manubrium, nare, antecubital fossa, volar forearm, hypothenar palm, plantar heel, toenail, and toe-web space) (10, 33). However, foot

sites are colonized by diverse fungal species which includes *Malassezia*, *Aspergillus, Cryptococcus, Rhodotorula, Epicoccum* among others (10). Notably, *Malassezia* is associated with various skin disorders as shown in Table 2.

2.3. Skin virome

Skin virome is one of the less investigated parts of skin microbiome despite their potential to modulate cutaneous health and disease. They are known to be associated with skin cancer (eg: Merkel cell polyomavirus causes Merkel cell carcinoma; HPV associated with SCC) and a multitude of cutaneous manifestations (eg: HPV causes warts). Eukaryotic DNA viruses are known to be rather individual specific and their representation is not dependent on the anatomical site unlike bacteria and fungi (10, 22). Since there is a lack of universally shared marker gene for viruses, shotgun metagenomics sequencing can be used to assess the skin virome (22, 34). Until now, no core virome has been identified which is conserved among individuals except bacteriophages which are dependent on skin bacteria (22, 34). Recent studies have shown the presence of resident or short-lived viruses on the skin such as α-HPV, β-HPV, and γ-HPV (35, 36). New viruses of the Polyomoaviridae family have also been revealed using functional metagenomic methods (37). These studies indicate the presence of cutaneous viral microbiome in healthy skin and their possible involvement in proliferative skin diseases.

2.4. Skin archaea

Lastly, the lesser known archaeal communities of skin microbiome are reported by Probst *et al*, by sequencing the 16S rRNA (38). 4% of the microbial genes were of archaea and 90% of the observed operational taxonomic units (OTUs) were of phylum Thaumarchaeota (39). Even though a range of different archaea are known to harbor the gut, mouth and vaginal microbiome, their abundance and functional roles are less studied. However, recent studies by Moissl-Eichinger *et al* and Koskinen *et al* signify the potential role of archaea in health and disease (39, 40).

Factors	Facts
Microbial density	$10^6/cm^2$
Microbial diversity	Bacteria are dominant (7-8 phyla, ~40 species/individual); up to 10% fungi and 40% viruses/phages
Niche	Stratum corneum (surface) and appendages (sebaceous glands, hair follicles and sweat glands) are the primary colonized habitats
Nutrients	Nutrient poor in comparison to gut, skin surface is covered in sweat with sebum and stratum corneum peptides and lipids as nutrients. Sweat also is replete with free fatty acids and AMPs. Urea present in sweat is also utilized as a nutrient by some strains of Staphylococcus (13)
Community establishment & change	Postpartum and during puberty
Effect on the immune system	Functional tuning and colonization resistance

Table 1. Summary of important skin microbiome factors. Adapted from (11).

3. Skin microbiota in disease

Changes in microbiota composition, called dysbiosis, are associated with many skin diseases like acne, eczema and chronic wounds (10, 41). Interestingly, often skin commensals are known to drive the dysbiosis in these diseases. In some cases, bacterial species that are usually known to be beneficial to their hosts could become pathogenic (10). For example, in acne vulgaris which is a chronic inflammatory skin condition, *P. acnes* (all healthy adults are colonized with abundant *P. acnes*) is known to be associated (42). Though all healthy adults harbor *P. acnes*, only a minority of them develop acne, indicating the importance of understanding a disease from the perspective of host genetics, the microbiome and its environment and immune and barrier defects (10). Skin microbes associated with important skin disease are summarized in Table 2.

Microbe	Associated diseases	References
Bacteria		
Staphylococcus aureus	atopic dermatitis (AD), skin and soft tissue infections, impetigo, cellulitis, folliculitis, subcutaneous abscesses, systemic lupus erythematosus with skin involvement, infected ulcers and wounds	(33, 43-51)
Propionibacterium acnes	acne vulgaris, dandruff, psoriasis,	(10, 42, 52-55)
Mycobacterium	skin and soft tissue infections, Buruli ulcer	(56-58)
Fungi		
Malassezia	atopic dermatitis, dandruff, tinea versicolor, psoriasis	(53, 59-61)
Mite		
Demodex follicularum	rosacea	(62)

Table 2. Microbes and their associated skin diseases

3.1. *Staphylococcus aureus*

Staphylococcus aureus is a Gram-positive bacterium which is known to be associated with many skin diseases as listed in Table 2. *S. aureus* is recognized as one of the most important pathogens of the skin, although more than 30 % of healthy individuals are asymptomatically colonized with this microbe (56, 63). The skin disease atopic dermatitis (AD) seems to be driven by *S. aureus* (44, 46). It has a wide range of virulence factors that play a major role in pathogenesis (49, 64, 65).

- Delta-toxin of *S. aureus* is known to induce degranulation of mast cells which promotes adaptive and innate immune responses (66).
- Alpha-toxin of *S. aureus* is known to induce production of IL-1ß from monocytes which promotes a T_H17 response (67).
- Lipoteichoic acid (*S. aureus* derived cell wall component*)* exposed T cells were unable to proliferate or produce cytokine indicating temporary T cell paralysis (68).
- *S. aureus* infection of skin has also shown to trigger dermal adipocyte proliferation leading to impaired adipogenesis resulting in increased infection. This host defense mechanism is known to be mediated by the production of cathelicidin AMP by adipocytes (69).
- In case of skin barrier defects in AD, *S. aureus* invades the epidermis and traverse into the dermis thereby interacting with viable immunocytes and stimulating the production of inflammatory cytokines IL-4, IL-13 and IL-22 cytokines (70).
- *S. aureus* produces the chemotaxis inhibitory protein (CHIPS) and formylated peptide receptor to inhibit neutrophil chemotaxis (49, 71).
- Protein A, fibrinogen binding protein and clumping factor A (ClfA) of *S. aureus* inhibit or impair phagocytosis (72, 73).
- Cytolytic toxin of *S. aureus* is known to cause osmotic lysis of host cells and prevents phagocytosis (72, 73).
- Human keratinocytes are known to upregulate the production of the AMPs hBD-2, -3 and LL-37 in response to *S. aureus* infection (74).

Even though dysbiosis is known to be associated with many skin diseases, it is currently unknown whether the changed microbiome is just a consequence of the disease or if it also initiates the disease (10).

4. Epithelial tumors: Impact of the microbiome

4.1. Skin tumor

Squamous cell carcinoma (SCC) and basal cell carcinoma (BCC) are the two most common non-melanoma skin cancers accounting for more than 90% of all skin malignancies (75) (76). Approximately 2-3 million cases are reported worldwide annually (77, 78). Other, less common forms of non-melanoma skin cancers are Merkel cell carcinoma, primary cutaneous

B-cell lymphoma, Kaposi sarcoma and Dermatofibrosarcoma protuberans (4). Cutaneous SCC (cSCC) often starts as precancerous lesion, called actinic keratosis (AK) which can progress into cancer over time (79). AK which is also known as solar keratosis is an intra-epidermal scaly lesion that usually develops on areas that are cumulatively exposed to UV radiation(80). Histologically, it is signified by an atypical keratinocyte proliferation within photo damaged skin which may progress to invasive SCC, but it might also regress (81-83) (Figure 7). Because of UV exposure, they occur typically on head, neck and forearms (84). UV radiation induces genetic mutations in keratinocytes (81). It initiates a complex cascade of genetic, cellular and immune events that impact the progression of AK to SCC (81, 85). In AK and SCC, defects in the maturation of superficial epidermal layers are prevalent, leading to hyperkeratosis (increased thickening of the keratin layer) and parakeratosis (retention of nuclei in the thickened keratin layer) (85) (Figure 8). In SCC, dysplastic keratinocytes penetrate the basement membrane and invade the subepithelial connective tissue. SCCs are often ulcerated (85) (Figure 7) and mostly metastasize into regional lymph nodes (86). The most common genetic alteration in SCCs is a mutation in the P53 tumor suppressor gene which allows the cells to escape apoptosis and propagate (4). SCC is also more prevalent in immunosuppressed individuals like organ transplant recipients (87, 88). BCC which arises from the basal cell layer of the epidermis rarely metastasizes, unlike SCC, but it shows a locally destructive (invasive) growth (4) (Figure 8). BCC is also caused mainly by exposure to UVB radiation, and also (inheritable) genetic mutations, ionizing radiation, immunosuppression and toxins play a role in its etiology (4). BCCs often show an intact skin surface and inflammation of the dermis is rarely prominent. BCC originates from the cells of the hair follicle and not from the surface epithelium (epidermis) like SCC.

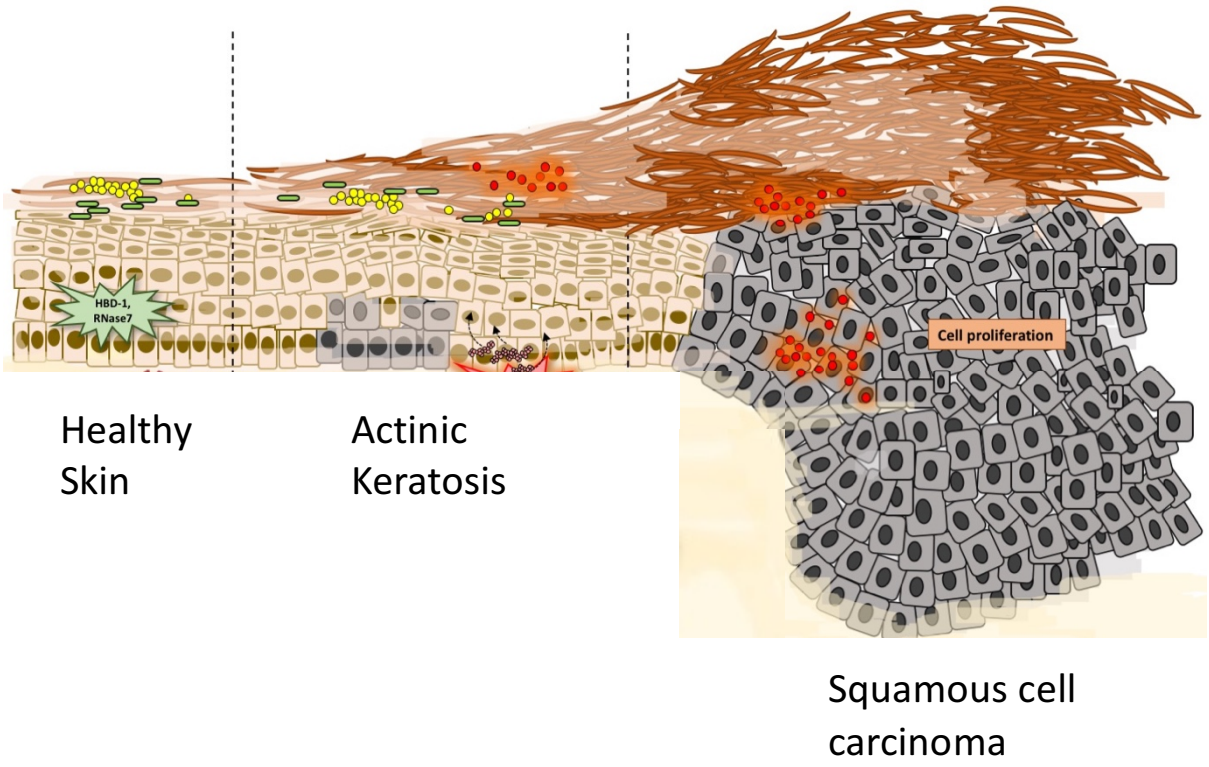

Figure 7. Scheme highlighting the progression of actinic keratosis to squamous cell carcinoma

Malignant tumors are usually composed of neoplastic cells intermixed with non-neoplastic cells like immune and stromal cells as well as microbes (89). A known driver of neoplasia development is inflammation leading to chronic tissue damage (Figure 8). In virtually all steps of carcinogenesis, including initiation, promotion, progression, and metastasis, specific roles of immune cells, cytokines and other immune mediators like chemokines, lymphokines and interleukins have been elucidated (90). In the context of AK to SCC progression, however, such factors are less clear (81). One of the main characteristics of AK is dyskeratosis, which is associated with a breach of the skin barrier, possibly resulting in microbial dysbiosis. This indicates the importance of understanding skin microbial compositions and their effect on cSCC development and progression (Figure 8).

The resident microbiome has been recognized as an important factor influencing inflammatory responses, tumor development and progression and also specific microbiome type are known to be associated with neoplasia (91, 92). Skin morphology and metabolism are significantly changed during carcinogenesis which in turn changes the microbial habitat leading to an altered

microbial colonization. This could potentially favor pro-tumorigenic microbes, which could in turn perpetuate tumorigenesis (1). An example of one such case is the overexpression of the carbohydrate Gal-GalNAc on neoplastic colonocytes acting as bacterial lectin to increased *Fusobacterium nucleatum* on the tumor (93). Hence, during tumor development, the homeostatic equilibrium between host and microbiota is altered and selection of a pro-inflammatory microbiome could possibly drive tumor progression (94).

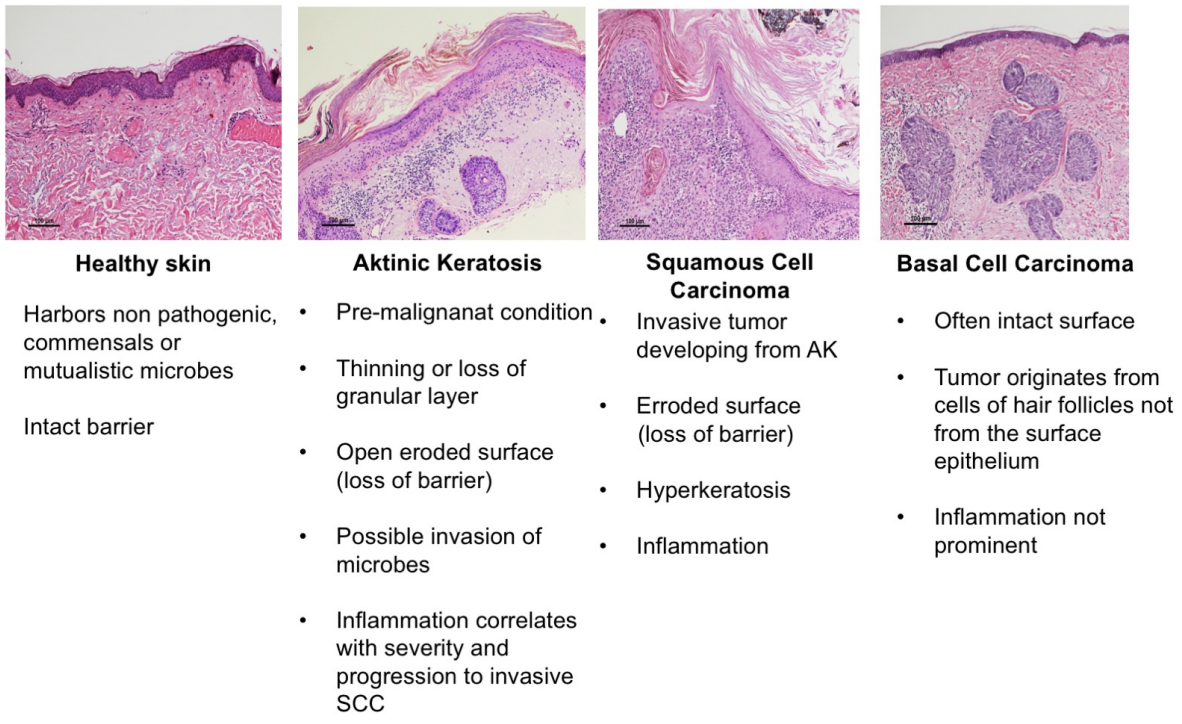

Figure 8. Histology of skin tumors

4.2. Colorectal cancer

Colorectal cancer (CRC) emerges by the formation of adenomatous polyps which undergoes dysplastic changes to become cancerous (95) (Figure 9). CRC pathogenesis has been thoroughly investigated. Characterization of the microbiota in CRC by using whole-genome sequencing has deduced a strong association of overabundant *Fusobacterium* with *F. nucleatum* being the most dominant species (89, 96, 97). Also, the mechanisms by which

Fusobacterium drives CRC has been investigated. Due to its unique adhesin FadA, it binds to E cadherin stimulating E-cadherin/beta-catenin signaling (98). Moreover, it favors a pro-inflammatory microenvironment by promoting the release of inflammatory cytokines like IL-8, IL-10 and tumor necrosis factor -α (TNF- α) in the vicinity of the tumor that is conducive for colorectal neoplasia progression. Also, via interaction between virulence factor Fap2 (autotransporter protein) of *F. nucleatum* and TIGIT which is a human inhibitory receptor (expressed on T cells and natural killer cells), lymphocytes cell death is induced and immunosuppressive tumor microenvironment is generated which in turn promotes colorectal tumor progression (99, 100).

Moreover, patients with Inflammatory Bowel Disease (IBD) are known to have an increased risk of colorectal carcinoma (101). Interestingly, *Fusobacterium* species have also been associated with IBD, including both ulcerative colitis and Crohn's disease (102, 103). Therefore, it would be noteworthy to explore the link between the role of *Fusobacterium* spp. in colitis-associated colorectal carcinoma pathogenesis.

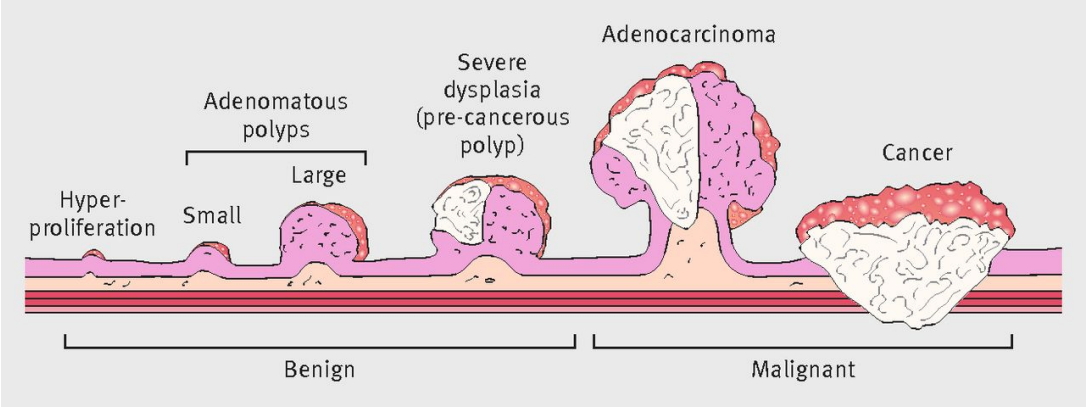

Figure 9. Scheme representing the progression of benign to malignant polyp to colorectal carcinoma. Reproduced from Thrumurthy S G et al., 2016 with permission of the publisher (104) -The BMJ (License no 4933041072421).

4.3. Different mechanisms of carcinogenesis modulated by the bacterial microbiome

The mechanisms through which bacteria can contribute to cancer development mainly include chronic inflammation, immune evasion and immune suppression (105). The association between inflammation and tumorigenesis is well-established (106).

Mechanisms of how bacteria might act in tumor development include:

a. Changes in the microbiome and host defense mechanisms lead to increased bacterial translocation which in turn activates Toll-like receptors (TLRs) in several cell types including macrophages, myofibroblasts, epithelial cells and tumor cells (94, 107-109).
b. Bacteria derived genotoxins (e.g. colibactin & cytolethal distending toxin [CDT]) induce direct DNA damage in the host cells (110-112). Induction of reactive oxygen species (ROS) released from inflammatory cells like macrophages are also known to be genotoxic (94).
c. Specific metabolites of the microbiome act as genotoxins, like acetaldehyde, nitrosamine and tumor-promoting secondary bile acids (94). Interestingly certain tumor suppressing effects of microbial metabolites have also been observed and they might act via inactivation of carcinogens. Such tumor suppressing metabolites might be short-chain fatty acids or certain phytochemicals (94).

Interestingly, a recent report showed that in an animal model of keratinocyte skin tumor caused by chronic inflammation, tumor formation was influenced by bacterial infection, specifically by bacterial flagellin which signals via TLR5, while antibiotic treatment inhibited tumor formation (113).

5. Antimicrobial peptides

Antimicrobial peptides (AMPs) are small peptides which are produced by all multicellular organisms as the first line of defense. They are evolutionarily conserved (commonly found from prokaryotes to humans) (114) and are known to have microbicidal activity. They are well studied and characterized in all multicellular organisms for their activity (114). More than 2500 AMPs are currently deposited in Antimicrobial Peptide Database (http://aps.unmc.edu/AP/main.php). Based on their secondary structure, AMPs are classified into α-helical (eg: human cathelicidin peptide LL-37), ß- sheet (eg: defensins) and extended

AMPs (eg: histidine, arginine, glycine and tryptophan). Human skin generates AMPs, which are innate immune factors acting as the first line of defense against microbes (74, 115-117). AMPs also have pro- or anti-inflammatory functions (118). While some AMPs are produced by keratinocytes in normal skin, others are induced during inflammation, infection or if the skin is wounded (119, 120). Some AMPs are even known to stimulate keratinocyte migration and proliferation (115, 121). Interestingly, keratinocytes are known to release an array of cytokines through G-protein coupled receptors when stimulated with ß-defensins or cathelicidins, both representing AMPs (122). At high concentrations, AMPs can damage human cells leading to necrosis or apoptotic cell death (123).

The most abundant AMPs produced by human keratinocytes are ß-defensins hBD-1, -2, -3, RNase 7 and the cathelicidin LL-37. hBD-1 is known to be constitutively expressed by epithelial tissues whereas hBD-2, -3, LL-37 and RNase 7 are induced by factors such as pathogenic bacterial colonization and certain cytokines like TNF- α, IL-1 ß and IL-17, (124-127). Interestingly, hBD-2, -3 and RNase 7 but not hBD-1 expression levels were induced in primary keratinocytes upon infection with the pathogen *S. aureus* but not by the commensal *Staphylococcus epidermidis*, suggesting differential induction of AMPs in the skin by specific microbes (74, 128)**.**

Cathelicidin is known to be produced by several cell types other than keratinocytes which includes eccrine sweat glands and sebocytes, bone-marrow-derived cells found within the skin, including neutrophils, mast cells and dendritic cells (114).

A potential role of hBD's in carcinogenesis of epithelial tumors has been described previously (129-132). The ability of hBDs to modulate proliferation of oral squamous cell carcinoma was shown by Winter J *et al*. (133). hBD-1 possibly acts as a tumor suppressor while hBD-2, -3 could act as tumor promoters. Moreover, hBD-2, -3 and -4 were shown to enhance keratinocyte proliferation and migration (115). Interestingly, hBD-2 was also known to promote the proliferation of lung cancer cells (134) and human cultured epithelial cells from the cervix (135). Their growth promoting effects in keratinocytes was shown to act via activation of epithelial growth factor receptor (EGFR) and downstream activation of STAT1 and STAT3 (115, 122, 136).

Besides, not just the skin but microbes also produce various AMPs in order to limit the growth of other microbes. However, these peptides are quite distinct from the mammalian AMPs (synthesized from nonribosomal peptide synthase). Examples of microbial AMPs are the cationic peptides polymyxin B which are produced by *Bacillus polymyxa* and the noncationic glycopeptide vancomycin by *Amycolatopsis orientalis* (114, 137, 138).

5.1. Cellular source of AMP s in the skin

AMPs	Cellular source in the skin
Alpha-defensin	Neutrophils
hBD-2	Keratinocytes, macrophages, dendritic cells
hBD-3	Keratinocytes
hBD-4	Keratinocytes
LL-37	Keratinocytes, macrophages and neutrophils
Dermicidin	Sweat glands
RNase 7	Keratinocytes

Table 3. AMPs produced by keratinocytes and immune cells (139, 140)

5.2. Chemotactic properties of AMPs

Defensins and cathelicidins are chemotactic for distinct subpopulations of leukocytes as well as some non-leukocytes (118).

- hBD (1-3) – memory T cells and immature dendritic cells
- hBD 2 – mast cells and activated neutrophils
- hBD 3 & 4- monocytes/macrophages
- Cathelicidins- neutrophils, monocytes/macrophages, CD4 T lymphocytes

ß-defensins and cathelicidins are the two main types of AMPs in the skin (141).

5.3. Beta defensins

Human ß-defensins account for one of the major class of AMPs found in human epithelia with mainly hBD-1, -2 & -3 expressed in the skin. (124, 126, 127, 142).

They are (143):

- 2-6 kDa in size
- cationic peptides

- contain three pairs of intramolecular disulfide bonds
- mainly generated by epithelial tissues
- 4 hBDs have been detected in human skin
- based on their size and pattern of disulfide bonding, defensins are classified into alpha, beta and theta categories
- known for their immune modulating properties

5.4. Structure of hBDs

A

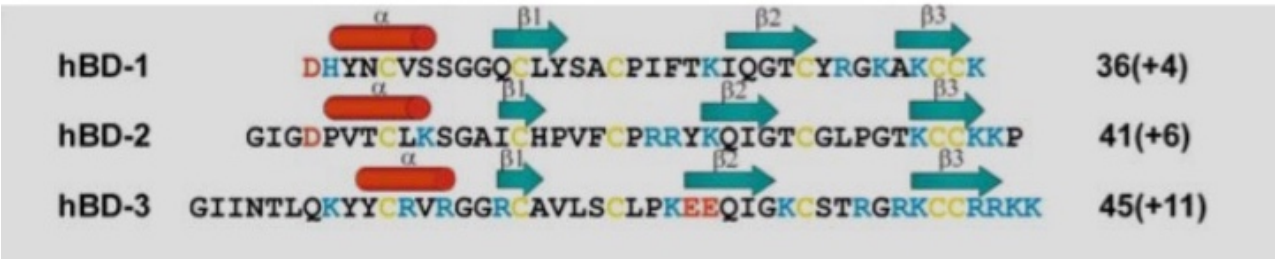

B

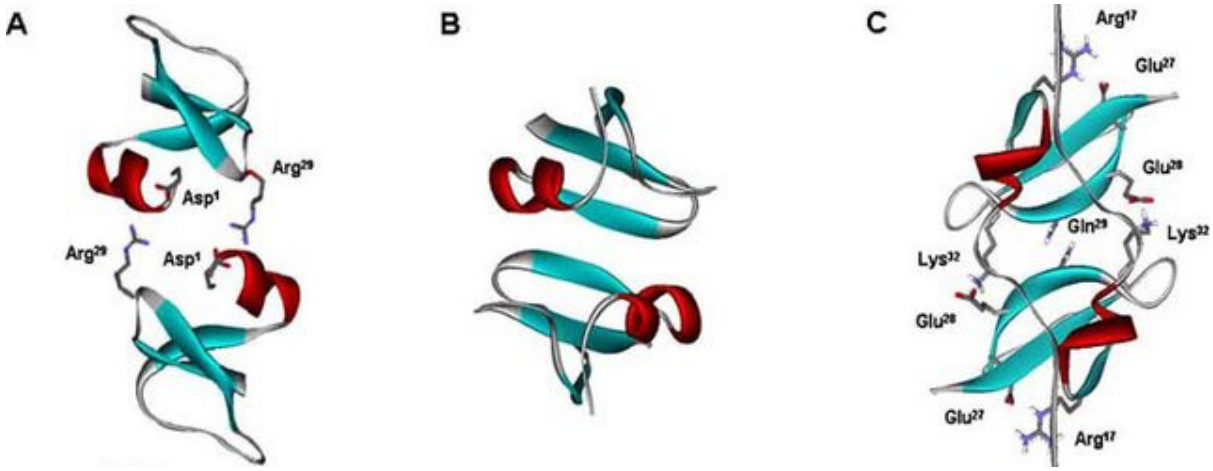

hBD-1 hBD-2 hBD-3

Figure 10. Structure of hBDs (A) Reproduced from Pazgier M et al., 2006 with permission of the publisher (143) –Springer nature (License no 4393871378538); (B) reproduced from Crovella S et al., 2005 with permission of publisher- Bentham science publisher ltd (License no 1049871-1).

- 6- cysteine residues
- high content of cationic residues Lys and Arg
- aggregation of these positive charges are important for antimicrobial activity
- tertiary structures are very similar
- core contains 3 beta strands arranged in anti parallel sheets
- limited AA sequence conservation
- N-terminus of hBD-3 appears unstructured

The main differences in structure, immune properties, expression and induction of hBDs are listed in Table 3. Though hBD-1 is structurally similar to hBD-2 and -3, it has no effect on cell proliferation or even the cytokine release (118).

Defensins	**hBD-1**	**hBD-2**	**hBD-3**
Structure	monomer	monomer	dimer
Immune properties	chemotaxin for memory T cells and immature dendritic cells	chemotactic migration of T cells and immature dendritic cells by binding to CCR6, mast cells and activated neutrophils	binds to TLRs, induce antigen uptake and processing, differentiation of APC; chemotaxin for monocytes/macrophages
Expression and induction	constitutively produced by epithelial tissues; no antimicrobial activity against *S. aureus*	isolated from lesional scales of psoriatic skin; inducible in inflamed skin lesions upon treatment with LPS, TNF- α, IL-1ß and bacterial products from commensals such as *S. epidermidis*; localized to uppermost layer of epidermis; produced by keratinocytes	isolated from lesional psoriatic scales; found in both epithelial and non-epithelial tissues; produced by keratinocytes and other epithelial tissues when induced by LPS, TNF-α, IL-1ß and bacterial products

Table 4. Differences in the biological properties of hBDs.

5.5. Cathelicidins

Only one cathelicidin gene *(camp)* is identified in humans so far and this encodes for LL-37 (144). LL-37 has 37 amino acids (49). It is constitutively expressed in neutrophils and is known to be induced in epithelial cells including keratinocytes (145, 146). Human keratinocytes have been shown to upregulate the production of LL-37 in response to *S. aureus* infections (49). It is also expressed in the gastrointestinal tract (squamous epithelium of tongue, mouth, esophagus and in colonocytes), epididymis and lungs (144, 147, 148).

II. Hypothesis

Specific microbes and microbiome types are associated with tumors (e.g. cSCC), which might change during development and progression from their precursor lesions (e.g. AK). The altered microbiome types and specific microbes therein can promote or inhibit tumor progression.

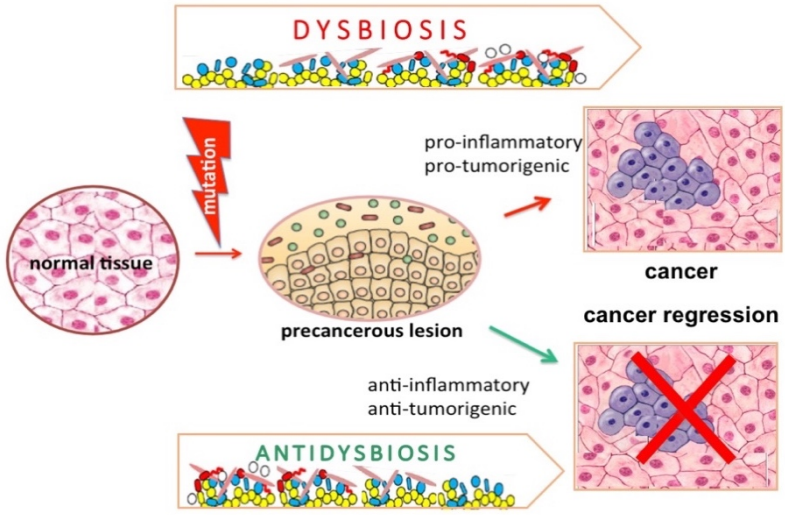

III. Aims

Part 1:

1. To decipher prevalent microbial communities in pre-invasive (AK) and invasive (SCC, BCC) keratinocyte tumors.
2. To investigate the in-situ localization of the specific bacteria in keratinocyte tumors.
3. To examine if the grade of inflammation is associated with specific microbial community changes.
4. To discern the role of the skin microbiome in promoting or preventing cSCC progression.

Part 2:

5. Comparative assessment of *Fusobacterium*, *F. nucleatum* and its virulence factor FadA adhesion gene expression via PCR in adenomatous polyps, colorectal carcinoma cases and healthy tissues.

Part 3:

6. To improve fungal DNA extraction from human skin Formalin-fixed paraffin-embedded (FFPE) samples and to discern the best region for internal transcribed spacer (ITS)-based PCR amplification for fungal microbiome characterization.

IV. Materials and methods

Parts of the methodological descriptions have also been published in original articles (1, 2).

1. Specimens

Skin tumor tissues (FFPE) were obtained from the Institute of Dermatology and Pathology at the Medical University of Graz (MUG) (Appendix 1). The entities used were as follows: AK (n=25), cSCC (n=22) and BCC (n=13) from the head, neck and arm regions. Ulcerated specimens were omitted from the study. Also, non-neoplastic skin samples (resection margins) without the lesions NS (n=10), healthy skin HS (n=5) and chronic plaque psoriasis PS (n=5) were included in the study for comparison. In total, specimens from total excision were n=54, punch biopsies n=24 and shave biopsies n=10 (1).

For fungal DNA isolation, the following entities were used: healthy skin (n=5); skin tumor BCC (n=2), SCC (n=1); Keratoacanthoma (n=1) and skin diagnosed with fungal infection (n=1) (Table 7). These tissues were obtained from the Institute of Pathology, MUG collected between the year 2014 and 2015 (2).

Colorectal tumor samples (FFPE) were obtained from the Institute of Pathology, MUG, collected in the year 2014 (Appendix 2). The following entities were used: adenocarcinoma (n=4), adenomatous polyp (n=7) and normal colon (n=4).

2. Histology and Immunohistochemistry

FFPE tissue specimen sections were either stained with hematoxylin and eosin (H&E) or PAS or Gram stains with the following parameters: microbial structures (bacteria, fungi; they were differentiated based on staining behavior in Gram and PAS stains as well as their cell size and shape): 0 = not visible, 1 = sparse, 2 = small clusters of microbial structures, 3 = abundant microbial structures; inflammation (i) % of papillary dermis infiltrated with inflammatory cells and (ii) semiquantitative (0 = none; 1 = focal; 2 = clusters of inflammatory cells in papillary dermis; 3 = dense bands of inflammatory cells in papillary dermis); neutrophilic granulocytes (no/high power field); hyper-/parakeratosis (average (mean ± SD) thickness in µm over the whole lesion)(1). All the analyses performed on these sections along with their clinical information are provided in the appendix section (Appendix 1 & 2) and Table 7 (1, 2).

Inflammation grades (low and high) of the skin tumors were semi-quantitatively scored using light microscopy based on the degree of infiltration using H&E staining. Low-grade inflammation: focal infiltrate of immune cells mainly surrounding small vessels; high-grade inflammation: papillary and upper reticular dermis are densely populated by immune cells, often represented as continuous bands of inflammatory cells. This was then correlated to the species richness as measured by alpha diversity (unpaired t-test; measure: observed species), microbial community type as measured by beta diversity (weighted unifrac) and relative genus abundance as assessed by Kruskal Wallis in AK, SCC & BCC.

For immunohistochemical staining (IHC), AK, SCC & BCC FFPE tissue sections (3.5 µm) were deparaffinized and rehydrated for staining. Slides were then incubated for heat-induced antigen retrieval in Dako Target Retrieval Solution Citrate pH 6.0 (Dako S2369) for 30 minutes in a steamer. The staining was then performed manually with antibody incubation at 4°C overnight using the Dako REAL™ Detection System, Peroxidase/AEC. The monoclonal antibodies were directed against: hBD2 (1:400; Abcam, #ab63982) and hBD3 (1:100; LSbio, #LS-B86). Images of staining were acquired with a DP71 digital camera (Olympus, Vienna, Austria), attached to an Olympus BX51 microscope. Quantitative analysis was performed by counting positively stained cells in 5 randomly selected microscopic fields or tumor sites at a magnification of 20x or 40x. Positive staining was scored in the epidermal layers. Scoring of microscopic slides was performed in a blinded manner by two individuals. Results of visual counts were averaged per patient and used further for statistical analysis.

3. Cell lines and culture

The human cutaneous squamous cell carcinoma cell lines HSC-1and SCL-1 were kindly provided by J C Becker, DKFZ, Essen, Germany. HaCaT cells (human immortal keratinocyte cell line) were obtained from the Center for Medical Research (CMR), MUG, Austria. HSC-1, SCL-1 and HaCaT cells were cultured in Dulbecco's modified Eagle's medium (DMEM) with low glucose (1g/l) (GE Healthcare, Vienna, Austria) and 10% fetal bovine serum (FBS) (Thermo Fischer Scientific). The cells were grown in a water-saturated atmosphere of 95% air and 5% CO_2 at 37^0C (1).

4. Bacterial strains and culture

Staphylococcus, *Streptococcus* and *Fusobacterium* strains were used for this study. The origin and designation of strains and their usage in the assays are given in Table 5. *Staphylococcus aureus* strains (DSM 799; DSM 11823 & DSM 1104) and *Staphylococcus epidermidis* (Hyg 9209-15) were cultured under aerobic conditions on Columbia blood agar plates (BioMerieux, France) at 37^0C for 24 hours (1). *Streptococcus parasanguinis* were cultured under aerobic conditions on Columbia blood agar plates at 37^0C for 72 hours. *Fusobacterium* strains were cultured anaerobically at 37^0C on Columbia blood agar plate for 67 hours.

Bacterial strains used in the study			
Species	Strains	Source	Usage
Staphylococcus aureus	DSM 799	DSMZ, Braunschweig, Germany	in vitro assay
	DSM 11823	DSMZ, Braunschweig, Germany	in vitro assay
	DSM 1104	DSMZ, Braunschweig, Germany	in vitro assay
		Institute of Hygiene and Microbiology, Graz, Austria	Positive control for qPCR & FISH
Staphylococcus epidermidis	DSM 1798	University Hospital Essen, Germany	in vitro assay
	ATCC 27626	University Hospital Essen, Germany	in vitro assay
	Hyg 9209-15	Institute of Hygiene and Microbiology, Graz, Austria	Positive control for qPCR & FISH
Streptococcus parasanguinis	10506	Institute of Hygiene and Microbiology, Graz, Austria	Positive control for qPCR
Fusobacterium nucleatum		Institute of Hygiene and Microbiology, Graz, Austria	Positive control for qPCR of *Fusobacterium* 16s, *F. nucleatum* and FadA
	20391		
	28310		

Table 5. Bacteria strains used for the study

5. DNA and RNA isolation

5.1. DNA isolation from human skin FFPE tissues

Two different DNA extraction kits were compared in this study along with additional mechanical and enzymatic treatments to get maximum yield of microbial DNA. These were QIAamp DNA FFPE tissue kit (Qiagen, Germany) and Maxwell 16 FFPE tissue LEV DNA Purification kit (Promega, USA). A two-step cell lysis (mechanical and enzymatic) was employed before the use of the kits according to the manufacturer's protocol. 5-µm thick 30-40 (depending on the tissue size) sections were cut from FFPE samples using a microtome. A new sterile blade was used for each tissue block and outer sections were discarded to avoid cross-contamination. The sections were deparaffinized and then subjected to mechanical lysis using a Magna Lyser instrument (Roche Diagnostics, Mannheim, Germany) with green beads (1.4 mm ceramic beads) for 30sec at 6000rpm twice, with 1 min cooling on ice in between and afterwards. Mechanical homogenization was carried out in 250 µl of bacteria lysis buffer. Subsequently, samples were subjected to enzymatic lysis with 2.5 ul of lysozyme (100 mg/ml; Carl Roth; Karlsruhe, Germany), 1.5 µl lysostaphin (4000U/ml; Sigma Aldrich; St. Luis, MO, USA) and 3µl mutanolysin (25KU/ml; Sigma Aldrich) and incubated at 37°C for 1 hour (149). Thereafter, 25µl proteinase K (20 mg/ml) was added and incubated at 70°C overnight with mild shaking (350rpm) (1). This mixture was then subjected to DNA with the commercial kits according to the manufacturer's protocols. DNA quality and concentration were determined spectrophotometrically with a NanoDrop ND-3300 instrument. Efficacy of bacterial DNA extraction was evaluated by using two qPCRs targeting the panbacterial 16S rRNA gene and a specific assay targeting *Propionibacterium acnes* (see below) (1).

5.2. Isolation of DNA from bacterial culture

A single bacterial colony of *S. aureus*, *S. epidermidis* and *Streptococcus parasanguinis* were cultured aerobically and *F. nucleatum* was cultured anaerobically and inoculated overnight in 1ml of bacterial culture media. Bacteria were pelleted, and the genomic DNA was isolated using the Wizard Genomic DNA purification kit (Promega, Wisconsin, USA) according to the manufacturer's protocol.

5.3. Isolation of DNA from human colorectal FFPE samples

5µm thick sections of FFPE sample blocks were used for DNA isolation. The initial 5 sections were discarded to exclude contamination. 10 subsequent sections were used for DNA extraction by using the QIAamp DNA FFPE tissue kit (Qiagen) according to the manufacturer's protocol.

5.4. Isolation of fungal DNA from FFPE material

The following sequence of steps were applied for fungal DNA isolation (2):

a. Pre-isolation step:

1. The microtome was cleaned with alcohol and xylene.
2. The FFPE blocks were cut into 5 µm thick sections and the first couple of slices were discarded.
3. 20 sections (for medium-sized tissues) and 25 sections (for tiny biopsies) were placed into a 1.5ml tube.
4. 1 ml of Xylene was added and centrifuged for 10 mins at 13000 rpm (RT). Following this, xylene was discarded.
5. 1 ml of 100% ethanol was added and mixed gently by vortexing. This was then centrifuged for 10 mins at 13000rpm (RT). Following this, ethanol was discarded.
6. The pellet was air-dried at RT for 1 hour and suspended in 180 ul ATL buffer (Qiagen kit).

b. Enzymatic Treatment:

1. 20 µl Proteinase K (Qiagen kit) was added to the above mixture and incubated overnight at 56 ºC with slight shaking (250 rpm) using a heat block.
2. Following day, the samples were spun down to remove drops from inside the lid.
3. Recombinant lyticase (2U/100 ul solution) was added to the above mixture and incubated for 45 min at 37 ºC.

c. Column DNA purification using QIAamp DNA FFPE Tissue Kit (Qiagen)

1. In order to partially reverse formaldehyde modification of nucleic acids, the above mixture was incubated at 90°C for 1 h and briefly centrifuged to remove drops from inside of the lid.
2. To this sample mixture, 200 µl Buffer AL was added and mixed thoroughly by vortexing. 200 µl ethanol (96–100%) was then added and mixed again thoroughly by vortexing.
3. QIAamp MinElute column was carefully opened and 500 µl Buffer AW1 was added without wetting the rim. This was then centrifuged at 6000 x g (8000 rpm) for 1 min. The QIAamp MinElute column was placed in a clean 2 ml collection tube, and the collection tube containing the flow-through was discarded.
4. The QIAamp MinElute column was carefully opened and 500 µl Buffer AW2 was added without wetting the rim. This was followed by centrifugation at 6000 x g (8000 rpm) for 1 min. The QIAamp MinElute column was then placed in a clean 2 ml collection tube, and the collection tube containing the flow-through was discarded.
5. Centrifugation was performed at full speed (20,000 x g; 14,000 rpm) for 3 min to dry the membrane completely.
6. The QIAamp MinElute column was then placed in a clean 1.5 ml microcentrifuge tube (not provided), and the collection tube containing flow-through was discarded. The column lid was carefully opened and 50 µl Buffer ATE was applied to the center of the membrane.
7. This was incubated at room temperature for 1 min and finally centrifuged at full speed (20,000 x g; 14,000 rpm) for 1 min (2).

5.5. Isolation of RNA from human skin FFPE samples

Total RNA from FFPE skin tumor samples (10 sections, each 5 µm thick) was isolated by using deparaffinization solution (Qiagen) and the RNeasy FFPE kit (Qiagen) which also included DNase treatment according to the manufacturer's specifications. 200ng of total RNA was used for cDNA synthesis with the GeneAmp RNA PCR kit (Thermo Fischer Scientific), according to the manufacturer's instructions for FFPE samples. RNA quality and quantity were determined spectrophotometrically using a NanoDrop instrument (ThermoScientific) (1).

5.6. Isolation of RNA from cells

RNA from cells was extracted using the PeqGOLD total RNA Kit (Peqlab, Erlangen, Germany) following the manufacturer's protocol. RNA was quantified using NanoDrop (Thermo Scientific). 200 ng of RNA was transcribed into cDNA with the Transcriptor First Strand cDNA Synthesis Kit (Roche Life Science, Indianapolis, IN, USA) according to the manufacturer's instructions (1).

6. 16S rRNA gene library preparation and sequencing

The V1–2 regions of the bacterial 16S rRNA gene were amplified using the oligonucleotide primers 27F (AGAGTTTGATCCTGGCTCAG) and 357R (CTGCTGCCTYCCGTA) [Eurofins (MWG, Ebersberg, Germany)], yielding a 349bp amplicon length (150)**.** For this purpose, 5µl of the total DNA (~15 ng/µl) extracted from FFPE skin samples was used as input for a 25µl PCR reaction. The reaction mixture contained 1X Fast Start High Fidelity Buffer (Roche), 1.25 U High Fidelity Enzyme (Roche), 200 µM dNTPs (Roche Diagnostic), 10 pmol primers and PCR-grade water (Roche). PCR amplification was performed as previously described (151). All PCR reactions were performed in triplicates. The amplification products were visually checked for quality on 1% agarose gel. Reactions resulting in a reliable PCR amplification were used further. Normalizations of the PCR products were performed using 15 µl of each pooled PCR products on a SequalPrep Normalization Plate (Life Technologies, Vienna, Austria) according to manufacturer's instructions. To introduce barcode sequences for each amplicon, 15ul of each normalized PCR product were used as the template in a 50 µl single reaction as described previously (152)**.** Cycling conditions were the same as for the 16S rRNA gene target with only eight cycles of amplification (151). Following the addition of index barcodes, 5 µl of each triplicate samples were pooled and 50 µl of the unpurified library was loaded onto a 1% agarose gel (Sigma–Aldrich). Products were then gel purified with the Qiaquick Gel Extraction Kit (Qiagen, Hilden, Germany) according to the manufacturer's instructions. Quantification of pooled products was performed with PicoGreen dsDNA reagent (Life Technologies) and visualized for size validation on an Agilent 2100 Bioanalyzer using a high sensitivity DNA assay (Agilent Technologies, Waldbronn, Germany). The sequencing library pool was resolved on a MiSeq desktop sequencer (Illumina, Eindhoven, Netherlands) and output FASTQ files were further processed for data analysis (1). 16S rRNA gene library preparation and sequencing was performed by me in collaboration with the core-facility Molecular biology at the center of medical research (ZMF), Graz, Austria.

7. Skin Microbiota analysis

The raw FASTQ files were processed with MOTHUR v.1.33.3 using the standard SOP of MOTHUR (153). Pyrosequencing errors were removed using pre.cluster (154)**.** UCHIME v.1.22 was used to remove chimeras (155). The Ribosomal Database Project (RDP) training set v.9 was used to remove non-bacterial contaminants (156). The high-quality reads were aligned to the SILVA database v.119 (157, 158). For operational taxonomic unit (OTU)-based analyses, the processed fasta files from MOTHUR were introduced into QIIME v.1.8.0 (159). OTUs were formed by clustering the sequences with UNCLUST (160), with a similarity score of 97% (OTU 97% identity). Taxonomy was assigned using the RDP classifier and Greengenes reference v.13.8. A *de novo* OTU picking strategy was employed. The biome file was further analyzed with the command core_diversity.py of QIIME. Differences in alpha-diversity measures were tested by unpaired t-tests with 999 Monte Carlo permutations while multiple comparison corrections were performed by the Bonferroni method. Principal coordinates analysis (PCoA) plots were created on the basis of a weighted-unifrac (161) distance matrix and statistical differences between groups were calculated with ANOSIM. Bacterial relative abundance was calculated using the Kruskal Wallis test with false discovery correction (FDR). The biomarker discovery program LEfSe (linear discriminant analysis effect size) was employed to determine differentially abundant OTUs. P-values ≤ 0.05 (* $p < 0.05$; ** $p < 0.01$; *** $p < 0.001$) were considered statistically significant. All presented values are always mean ± SD if not indicated otherwise. Batch files containing detailed parameters used in the analysis are specified in appendix 3. Heat maps were created on the basis of log(10)-transformed abundance data, which were obtained from OTU's with more than 1% overall abundance. The EzBioCloud database was used to assign species level taxonomy (162). Visualization and hierarchical clustering (hclust) were implemented in R using the heatmap.2 function provided by the gplots_3.0.1.1 package. Pearson correlation was used to calculate associations between assessed features which were computed with R 3.4.4 using the method corr.test implemented in the package psych vers.1.8.12 (163). The p-values were corrected using Holm correction to adjust for multiple comparisons (1, 164). Skin microbiota analysis was performed by Bettina Halwachs (MUG, Graz, Austria), Marija Durdevic (MUG, Graz, Austria), and I (MUG, Graz, Austria).

8. Quantitative real-time PCR

8.1. Quantitative real-time PCR (qRT-PCR) was performed with an ABI PRISM 7900HT instrument (Applied Biosystems) using SYBR Green PCR core reagents (Applied Biosystems). Amplification was carried out in a 96-well plate. Each reaction was run in triplicates in a 20µl reaction volume. For determination of bacterial load, the pan bacterial gene marker (16S rRNA gene) was used (165). A 16S rRNA gene region specific for the genus *Staphylococcus* was used (166, 167)**.** For specific detection of *S. aureus*, the thermostable nuclease gene (*nuc A*) was used (168, 169). For specific detection of *Staphylococcus epidermidis*, *the g*lutamic acid-specific serine protease (*GluSE*) was employed *(166, 170, 171)*. PCR amplification specific for amplification of the genus *Streptococcus*, the elongation factor Tu (*tuf*) gene was employed. To determine the loads of *P. acnes*, a specific region of the 16S rRNA gene was amplified (172)**.** 20ng of total DNA was used as a normalized input for real-time PCR amplification of bacterial targets from skin samples. The oligonucleotide primer sequences are indicated in the supplementary material (Appendix 4). Reaction mixtures were incubated for 10 min at 95 °C, followed by 40 cycles of 15 s at 95 °C and 1 min at the respective annealing temperatures (i.e., 16s pan-bacterial: 55°C, *Staphylococcus* and *S. aureus*: 62°C, *S. epidermidis, Streptococcus, P. acnes*: 60°C) and a final step for 15s at 95°C, 1 min at 60°C and 15s at 95°C. Each PCR reaction was performed in triplicates (1).

8.2. 50ng of the total DNA isolated from colon FFPE samples were used to amplify *Fusobacterium* species, *Fusobacterium nucleatum* and the gene for FadA. The oligonucleotide primer sequences are indicated in the supplementary material (Appendix 4). qRT-PCR was performed with an ABI PRISM 7900HT instrument (Applied Biosystems) using SYBR Green PCR core reagents (Applied Biosystems). Amplification was carried out in a 96-well plate. Each reaction was run in triplicates in a 20µl reaction volume. Reaction mixtures were incubated for 10 min at 95 °C, followed by 40 cycles of 15 s at 95 °C, 1 min at 55°C and finally 15s at 95°C, 1 min at 60°C and 15s at 95°C.

8.3. Fungal DNA amplification was performed on extracted DNA from FFPE skin samples and the ITS1 (ITS1-F CTTGGTCATTTAGAGGAAGTAA and ITS2-R

GCTGCGTTCTTCATCGATGC) and ITS2 (ITS3-F GCATCGATGAAGAACGCAGC and ITS4-R TCCTCCGCTTATTGATATGC) regions were targeted. Quantitative real-time PCR was performed on a CFX96 detection system (Bio-rad, Munich, Germany) using the LuminoCt® SYBR® Green qPCR ReadyMix™ (Sigma-Aldrich, Steinheim, Germany). The PCR reaction mixtures contained 50ng of total DNA in each reaction in a total volume of 20 µl. The amplification program consisted of 3 mins at 95^0C, followed by 40 cycles of 5s at 95^0C, 15 s at 51^0C and finally a melting curve analysis by gradually increasing the temperature by 0.5^0C, from 65^0C to 95^0C with simultaneous recording of fluorescence signals. Each PCR reaction was performed in triplicates. The CT values obtained for the samples were subtracted from the no template control (△ CT)(2).

9. Reverse transcription quantitative PCR (RT-qPCR)

9.1. Total RNA was extracted from FFPE skin samples; 10 sections, with 5 µm in thickness from each FFPE sample served as input and were first deparaffinized using a deparaffinization solution (Qiagen). RNA isolation was then performed by using the RNeasy FFPE kit according to the manufacturer's protocol, which also includes a DNase digestion step (Qiagen). 200ng of extracted total RNA served as input for cDNA synthesis using the GeneAmp RNA PCR kit (Thermo Fischer Scientific) according to the manufacturer's instructions for FFPE samples. RNA quality and quantity were determined spectrophotometrically using a NanoDrop instrument (ThermoScientific). qPCR was performed with an ABI PRISM 7900HT instrument (Applied Biosystems) and the SYBR Green PCR core reagents (Applied Biosystems). Reaction mixtures were set up as described above. Each PCR reaction was performed in triplicates (1).

9.2. RNA from cell culture experiments challenged with bacteria were extracted using the PeqGOLD total RNA Kit (Peqlab, Erlangen, Germany) and transcribed into cDNA with the Transcriptor First Strand cDNA Synthesis Kit (Roche Life Science, Indianapolis, IN, USA). qRT-PCR for these samples were performed using SYBR green PCR master mix (Sigma) on the StepOnePlus Real-Time PCR system (Applied Biosystems) (1). The oligonucleotide primer sequences for measurements of antimicrobial peptide expressions (hBD-1, -2, -3, RNase 7 and psoriasis) (173-176) are shown in appendix 4. For each mRNA target, the expression level was normalized using the beta-actin gene

(ACTB) as a reference and relative quantification was calculated by the ΔΔCt method (1, 177).

10. Fluorescent *In Situ* Hybridization (FISH)

A modified method of a previously described FISH protocol was employed (178, 179). 5 µm thick sections of skin FFPE samples were placed on adhesive super frost slides (DAKO FLEX slides, Sigma Aldrich). The slides were first incubated at 70°C for 1 hour in a non-CO2 incubator followed by 2 times for 10 mins in Xylene (Sigma Aldrich) for deparaffinization. Subsequently, slides were incubated for 5 mins in 100% ethanol and air-dried. Next, the slides were dehydrated using 50%, 80% and 99% ethanol for 3 mins each. Before hybridization, each section was pretreated with lysozyme (20mg/ml) (Carl Roth) (180) by incubation for 30 min at 37°C, followed by incubation in lysostaphin (1mg/ml) (Sigma Aldrich) for another 30 min at 37°C. The reaction was stopped by absolute methanol for 1 min at RT. The positive and negative control slides contained fixed *E. coli*, *S. epidermidis*, and *S. aureus* cells derived from bacterial culture. Hybridization of FISH probes was performed as described earlier with slight modifications (178, 179). Briefly, samples were first incubated with the hybridization buffer containing 20% (v/v) formamide (PanReac AppliChem, Barcelona, Spain), 20 mmol/L Tris-HCl pH7 (AMRESCO, OH, USA), 2% (w/v) sodium dodecyl sulfate (Sigma), 0.9 M NaCl (VWR Chemicals, Pennsylvania, USA) for 15 min at 46°C. A mixture of probes was then added to the slides (50 ng of each probe) encompassing a Cy3-labeled EUB338/I probe (38) directed against bacteria and a Cy5-labelled Sau probe for *S. aureus* (181)**.** A Cy3-labeled NONEUB-probe was used as a nonsense negative control. All probe sequences are given in table 6. The slides were transferred to the humid chamber and incubated for 2h at 46°C. After incubation, the slides were washed at 46°C for 15 min. The washing solution was preheated at 48°C and contained 10 mM Tris/HCl (AMRESCO) at pH 7, 0.225 M NaCl (VWR Chemicals), and 2% sodium dodecyl sulfate (Sigma). The slides were washed again with cold water and dried at room temperature before being counterstained with DAPI (Sigma Aldrich). Slides were analyzed using the Zeiss LSM 510 confocal microscope (Carl Zeis, Jena, Germany). Fluorescence microscopy was performed using the following filters with excitation and emission as follows: DAPI (358nm/ 463nm), CY3 (549nm/562nm) and CY5 (646nm/664nm) (1). FISH signals were scored according the following system: 0 = no signal, 1 = single signals, 2 = small groups of signals, 3 = large clusters of signals (1).

Gene	Gene name	Dye	Sequence (5' to 3')	Reference
EUB338/I	16S ribosomal RNA (338–355)	Cy3	GCTGCCTCCCGTAGGAGT	(38)
Sau	16S ribosomal RNA (*Staphylococcus aureus*)	Cy5	GAAGCAAGCTTCTCGTCCG	(181)
NONEUB		Cy3	ACTCCTACGGGA GGC AGC	(38)

Table 6. Probes used for FISH analysis

11. Cell culture and infection assay

Staphylococcus aureus (DSM799, DSM11823 and DSM1104) and *S. epidermidis* (Hyg9209-15) strains were cultured under aerobic conditions on Columbia blood agar plates (BioMerieux, Marcy l'Etoile France) at 37^0C for 24hrs (1). Human cutaneous squamous cell carcinoma cells HSC-1 (Human cutaneous squamous cell carcinoma) and SCL-1 (182, 183) were kindly provided by J C Becker, DKFZ, Essen, Germany. The human keratinocyte cell line HaCaT (183) were obtained from ZMF, Medical University of Graz, Austria. 2 x 10^5 cells were seeded per well in six-well plates in 2 ml of Dulbecco's modified Eagle's medium (DMEM) low glucose (1g/l) (GE Healthcare, Vienna, Austria) containing 10% fetal bovine serum (FBS) (Thermo Fischer Scientific) and grown to 80% confluence in a water-saturated atmosphere of 95% air and 5% CO_2 at 37^0C. Prior to the infection assay, a single colony of *S. aureus* was inoculated into a 100-ml culture flask containing 30 ml of DMEM low glucose (1g/l) with 1.5% FBS corresponding to an OD_{600nm} of 0.03. The culture was incubated with gentle agitation (160 rpm) at 37^oC for 14 hrs. Subsequently, HSC-1 cells were infected with *S. aureus* at a multiplicity of infection (MOI) of 1:2, 1:20 & 1:50 for 24 h (74). After 24 hours, the cells were collected using the lysis buffer from the PeqGOLD total RNA Kit (Peqlab, Erlangen, Germany) for RNA isolation (74). Simultaneously the supernatant was collected to assess the growth (cfu/ml) of bacteria after 24hrs infection. Bacterial colony forming units (CFU) were determined by serial dilution and plating on Columbia blood agar plates (BioMerieux). Experiments were repeated three times. Simultaneously, viability, apoptosis and cell numbers were determined by flow cytometry (1).

12. Flow cytometry

HSC-1, SCL-1 and HaCaT cells were harvested after 24 hrs of infection using trypsin (Thermo Fischer Scientific) for cell viability and apoptosis measurements. For this purpose, 7-AAD viability staining solution (eBioscience, CA, USA) or the Annexin V Apoptosis Detection Kit APC (eBioscience) were used following the manufacturer's protocol. Cells were analyzed using the CytoFLEX flow cytometer (Beckman Coulter, California, USA) and results were calculated using CytExpert Software (Beckman Coulter) (184). Each experiment was repeated three times (1).

13. CCK-8 assay

1 x 10^4 cells/well of HSC-1 and SCL-1 cells were plated in 96-well plates in a water-saturated atmosphere of 95% air and 5% CO_2 at 37^0C overnight. The cells were then treated with 20 µg/ml of hBD-1, -2 & -3 (PeptaNova, Sandhausen, Germany) for 24 hours (98). Subsequently, cell proliferation was evaluated using the CCK-8 kit (Sigma-Aldrich) after 24 hrs of treatment according to a published protocol (115). The absorbance was measured at 450 nm using a SPECTROstar Omega microplate reader (BMG Labtech, Offenburg, Germany)(1).

14. xCELLigence real-time cell proliferation assay

The xCELLigence Real-Time Cellular Analysis (RTCA) system (Roche and ACEA Biosciences) was used to monitor cell proliferation, using impedance as the readout. The impedance measurement, displayed as cell index (CI), takes into account cell number, viability and morphology of cells. 1 x 10^4 HSC-1 or SCL-1 cells were treated with 20 µg/mL hBD-1, -2 & -3 (115) and seeded in DMEM low glucose (1g/l) with 1.5% FBS in E-plates "16" (ACEA Biosciences). Proliferation was monitored every 15 min by the xCELLigence system (185) for up to 24 hours. Growth curves were normalized to the time point of cell adherence (~4 h). Evaluations were performed using xCELLigence 1.2.1 software (ACEA Biosciences). Each experiment was repeated three times (1).

15. Statistical analysis

Quantitative PCR and cell proliferation data were assessed with the Shapiro-Wilk normality test for their normal distribution. Data are given as mean $\pm$ standard error of mean if not

specified otherwise. Statistical analyses were performed with GraphPad Prism 5 software. P-Values < 0.05 were considered to be statistically significant (1).

16. Data deposition

The sequencing data generated for this study is available on EBI short read archive (EBI SRA) with the accession number PRJEB23563 (1).

17. Ethics Statement

The usage of human tissue specimens was approved by the institutional review board of the Medical University of Graz (24-167ex11/12; 25-293ex12/13) (1).

V. Results

Cancer development is a sequential process; wherein invasive tumors arise from non-invasive lesions. This stepwise process also alters the host-microbiome equilibrium, i.e. the microbes colonizing the (pre-)neoplastic epithelia which is also mirrored by an alteration of the local immunological environment. Thus, we studied the microbiome of pre-invasive neoplastic lesions (AK / adenomatous polyp) with invasive lesions of cSCC (part 1) and CRC (part 2) respectively. Also, the role skin microbiome plays in cSCC promotion was assessed (part 1). Additionally, methodological optimization for microbial community analyses was performed for bacteria (part 1) and fungi (part 3) from skin FFPE samples.

Parts of results and figures used are adopted according to the published manuscripts: Madhusudhan, Pausan (1) and Halwachs, Madhusudhan (2).

Part 1:

Published in https://doi.org/10.3390/cancers12030541

1. Molecular profiling of keratinocyte skin tumors links *Staphylococcus aureus* overabundance and increased Human β-Defensin-2 expression to growth promotion of squamous cell carcinoma

In total 88 skin samples originating from sun exposed skin sites representing excised tissue specimens (total excision: n=54; punch biopsies: n=24; shave biopsies: n=10) were used for the study. These consisted of 60 tumor samples (25 AKs, 22 SCCs & 13 BCCs) and 28 skin samples without neoplasia which consisted of healthy skin, non-neoplastic skin adjacent to tumor and psoriasis samples which served as controls (1).

1.1. Skin habitat change in AK and SCC is associated with microbial colonization

During neoplasia development, skin undergoes significant alterations in architecture which in turn leads to a change in the microbial habitat. A histological hallmark of AK & SCC is hyper- and parakeratosis characterized by increased lamellar keratin on the lesional surface. Especially in AK & SCC hyper- and parakeratosis are prominent features, whereas in BCC it is less pronounced (Figure 11) (1).

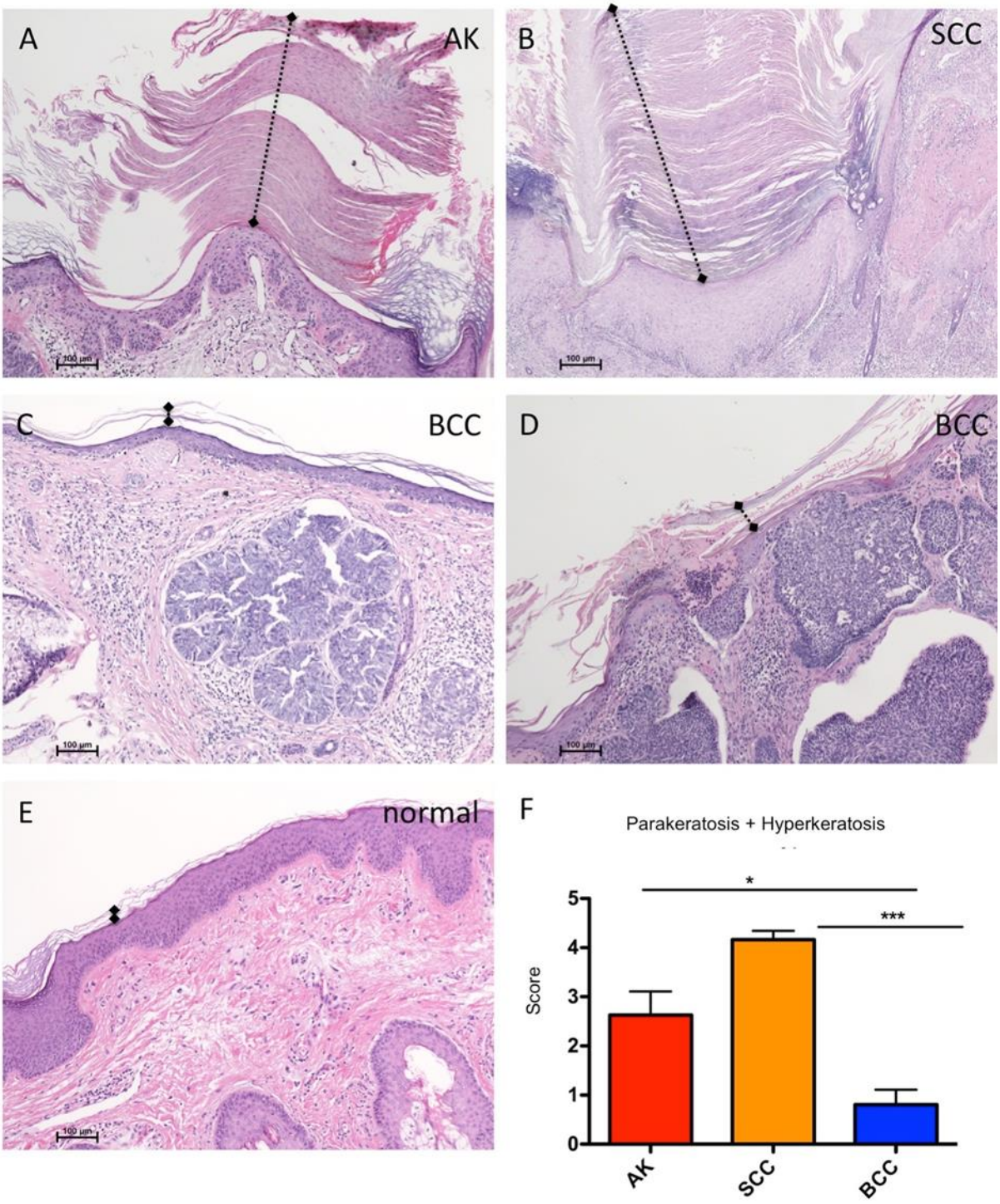

Figure 11. Hyper- and parakeratosis are associated with AK and SCC. Dotted lines represent the keratin layer. (A& B) H & E staining representing excessive production of layered keratin in AK (A) & SCC (B), while BCC (C, D) shows no or sparse hyper-or parakeratosis. (E) Healthy normal skin originating from chest is used for comparison. (D) Microscopic scoring of hyper- and parakeratosis indicating prevalence in AK and SCC (*p< 0.05; ***p<

0.005, Kruskal Wallis test; Dunn's multiple comparison test; AK, n=12; SCC, n=12; BCC, n=13). Adopted from (1).

Microscopy revealed numerous microbial structures associated with hyper- and parakeratotic areas in AK and SCC (Figure 12 A-C) (1). Abundant microbial structures were not only present on the lesional surface of AK and SCC, but also in deeper (invasive) parts of tumor tissue in SCC (Figure 12C). Interestingly, microbial structures often appeared as clusters of cocci (Figure 12 D-E). These observations were only rarely detected in BCC and normal skin.

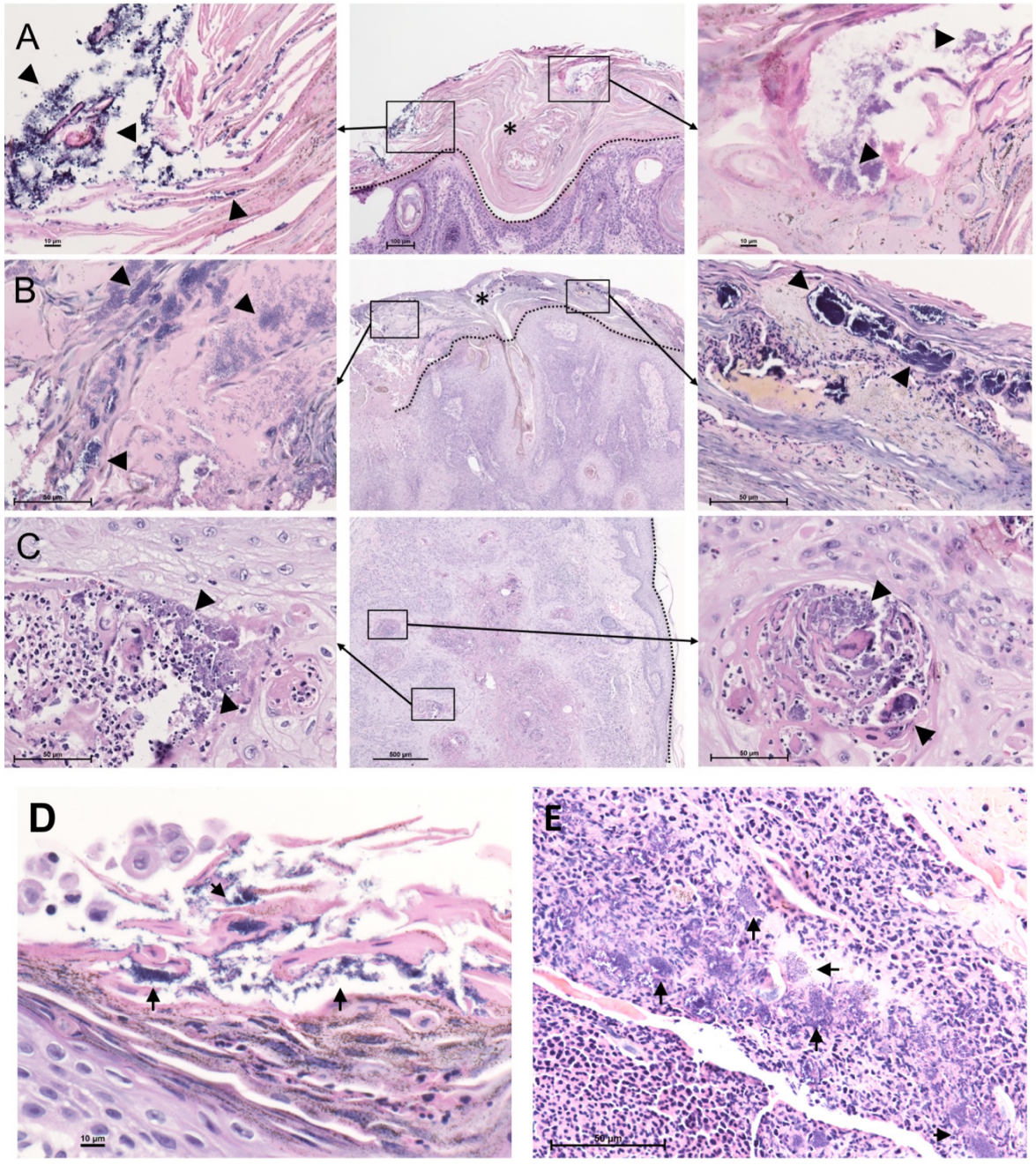

Figure 12. Increased microbial biomass associated with hyper- and parakeratosis in AK and SCC. Abundant microbial structures in AK (A) and SCC (B) associated with hyperkeratosis (marked with * in panels A-B). Microbes are not just present on the surface but also emerge in deeper layers of invasive SCC (C). The dotted lines specify the skin surface (D and E). Coccoid bacteria are associated with hyper and parakeratosis regions in AK & SCC. Adopted from (1).

Microbial structures mainly resembled bacteria and to a lesser extent also fungi, which were microscopically differentiated based on morphology and staining pattern (refer materials and methods for details) (Figure 13 A-F). These structures were microscopically scored indicating a significant increase of bacteria in AKs & SCCs compared to BCC and normal skin (Figure 13 G). Also, fungi were increased in AK (Figure 13 H)(1).

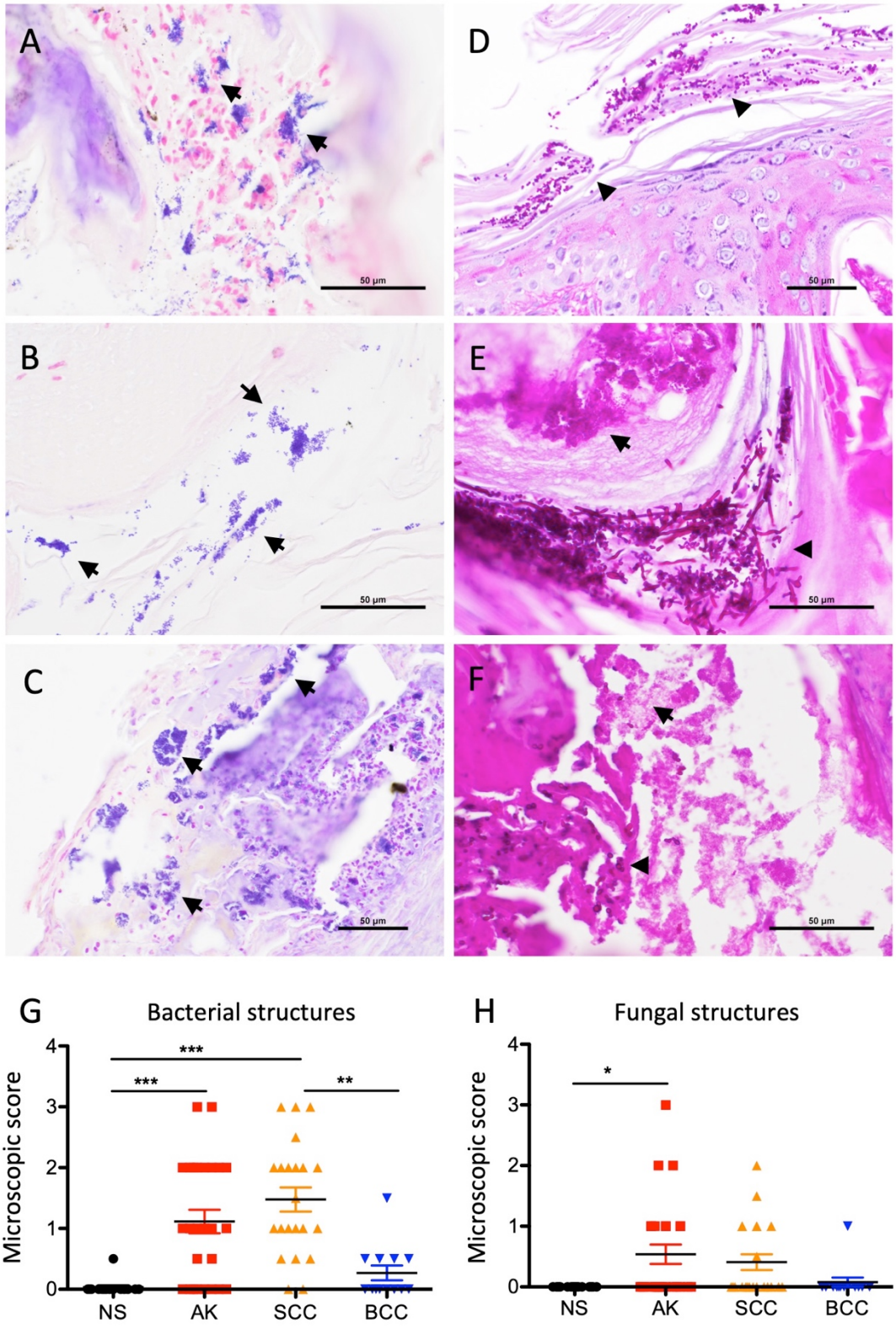
A
D
B
E
C
F
50 µm
G
Bacterial structures
Microscopic score
***
***
**
NS
AK
SCC
BCC
H
Fungal structures
Microscopic score
*
NS
AK
SCC
BCC

Figure 13. Bacterial and fungal structures in AK and SCC. (A-F) Bacterial (arrows) and fungal (arrow heads) structures in AK (A, D, E) and SCC (B, C, F) specimens (A-C: Gram stain; D-F: PAS stain). (G) Microscopic scoring indicates significantly increased bacterial structures in AK and SCC compared to basal cell carcinoma (BCC) and NS (normal skin) samples (** $p < 0.01$; *** $p < 0.005$; Kruskal–Wallis test; Dunn's multiple comparison test). (H) Increased fungal structures in AK samples (* $p < 0.05$; Kruskal–Wallis test; Dunn's multiple comparison test). Adopted from (1).

1.2. Keratinocyte skin tumors show a different microbial community type with increased *Staphylococcus* abundance in AK & SCC.

Microbial communities are modified in neoplastic tissue (91). To investigate alterations in microbial composition in keratinocyte tumors, AK (n=12), SCC (n=12) and BCC (n=13) specimens were subjected to comparative microbiota analysis using 16S rRNA gene-based microbial community profiling. 8 normal skin specimens were included as controls.

First, we optimized the DNA isolation procedure to maximize the output of microbial DNA from skin FFPE samples.

1.2.1. Optimization of microbial DNA extraction from FFPE skin samples

We compared DNA yield and amplification of skin samples extracted with 2 different DNA isolation kits: the QIAamp DNA FFPE tissue kit and the Maxwell 16 FFPE Plus LEV DNA purification kit. Two additional steps viz mechanical disruption and enzymatic lysis were added sequentially to this extraction procedure. Maxwell DNA purification kit together with both mechanical and enzymatic lysis turned out to be the most efficient method in terms of DNA yield and amplification in the extracted samples. This method yielded higher microbial abundance as measured using pan-bacteria specific primers (Figure 14 A) and higher detectable levels of *P. acnes* as measured by *P. acnes* specific primers (Figure 14 B) (Appendix 4 for sequence) in comparison to QIAamp DNA FFPE kit alone or in combination with the lysis steps (Figure 14)(1).

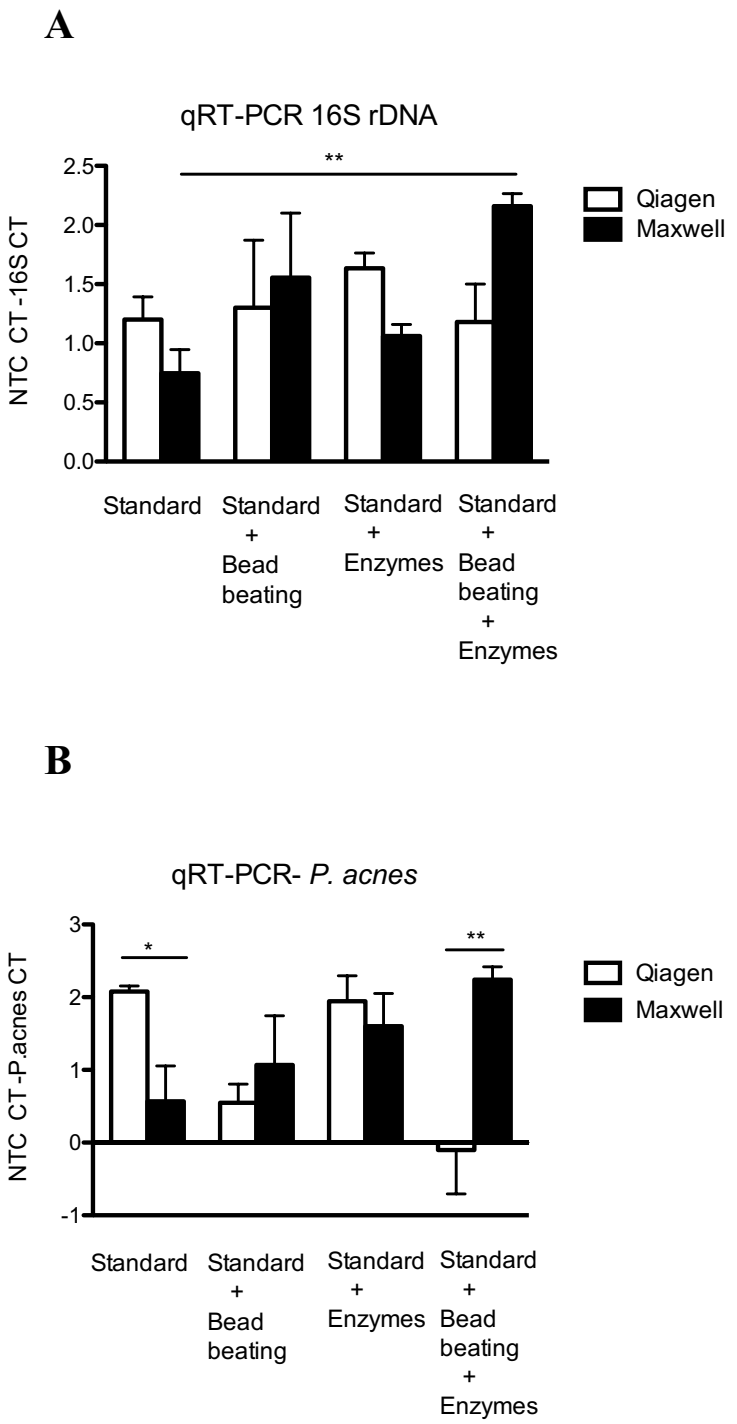

Figure 14. Optimization of DNA extraction for skin FFPE specimens. Two commercially available kits were compared with sequential addition of bead-beating and enzymes. Real-time PCR was used to determine DNA yield and amplification using pan-bacterial (A) and *P. acnes* (B) specific primers (n=3, *p<0.05, **p<0.01, one-way ANOVA, Bonferroni correction). Adopted from (1).

Since Maxwell 16 FFPE Plus LEV DNA purification kit proved superior, we then checked for 16S rRNA gene specificity and sensitivity of the extracted samples from this method (Figure 15). The V1-2 region of the 16S rRNA gene was amplified via PCR using oligonucleotide primers 27F and 357R. 5 µl of input DNA (~15 ng/µl) containing 1X Fast Start High Fidelity Buffer (Roche), 1.25 U High Fidelity Enzyme (Roche), 200 µM dNTPs (Roche), 10 pmol primers and PCR grade water (Roche) to a final volume of 25 µl. Triplicates from each sample were pooled and the amplicons were checked visually on 1% agarose gels. Specific PCR products (molecular weight ~400bp) were generated from the skin tumor entities (Lane 2-13) (Figure 15), while a faint or no band was observed in the three negative controls (blank extraction, paraffin extraction and no template control) (Lane 14-16) (Figure 15).

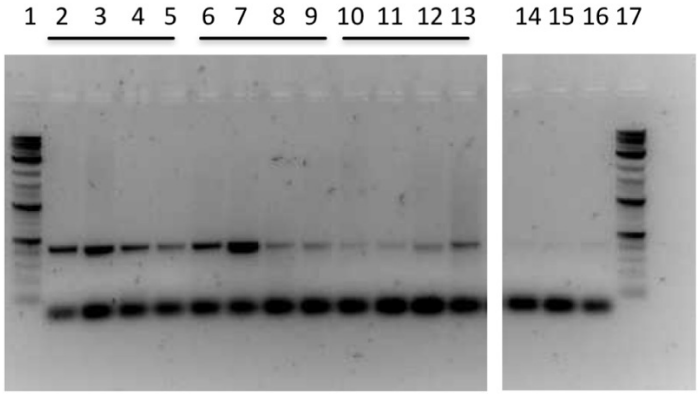

LANE	SAMPLE
1	Ladder
2-5	Aktinic Keratosis
6-9	Squamous Cell Carcinoma
10-13	Basal Cell Carcinoma
14	NTC
15	Blank extraction
16	Paraffin extraction
17	Ladder

Figure 15. Agarose gel electrophoresis of the PCR products amplified with 27F and 357R primers (16S V1-2 region) with DNA extracted from Maxwell 16 FFPE Plus LEV DNA purification kit of AK, SCC & BCC tumor entities along with negative control for specificity.

1.2.2. Different microbial community types in keratinocyte skin tumors

To classify the microbes associated with different skin tumors, we subjected surgically removed tumor specimens to comparative microbiota analysis. A subset of AK (n = 12), SCC (n = 12), and BCC (n = 13) samples were used for this analysis. In addition, 8 normal skin specimens were included. The variable V1-2 region of the bacterial 16S rRNA gene was amplified by PCR and products were resolved on an Illumina TM Miseq next generation sequencer. 16S rRNA gene library preparation and sequencing was performed by me in

collaboration with the core-facility Molecular biology at the center of medical research (ZMF), Graz, Austria.

A total of 17,747,248 reads were generated which corresponds to 199,630 ± 132,100 reads per sample on average. The data set was denoised, quality filtered and analyzed using MOTHUR and QIIME. 117±37 operational taxonomic units (OTU, 97% ID) were generated per sample on average. Skin microbiota analysis was performed by Bettina Halwachs (MUG, Graz, Austria), Marija Durdevic (MUG, Graz, Austria), and I (MUG, Graz, Austria).
Microbial richness, which measures the total number of taxa detected in the respective samples, was significantly higher in AK and SCC compared to BCC (Figure 16A). In contrast, diversity and evenness, which are measures of how diverse a microbial community is and how equally the number of each taxon are distributed respectively, were significantly lower in AK & SCC compared to BCC (Figure 16 A-C). A scheme summarizing the results of richness, evenness and diversity is represented in figure 16D. From these findings, it could be hypothesized that certain taxa are overrepresented in AK & SCC leading to an uneven community composition, which could potentially represent driver bacteria of neoplasia development (1).

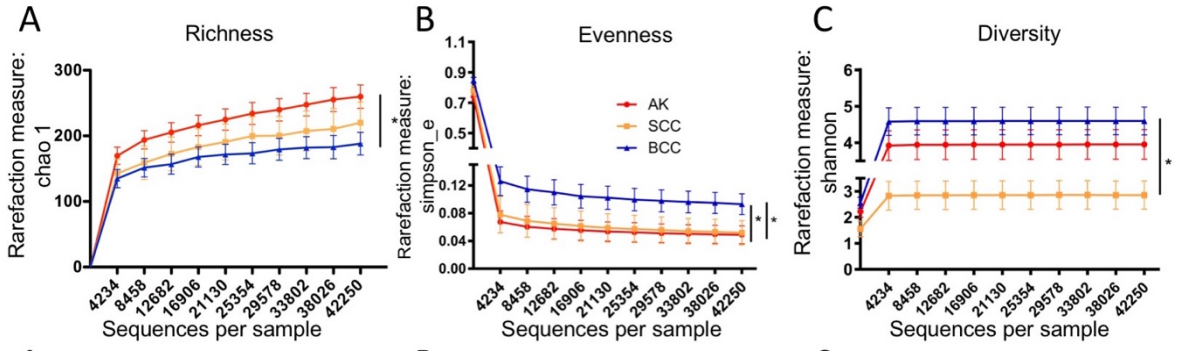

D

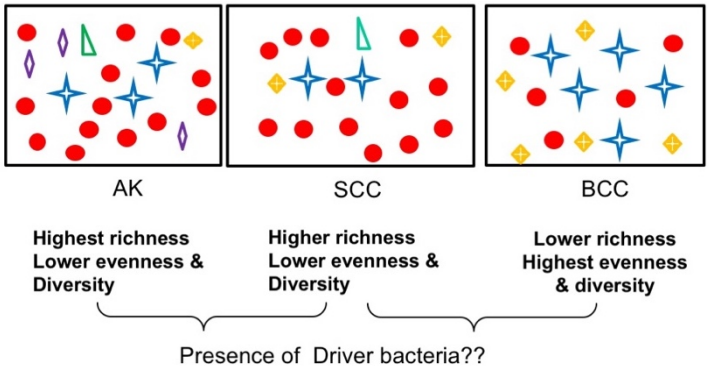

Figure 16. Microbial community type differs in keratinocyte skin tumors (A) Microbial richness was significantly higher (Chao 1; $p<0.05$) but (B) evenness (Simpson index; $p<0.05$) and (C) diversity (Shannon index; $p<0.05$) were significantly lower in AK & SCC compared to BCC (unpaired t-test). (D) Scheme indicating the results of microbial richness, evenness and diversity in AK, SCC & BCC. Adopted from (1).

Interestingly, alpha diversity measures (richness, evenness and diversity) were significantly different between healthy skin and all keratinocyte tumors (AK, SCC &BCC) (Figure 17 A-C) (1).

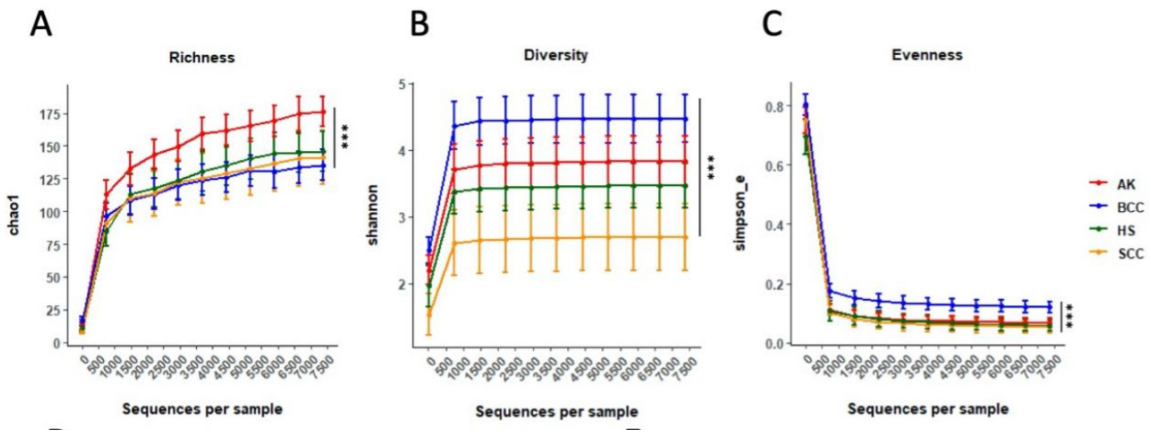

Figure 17. Healthy skin and skin tumors exhibit different microbial community types. (A-C): Microbial richness as measured by Chao1, diversity as assessed by Shannon and evenness as measured by Simpson were significantly different between all groups (Kruskal-Wallis rank- sum test; $p < 0.0001$). Adopted from (1).

Principal coordinate analysis PCoA (measure: weighted unifrac distance) performed in a pairwise fashion on tumor samples showed significantly different microbial community structures in AK & SCC in comparison to BCC, whereas no significant difference in the microbial community structure was observed between AK & SCC samples (Figure 18 A-C). This indicates that more similar microbial community types are prevalent between AK & SCC in comparison to BCC (1).

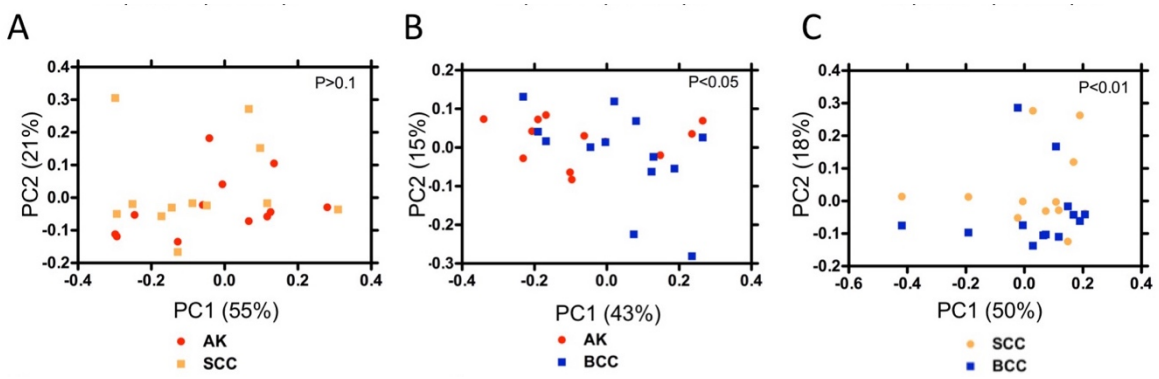

Figure 18. Microbial community type differs in keratinocyte skin tumors. (A-C) Principal coordinate analysis indicates significantly different microbial communities in AK & SCC compared to BCC (measure: weighted unifrac; ANOSIM; $p<0.05$). Adopted from (1).

However, significantly different microbial communities were identified in all sample types (healthy skin and skin tumor samples) as assessed by PCoA analysis (Fig 19 A-B)(1).

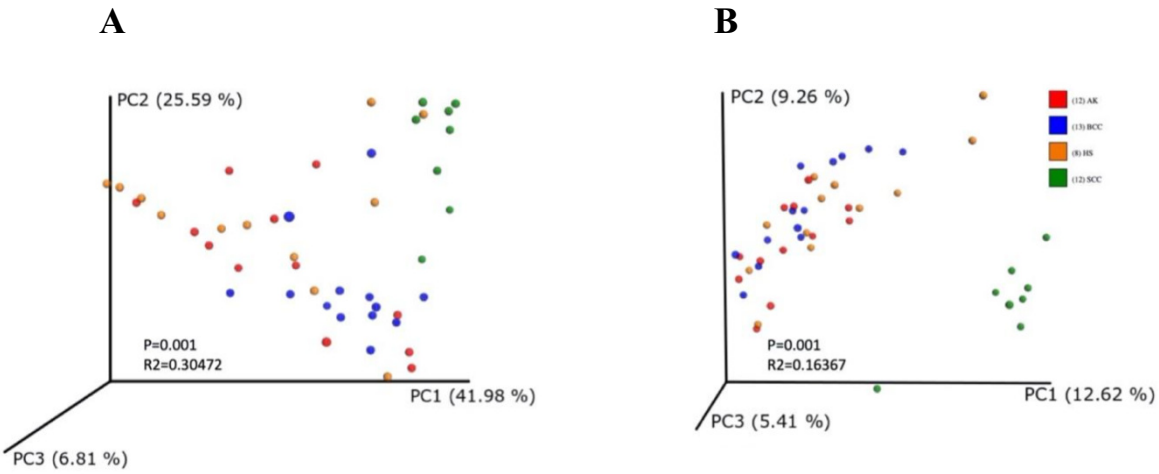

Figure 19. Healthy skin and skin tumors exhibit different microbial community type. PCoA analysis (A-B) of healthy skin and skin tumor samples showed significantly different microbial communities in all 4 entities as measured by weighted unifrac (A) and unweighted unifrac (B) (measure: ANOISM). Adopted from (1).

Next, we assessed which microbes are specifically associated with tumor entities. At phylum level, a significant decrease in the phyla *Proteobacteria* and *Bacteroidetes* in SCC compared to BCC were evident (Figure 20 A). At the genus level, a significantly higher relative

abundance of *Staphylococcus* in AK & SCC as compared to BCC was observed, while a significant increase in *Streptococcus* was seen in BCC (Figure 20 B). Next, we determined which microbes are specifically associated with healthy skin along with skin tumors at the genus level and significantly different relative abundance of *Staphylococcus*, *Streptococcus*, *Propionibacterium* and *Bacteroides* were detected (Figure 20 C)(1).

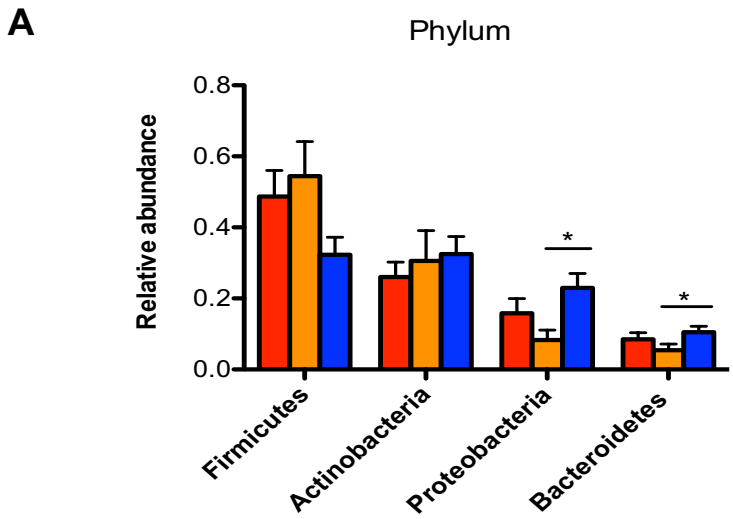

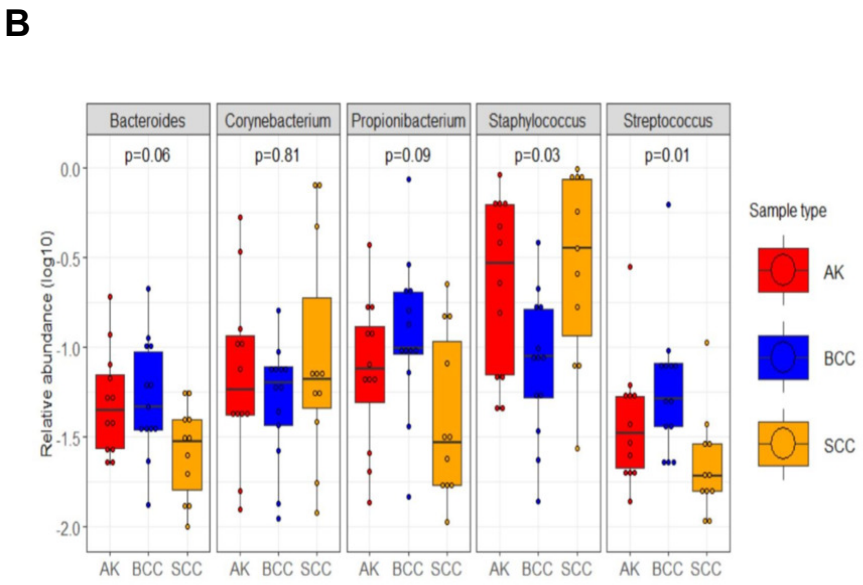

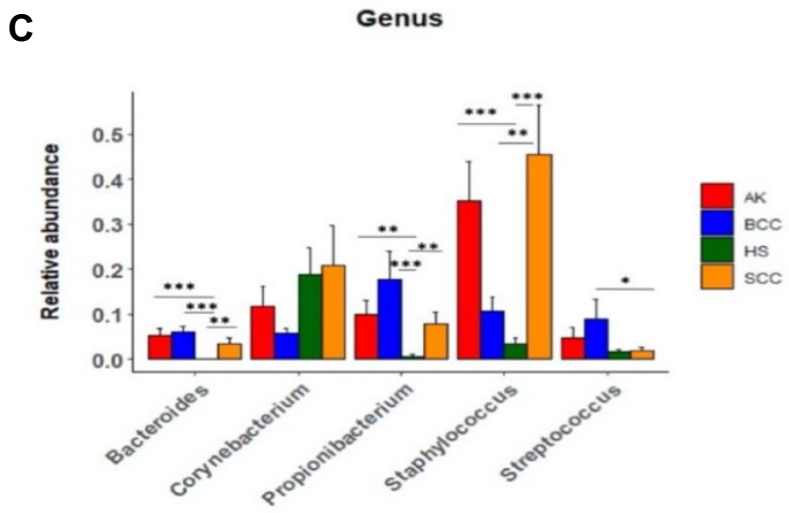

Figure 20. Relative abundance of most abundant taxa in skin tumor and healthy skin entities. (A) Relative abundance of the phyla *Proteobacteria* and *Bacteroidetes* were significantly lower in SCC compared to BCC ($p<0.05$; Kruskal Wallis); (B) Differential abundant taxa of log(10)-transformed read data identifies significantly increased *Staphylococcus* in AK and SCC compared to BCC and significantly increased *Streptococcus* in BCC compared to SCC (Kruskal Wallis) (C) Significantly different relative abundance of *Staphylococcus*, *Streptococcus*, *Propionibacterium* and *Bacteroides* in skin tumors and healthy skin (Dunn's post hoc test, Benjamini- Hochberg correction; **$p<0.01$; **$p<0.01$; ***$p<0.005$). Adopted from (1).

Additionally, comparative linear discriminant analysis effect size (LEfSe) analysis confirmed the increased relative abundance of *Staphylococcus* based on the linear discriminant analysis (LDA) score in SCCs (LDA > 5; 50.07± 14.43%) and AKs (38.62 ±14.05%) while *Streptococcus* was significantly higher in BCC (LDA >4; 17.42 ± 10.51%) (Figure 21 A-B). Other differentially abundant taxa were revealed by LEfSe analysis, which were mainly associated with BCC like *Betaproteobacteria* and *Bacteroidetes*, although their overall relative abundance was low. Healthy skin showed significantly increased *Streptomyces* compared to keratinocyte tumors in the LEfSe analysis (Figure 22A-B). A complete list of taxa specified by LEfSe analysis is shown in appendix 5 and 6 (1).

A

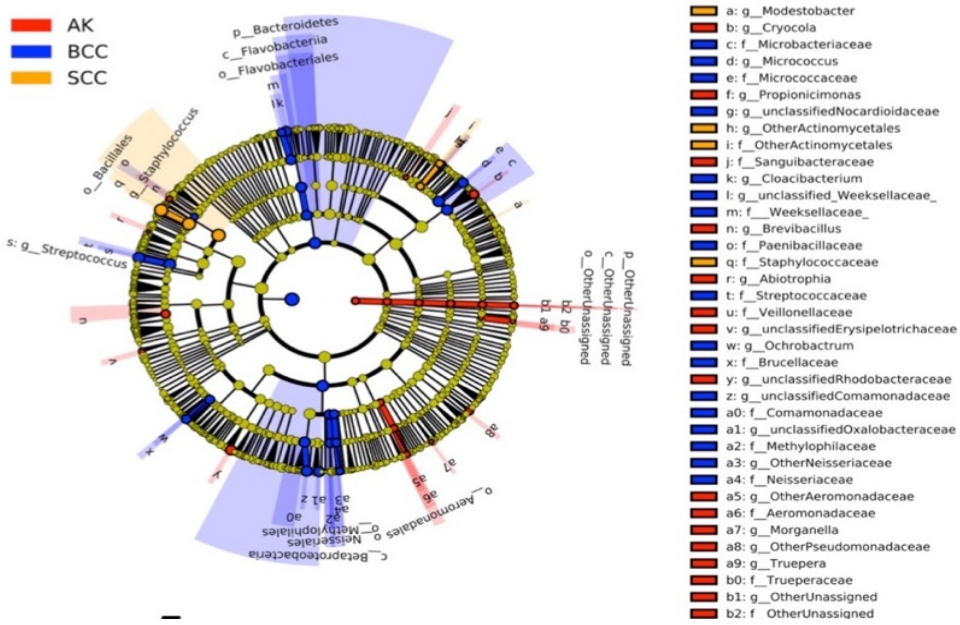
AK
BCC
SCC
p__Bacteroidetes
c__Flavobacteriia
o__Flavobacteriales
o__Bacillales
f__Staphylococcaceae
s: g__Streptococcus
p__OtherUnassigned
c__OtherUnassigned
o__OtherUnassigned
c__Betaproteobacteria
o__Neisseriales
o__Methylophilales
o__Aeromonadales
a: g__Modestobacter
b: g__Cryocola
c: f__Microbacteriaceae
d: g__Micrococcus
e: f__Micrococcaceae
f: g__Propionicimonas
g: g__unclassifiedNocardioidaceae
h: g__OtherActinomycetales
i: f__OtherActinomycetales
j: f__Sanguibacteraceae
k: g__Cloacibacterium
l: g__unclassified_Weeksellaceae_
m: f__Weeksellaceae_
n: g__Brevibacillus
o: f__Paenibacillaceae
q: f__Staphylococcaceae
r: g__Abiotrophia
t: f__Streptococcaceae
u: f__Veillonellaceae
v: g__unclassifiedErysipelotrichaceae
w: g__Ochrobactrum
x: f__Brucellaceae
y: g__unclassifiedRhodobacteraceae
z: g__unclassifiedComamonadaceae
a0: f__Comamonadaceae
a1: g__unclassifiedOxalobacteraceae
a2: f__Methylophilaceae
a3: g__OtherNeisseriaceae
a4: f__Neisseriaceae
a5: g__OtherAeromonadaceae
a6: f__Aeromonadaceae
a7: g__Morganella
a8: g__OtherPseudomonadaceae
a9: g__Truepera
b0: f__Trueperaceae
b1: g__OtherUnassigned
b2: f__OtherUnassigned

B

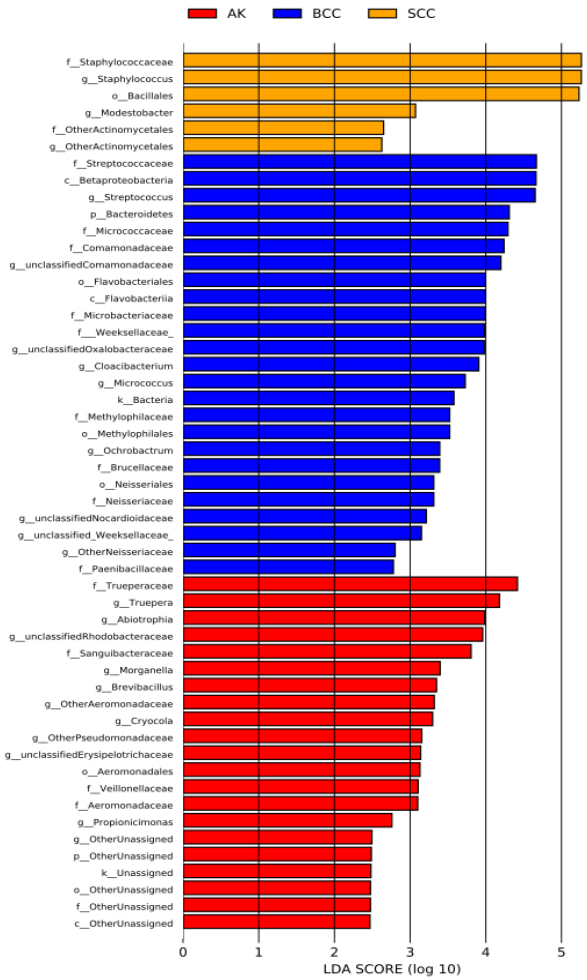
AK
BCC
SCC
f__Staphylococcaceae
g__Staphylococcus
o__Bacillales
g__Modestobacter
f__OtherActinomycetales
g__OtherActinomycetales
f__Streptococcaceae
c__Betaproteobacteria
g__Streptococcus
p__Bacteroidetes
f__Micrococcaceae
f__Comamonadaceae
g__unclassifiedComamonadaceae
o__Flavobacteriales
c__Flavobacteriia
f__Microbacteriaceae
f__Weeksellaceae_
g__unclassifiedOxalobacteraceae
g__Cloacibacterium
g__Micrococcus
k__Bacteria
f__Methylophilaceae
o__Methylophilales
g__Ochrobactrum
f__Brucellaceae
o__Neisseriales
f__Neisseriaceae
g__unclassifiedNocardioidaceae
g__unclassified_Weeksellaceae_
g__OtherNeisseriaceae
f__Paenibacillaceae
f__Trueperaceae
g__Truepera
g__Abiotrophia
g__unclassifiedRhodobacteraceae
f__Sanguibacteraceae
g__Morganella
g__Brevibacillus
g__OtherAeromonadaceae
g__Cryocola
g__OtherPseudomonadaceae
g__unclassifiedErysipelotrichaceae
o__Aeromonadales
f__Veillonellaceae
f__Aeromonadaceae
g__Propionicimonas
g__OtherUnassigned
p__OtherUnassigned
k__Unassigned
o__OtherUnassigned
f__OtherUnassigned
c__OtherUnassigned
0
1
2
3
4
5
LDA SCORE (log 10)

Figure 21. LEfSe analysis describing taxa with increased relative abundance in keratinocyte skin tumors. (A) The association of *Staphylococcus* with LDA>5 with SCC, *Streptococcus* with LDA >4 and *Betaproteobacteria* with LDA > 4 with BCC is emphasized. (B) LEfSe output signifying the differentially abundant taxa and respective LDA scores. Tabular representation of the LEfSe output is given in Table. Adopted from (1).

A

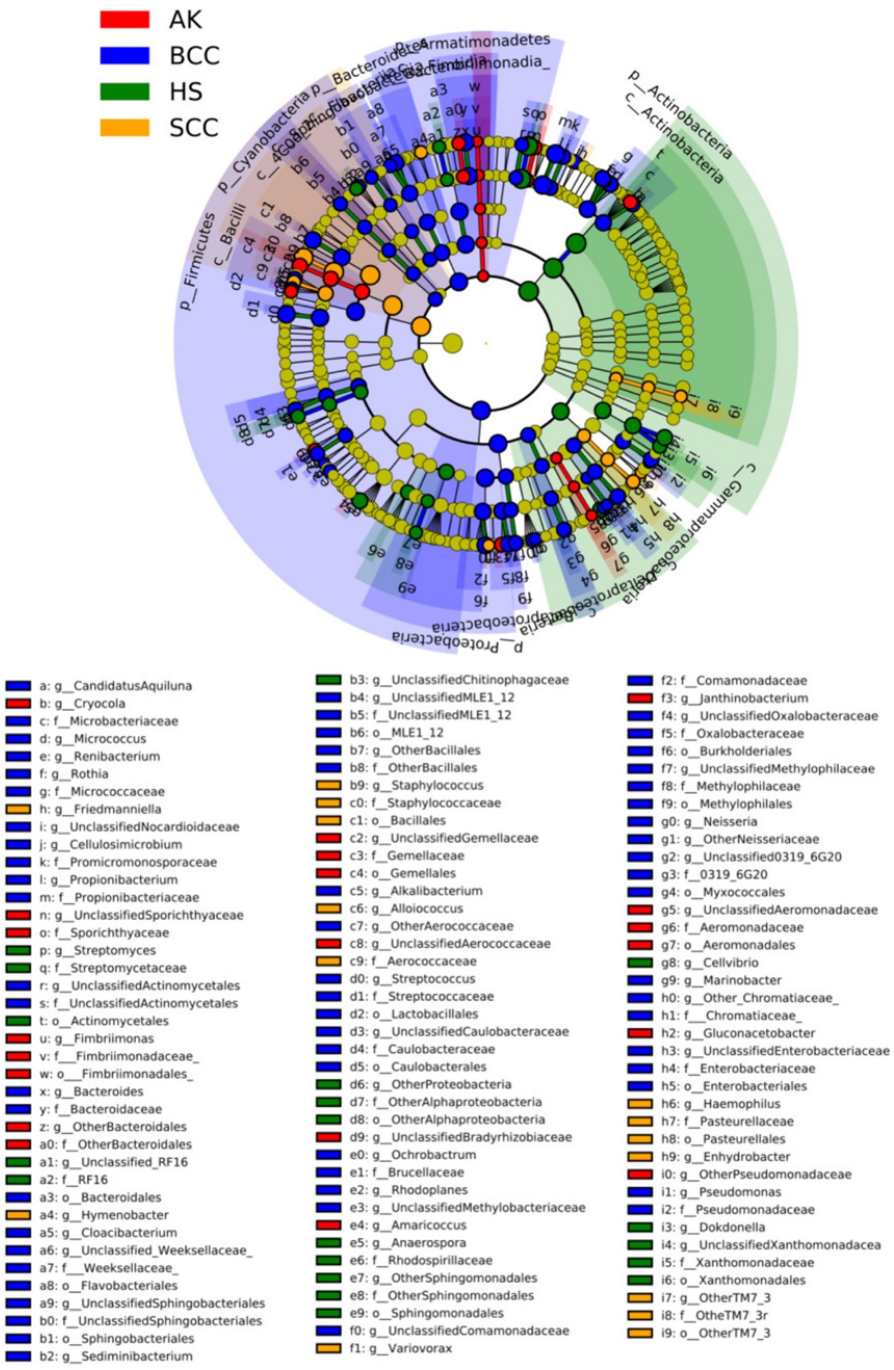

B

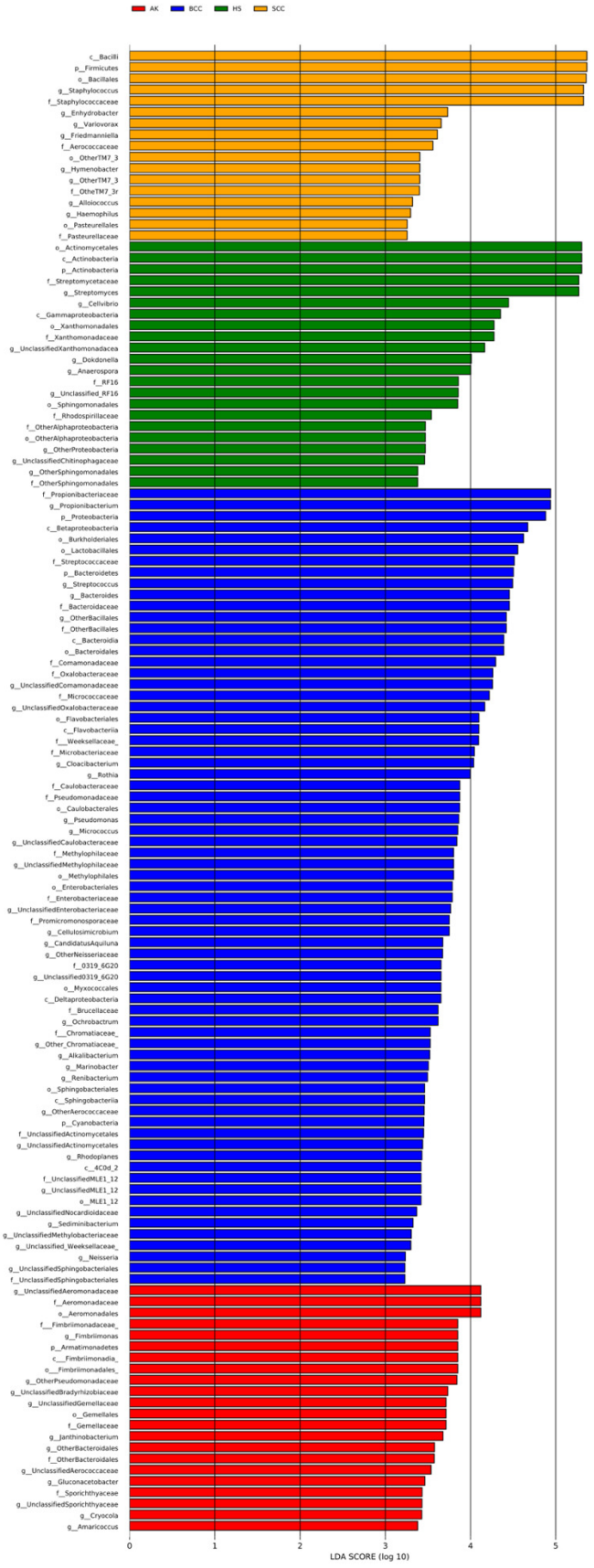
AK
BCC
HS
SCC
c__Bacilli
p__Firmicutes
o__Bacillales
g__Staphylococcus
f__Staphylococcaceae
g__Enhydrobacter
g__Variovorax
g__Friedmanniella
f__Aerococcaceae
o__OtherTM7_3
g__Hymenobacter
g__OtherTM7_3
f__OtheTM7_3r
g__Alloiococcus
g__Haemophilus
o__Pasteurellales
f__Pasteurellaceae
o__Actinomycetales
c__Actinobacteria
p__Actinobacteria
f__Streptomycetaceae
g__Streptomyces
g__Cellvibrio
c__Gammaproteobacteria
o__Xanthomonadales
f__Xanthomonadaceae
g__UnclassifiedXanthomonadacea
g__Dokdonella
g__Anaerospora
f__RF16
g__Unclassified_RF16
o__Sphingomonadales
f__Rhodospirillaceae
f__OtherAlphaproteobacteria
o__OtherAlphaproteobacteria
g__OtherProteobacteria
g__UnclassifiedChitinophagaceae
g__OtherSphingomonadales
f__OtherSphingomonadales
f__Propionibacteriaceae
g__Propionibacterium
p__Proteobacteria
c__Betaproteobacteria
o__Burkholderiales
o__Lactobacillales
f__Streptococcaceae
p__Bacteroidetes
g__Streptococcus
g__Bacteroides
f__Bacteroidaceae
g__OtherBacillales
f__OtherBacillales
c__Bacteroidia
o__Bacteroidales
f__Comamonadaceae
f__Oxalobacteraceae
g__UnclassifiedComamonadaceae
f__Micrococcaceae
g__UnclassifiedOxalobacteraceae
o__Flavobacteriales
c__Flavobacteriia
f__Weeksellaceae_
f__Microbacteriaceae
g__Cloacibacterium
g__Rothia
f__Caulobacteraceae
f__Pseudomonadaceae
o__Caulobacterales
g__Pseudomonas
g__Micrococcus
g__UnclassifiedCaulobacteraceae
f__Methylophilaceae
g__UnclassifiedMethylophilaceae
o__Methylophilales
o__Enterobacteriales
f__Enterobacteriaceae
g__UnclassifiedEnterobacteriaceae
f__Promicromonosporaceae
g__Cellulosimicrobium
g__CandidatusAquiluna
g__OtherNeisseriaceae
f__0319_6G20
g__Unclassified0319_6G20
o__Myxococcales
c__Deltaproteobacteria
f__Brucellaceae
g__Ochrobactrum
f__Chromatiaceae_
g__Other_Chromatiaceae_
g__Alkalibacterium
g__Marinobacter
g__Renibacterium
o__Sphingobacteriales
c__Sphingobacteriia
g__OtherAerococcaceae
p__Cyanobacteria
f__UnclassifiedActinomycetales
g__UnclassifiedActinomycetales
g__Rhodoplanes
c__4C0d_2
f__UnclassifiedMLE1_12
g__UnclassifiedMLE1_12
o__MLE1_12
g__UnclassifiedNocardioidaceae
g__Sediminibacterium
g__UnclassifiedMethylobacteriaceae
g__Unclassified_Weeksellaceae_
g__Neisseria
g__UnclassifiedSphingobacteriales
f__UnclassifiedSphingobacteriales
g__UnclassifiedAeromonadaceae
f__Aeromonadaceae
o__Aeromonadales
f__Fimbriimonadaceae_
g__Fimbriimonas
p__Armatimonadetes
c__Fimbriimonadia_
o__Fimbriimonadales_
g__OtherPseudomonadaceae
g__UnclassifiedBradyrhizobiaceae
g__UnclassifiedGemellaceae
o__Gemellales
f__Gemellaceae
g__Janthinobacterium
g__OtherBacteroidales
f__OtherBacteroidales
g__UnclassifiedAerococcaceae
g__Gluconacetobacter
f__Sporichthyaceae
g__UnclassifiedSporichthyaceae
g__Cryocola
g__Amaricoccus
0
1
2
3
4
5
LDA SCORE (log 10)

Figure 22. LEfSe analysis identifying taxa with increased relative abundance in tumors. (A) LEfSe output specifying taxa with increased relative abundance in tumors (B) LEfSe bar-chart output (keratinocyte tumors and healthy skin). Adopted from (1).

Further, unsupervised hierarchical clustering was employed, in which we assigned OTUs to species level taxonomy using EzBioCloud database (162). A highly individualized microbiota composition was indicated from this analysis for different specimens. However, we observed a strong but not specific association of *Staphylococcus aureus* with AK and SCC samples (Figure 23 A-B). Interestingly, when *S. aureus* was abundant, other typical skin microbes like *Cutibacterium acnes* were low, indicating a possible competitive exclusion between these taxa (1).

A

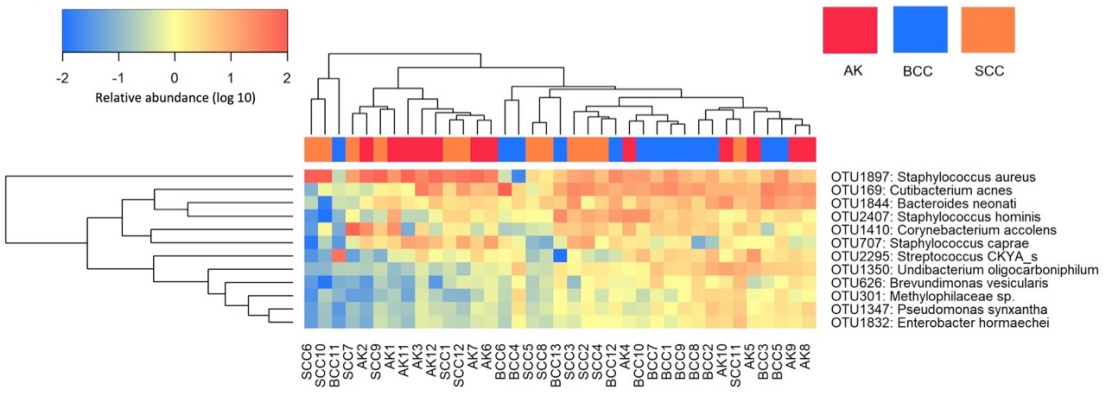

B

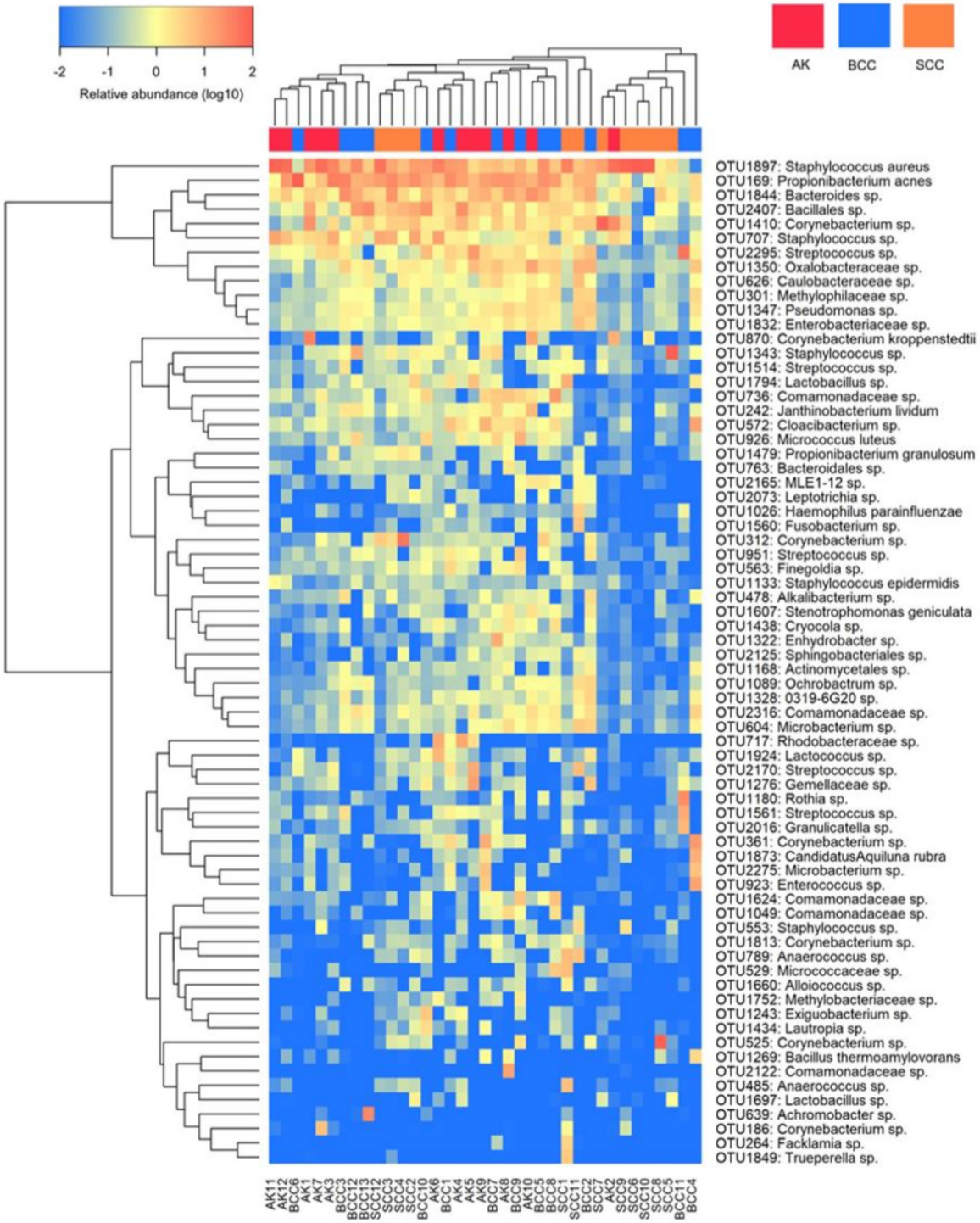
-2
-1
0
1
2
Relative abundance (log10)
AK
BCC
SCC
OTU1897: Staphylococcus aureus
OTU169: Propionibacterium acnes
OTU1844: Bacteroides sp.
OTU2407: Bacillales sp.
OTU1410: Corynebacterium sp.
OTU707: Staphylococcus sp.
OTU2295: Streptococcus sp.
OTU1350: Oxalobacteraceae sp.
OTU626: Caulobacteraceae sp.
OTU301: Methylophilaceae sp.
OTU1347: Pseudomonas sp.
OTU1832: Enterobacteriaceae sp.
OTU870: Corynebacterium kroppenstedtii
OTU1343: Staphylococcus sp.
OTU1514: Streptococcus sp.
OTU1794: Lactobacillus sp.
OTU736: Comamonadaceae sp.
OTU242: Janthinobacterium lividum
OTU572: Cloacibacterium sp.
OTU926: Micrococcus luteus
OTU1479: Propionibacterium granulosum
OTU763: Bacteroidales sp.
OTU2165: MLE1-12 sp.
OTU2073: Leptotrichia sp.
OTU1026: Haemophilus parainfluenzae
OTU1560: Fusobacterium sp.
OTU312: Corynebacterium sp.
OTU951: Streptococcus sp.
OTU563: Finegoldia sp.
OTU1133: Staphylococcus epidermidis
OTU478: Alkalibacterium sp.
OTU1607: Stenotrophomonas geniculata
OTU1438: Cryocola sp.
OTU1322: Enhydrobacter sp.
OTU2125: Sphingobacteriales sp.
OTU1168: Actinomycetales sp.
OTU1089: Ochrobactrum sp.
OTU1328: 0319-6G20 sp.
OTU2316: Comamonadaceae sp.
OTU604: Microbacterium sp.
OTU717: Rhodobacteraceae sp.
OTU1924: Lactococcus sp.
OTU2170: Streptococcus sp.
OTU1276: Gemellaceae sp.
OTU1180: Rothia sp.
OTU1561: Streptococcus sp.
OTU2016: Granulicatella sp.
OTU361: Corynebacterium sp.
OTU1873: CandidatusAquiluna rubra
OTU2275: Microbacterium sp.
OTU923: Enterococcus sp.
OTU1624: Comamonadaceae sp.
OTU1049: Comamonadaceae sp.
OTU553: Staphylococcus sp.
OTU1813: Corynebacterium sp.
OTU789: Anaerococcus sp.
OTU529: Micrococcaceae sp.
OTU1660: Alloiococcus sp.
OTU1752: Methylobacteriaceae sp.
OTU1243: Exiguobacterium sp.
OTU1434: Lautropia sp.
OTU525: Corynebacterium sp.
OTU1269: Bacillus thermoamylovorans
OTU2122: Comamonadaceae sp.
OTU485: Anaerococcus sp.
OTU1697: Lactobacillus sp.
OTU639: Achromobacter sp.
OTU186: Corynebacterium sp.
OTU264: Facklamia sp.
OTU1849: Trueperella sp.
AK11
AK12
BCC6
AK1
AK7
AK3
BCC3
BCC12
BCC13
SCC12
SCC3
SCC4
SCC2
BCC10
AK6
BCC1
AK4
AK5
AK9
BCC7
AK8
BCC9
AK10
BCC5
BCC8
SCC1
SCC11
BCC2
SCC7
AK2
SCC9
SCC6
SCC10
SCC8
SCC5
BCC11
BCC4

Figure 23. Dominant taxa in keratinocyte skin tumors. (A) Unsupervised hierarchical clustering of log (10)-transformed data (heat map representation) of dominant taxa shows a predominant but not exclusive association of *S. aureus* with AK and SCC samples. EzBioCloud database was used to assign species level taxonomy. Complete heat map representation of dominant taxa revealed by unsupervised hierarchical clustering is shown in (B). Adopted from (1).

To further quantify the microbial load in tumor entities and normal skin and to confirm the dominant colonization of *Staphylococcus aureus* in AK and SCC, quantitative PCR (qPCR) was employed with an increased sample set. Bacterial load assessed using the pan-bacterial 16S rRNA gene showed no significant change in AKs and SCCs compared to normal skin, however, a significant decrease in bacterial load was observed in BCC (Figure 24 A). Next, *Staphylococcus* (genus) loads were assessed and a significant increase in *Staphylococcus* abundance was observed in AK and SCC compared to BCC and normal skin (Figure 24 B). Notably, *Staphylococcus aureus* (species) load was significantly increased only in SCCs compared to other entities (Figure 24 C). Furthermore, in paired samples, a significant increase in *S. aureus* loads was observed in adjacent non-lesional skin (NS) compared to neoplastic skin (Figure 25). Notably, a known antagonist of *S. aureus*, *S. epidermidis* (10) was significantly reduced in AK, SCC & BCC in comparison to healthy skin (HS) and non-lesional skin indicating a possible competition with *S. aureus* (Figure 24 D) (1). Of note, we were not able to detect *Streptococcus* by qPCR in tumor entities (data not shown), which could possibly be due to very low *Streptococcus* loads in skin tumor samples which were below the limit of detection of our qPCR assay.

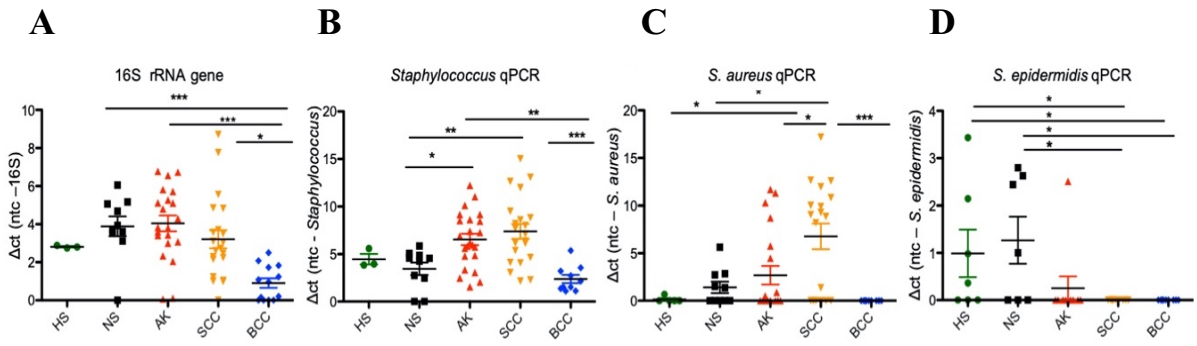

Figure 24. Bacterial, *Staphylococcus*, *S. aureus* and *S. epidermidis* loads in keratinocyte skin tumors. (A) Bacterial load (16S rRNA gene) is significantly decreased in BCC, (B) *Staphylococcus* (genus) loads are significantly increased in AK and SCC, and (C) *S. aureus* loads are significantly increased in SCC. (D) *S. epidermidis* loads are significantly reduced in tumors (Kruskal–Wallis test; Dunn's multiple comparison test; C and D: ANOVA; Turkey's multiple comparison test; * $p < 0.05$; ** $p < 0.01$; *** $p < 0.005$). Adopted from (1).

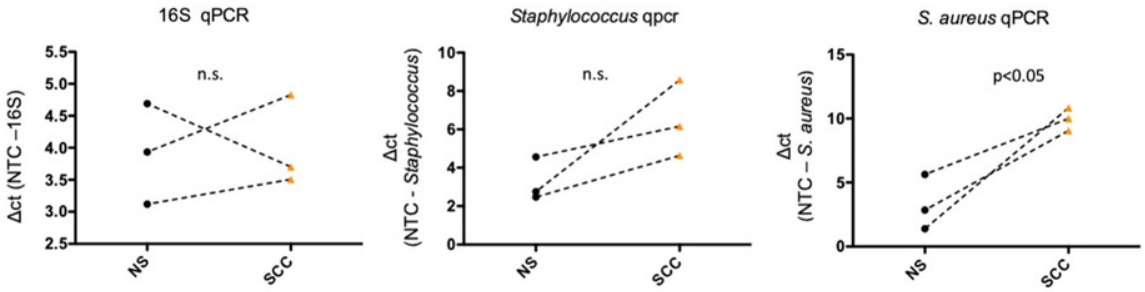

Figure 25. Bacterial, *Staphylococcus*, *S. aureus* abundance in paired samples. Significant increase of *S. aureus* abundance in cSCC compared to its adjacent non-lesional skin (NS) as assessed by qPCR in paired samples (*$p<0.05$; paired t-test; n=3). Adopted from (1).

Interestingly, assessing chronic plaque psoriasis samples (n=5) which are characterized by vigorous hyper- and parakeratosis, no increase in *Staphylococcus* or *S. aureus* loads were measured using qPCR analysis. No significant changes in bacterial, *Staphylococcus* and *S. aureus* loads were observed in psoriasis samples when compared to HS and NS (Figure 26 A-C) (1). This indicates that the observed *S. aureus* overabundance in AK and SCC is not solely driven by high amounts of keratin on the tumor surface but might be a tumor specific phenomenon.

To summarize, these data collectively indicate a significantly different microbial community type in skin tumors, which deviate from normal skin. Taxon *Staphylococcus* dominates in AKs and SCCs while *S. aureus* is the most abundant taxon in SCC. This microbial change is associated with reduction of typical skin commensals like *S. epidermidis* or *C. acnes*. BCCs show a reduced bacterial load and represent a more variable community composition (1).

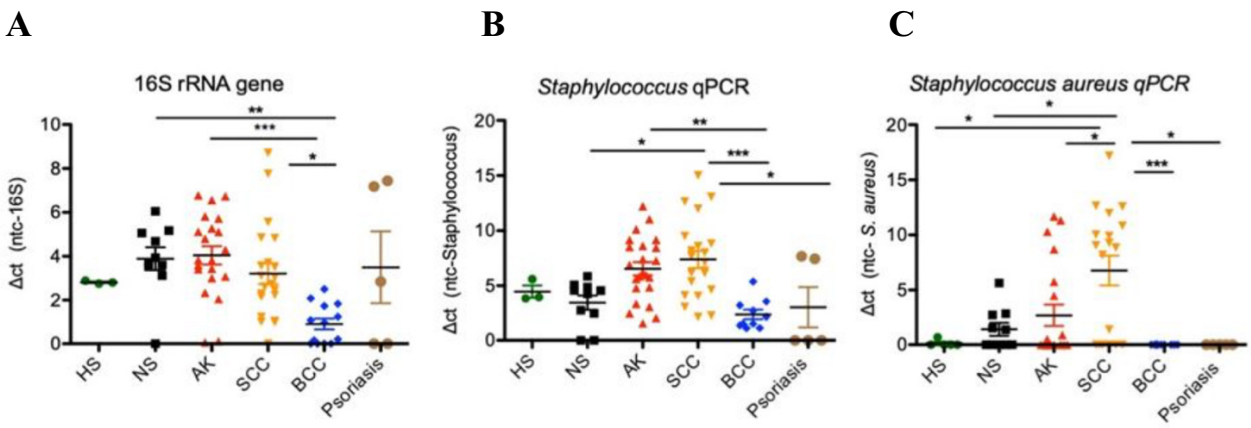

Figure 26. Bacterial, *Staphylococcus*, *S. aureus* abundance in psoriasis, skin tumors, NS and HS (normal skin) entities. Bacterial load as measured by 16S rRNA gene, *Staphylococcus* (genus) loads and *S. aureus* loads are not significantly changed in psoriasis compared to HS and NS (ANOVA; Turkey's multiple comparison test; *p<0.05; **p<0.01; ***p<0.005). Adopted from (1).

1.3. *S. aureus* is mostly localized to hyperkeratotic regions and in areas with invasive tissue of the cutaneous SCC and its precursor AK.

FISH was employed to determine the *in-situ* localization of bacteria and *S. aureus* in our tumor entities. A pan-bacterial 16S rRNA (EUB338) probe was used for overall bacterial detection and a *S. aureus* specific (*Sau)* probe was used for this taxon. The specificity of the FISH probes was assessed ahead by using mixed cultures of *S. aureus* and *S. epidermidis* (Figure 27).

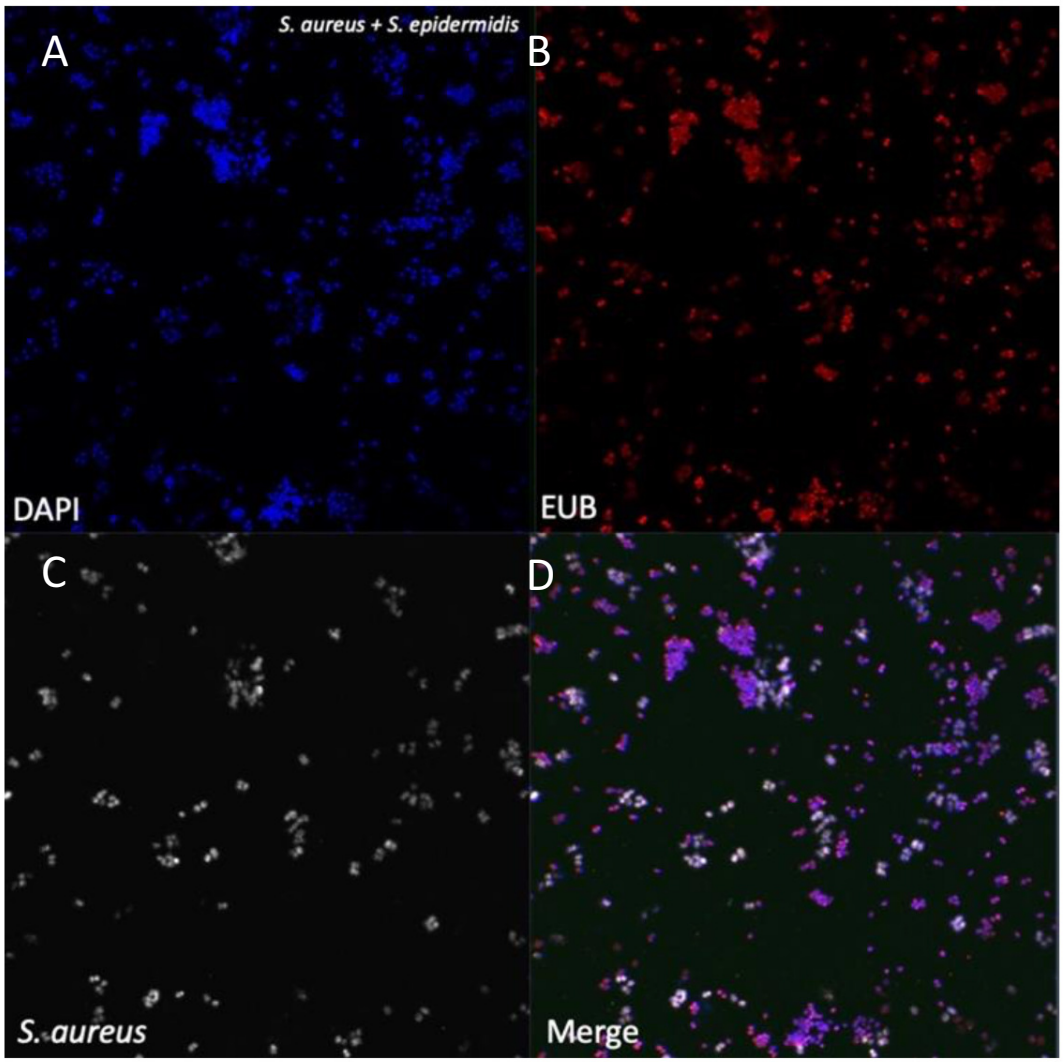

Figure 27. Assessment of the specificity of FISH probes used in the study. Mixed cultures of *S. aureus* and *S. epidermidis* were stained with (A)DAPI, (B) a panbacterial (EUB) probe and (C) a *S. aureus* specific probe. The *S. aureus* probe specifically stains just *S. aureus* cells as specified in the merged (D) image.

A significant number of *S. aureus* specific fluorescence signals were detected in the hyperkeratotic regions of AK & SCC samples (Figure 28 A-B) which were absent in BCC samples. *S. aureus* signals were also detected in the invasive tissue areas of SCC samples and only sparse signals in BCC samples (Figure 28 B-C). Bacterial signals were absent in the dermis of any of the tumor entities. To that end, these findings confirm the *S. aureus* colonization of hyperkeratotic surface areas of AK and SCC as well as invasive tumor tissue in SCC. Moreover, these findings reassure the histologic representation of abundant coccoid microbial structures visible in AK and SCC specimens (Figure 12 D-E) (1).

A

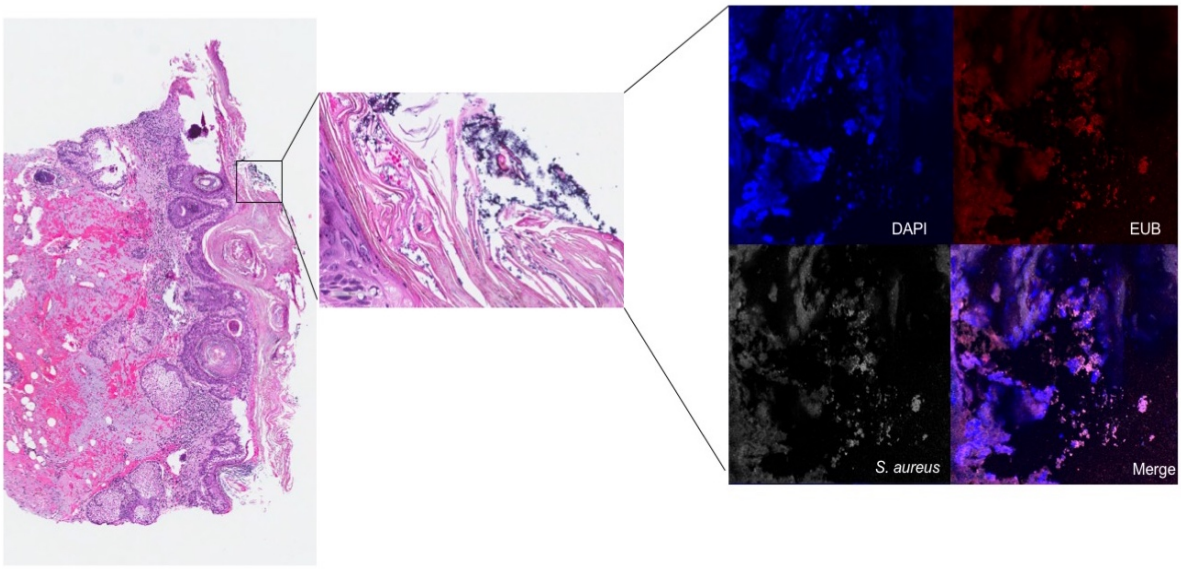

B

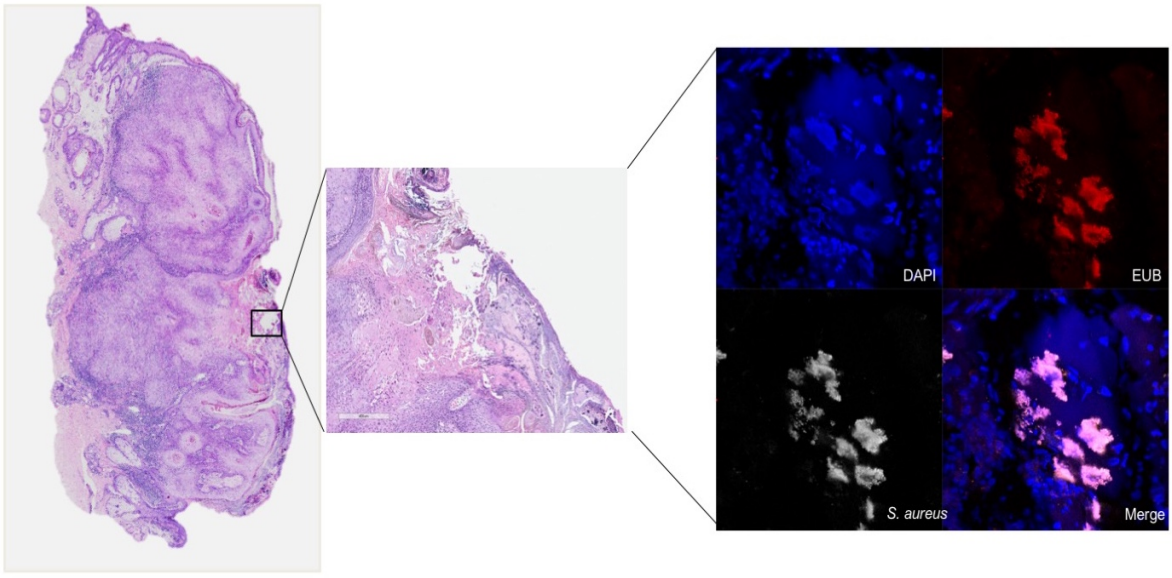

C

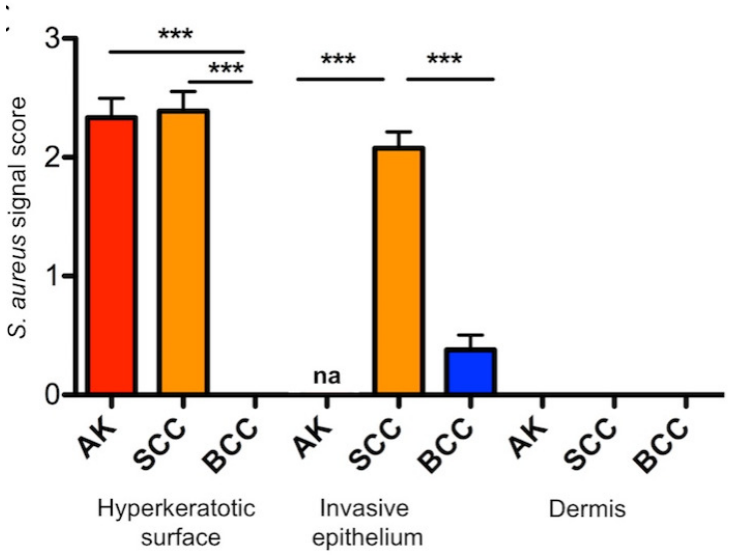

Figure 28. ***In situ*** **visualization of** ***S. aureus*** **shows its association with hyperkeratotic areas in (A) AK and (B) SCC using FISH** (DAPI: blue, EUB338: red; *S. aureus*: grey; magnification 650x). (C) Semi-quantitative scoring of *S. aureus* specific signals in hyperkeratotic surface areas and invasive tumor parts in AK, SCC and BCC specimens, respectively (***p<0.005; Kruskal Wallis; na, not applicable; AK, n=5; SCC, n=5; BCC, n=5). Adopted from (1).

1.4. Inflammation severity significantly correlated to altered microbial community in AK but not in SCC or BCC

The dermal immune infiltrates in skin tumors is a known predictor of tumor progression and disease prognosis (14, 90). AK, SCC and BCC typically show increased dermal inflammation compared to healthy skin. Thus, we investigated whether the grade of inflammation is associated with specific microbial community changes. Tumor samples were histologically graded into low- and high-inflammation categories (Figure 29 A). A significantly increased richness ($p<0.05$, unpaired t-test) and different microbial community composition in PCoA ($p<0.05$, ANOSIM; measure: weighted unifrac) were identified in high grade inflamed AK (Figure 29 B-C). Higher inflamed lesions were characterized by gradually increased *Staphylococcus* reads (Figure 29 D; $p=0.06$, Kruskal Wallis), validated by performing qPCR specific for *Staphylococcus* genus (figure 29 E). No significant differences in microbial community structure could be discerned among low- and high inflammation specimens in SCC and BCC, which might be attributed to an underrepresentation of low inflammation cases in

both entities in our sample set (only 2 out of 12 specimens in SCC and 3 out of 13 in BCC were "low"). Of note, a higher dermal inflammation is typical for SCC and BCC since they represent advanced tumor entities in general. Together, these findings suggest that higher dermal inflammation levels are associated with higher microbial richness and that *S. aureus* is at least gradually increased in higher inflamed AK lesions.

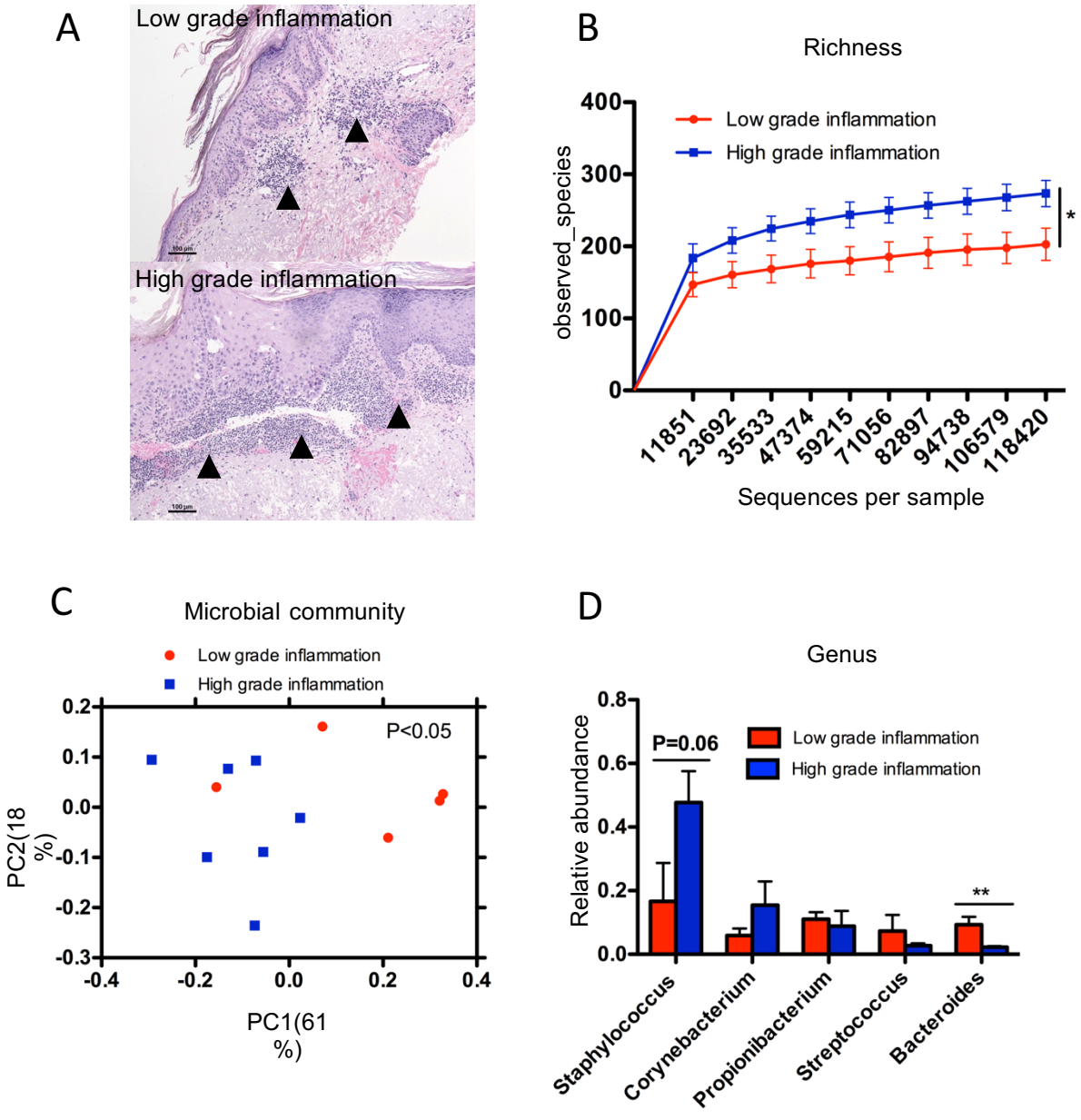

E

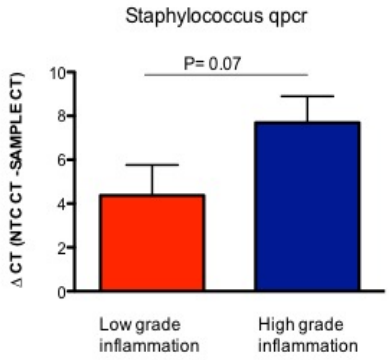

Figure 29. Higher inflammation is associated with increased richness and altered microbial community in AK. (A) Representative images of low grade (upper panel) and high grade (lower panel) inflammation (arrows; low grade: focal immune infiltrate mainly surrounding small vessels; high grade: papillary and upper reticular dermis are densely populated by immune cells, often representing as continuous bands of inflammatory cells). (B) Significantly increased microbial richness ($p<0.05$; unpaired t-test at 118420 reads). (C) Different microbial community composition in low vs. high grade inflamed AK (PCoA; measure: weighted unifrac; $p<0.05$, ANOSIM). (D) *Staphylococcus* relative abundance is gradually increased in higher inflammation in addition to significantly reduced Bacteroides (**$p< 0.01$; Kruskal Wallis). Inflammation levels were semi-quantitatively scored using light microscopy (low grade, n=5; high grade, n=7; data are mean±SEM). (E) *Staphylococcus* abundance as assessed by qPCR also shows a correlation trend with grade of inflammation in AK.

1.5. Antimicrobial peptides (AMP) are differently expressed in epithelial skin tumors.

In addition to immune cells, humoral immune factors like AMPs are also important in skin defense. Interestingly, several AMPs have been implicated in tumor development (118, 141, 186). Consequently, in order to understand the expression of these AMPs in association with *S. aureus* colonization and tumorigenesis, we measured the major skin AMPs, i.e., hBD-1, -2 and -3, RNase7 and psoriasin (S100A7) in our samples via qRT-PCR. These AMPs, except hBD-1 which is reported to be constitutively expressed in skin, are known to be modulated via microbes (187, 188). They are also known to modulate epithelial cell growth and migration

(118, 141, 186-188). Significantly increased transcription levels of *hBD-2* and *-3* were detected in SCCs and AKs compared to both normal skin as well as BCC (Fig. 30 B, C). *Psoriasin* mRNA also increased, but to a lesser extent in SCC compared to normal skin and BCC (Fig. 30 E). In contrast, transcription levels of *hBD-1* and *RNase7* were significantly increased in AK, although at a relatively low level (Figure 30 A, D) (1).

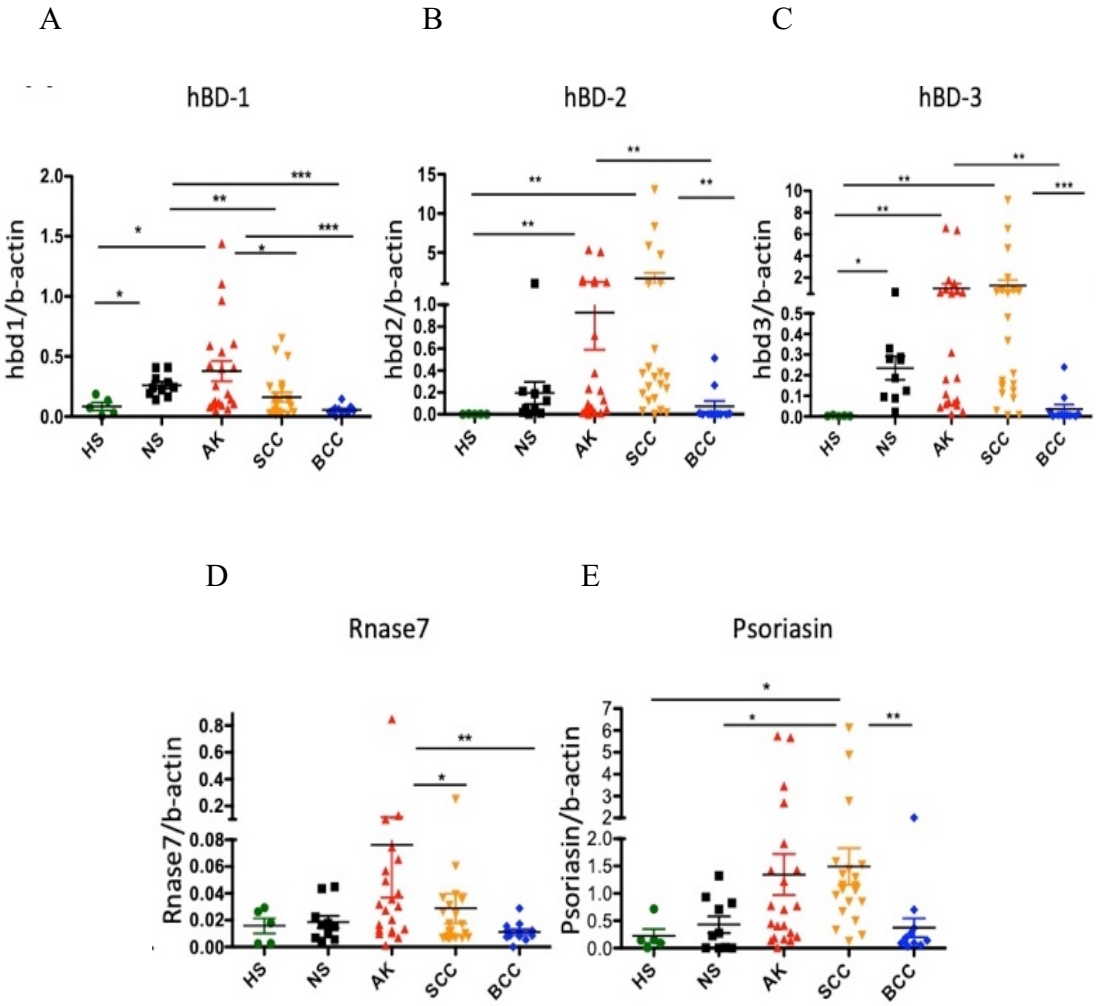

Figure 30. Expression of AMPs in human skin tumors as assessed by qRT-PCR. Significantly increased mRNA expression of *hBD-2, hBD-3* (B, C) and to lesser extent *psoriasin* (S100A7) (E) in AK and SCC compared to normal skin and BCC. Increased mRNA expression of *hBD-1* (A) and *Rnase7* (D) in AK (*p< 0.05, **p< 0.05; ***p<0.005; Kruskal-Wallis; HS, healthy skin, n=5; AK, n=21; SCC, n=22; BCC, n=11; data are mean±SEM). Adopted from (1).

To confirm the increased expression on the protein level, we used immunohistochemical scoring emphasizing hBD-2 and hBD-3 specific antibodies on a subset of samples. This analyses confirmed increased protein expression of hBD-2 in SCC (Fig. 31A-B) whereas, hBD-3 protein expression was significantly increased in AK compared to SCC and BCC, which is in line with a previous report (189).

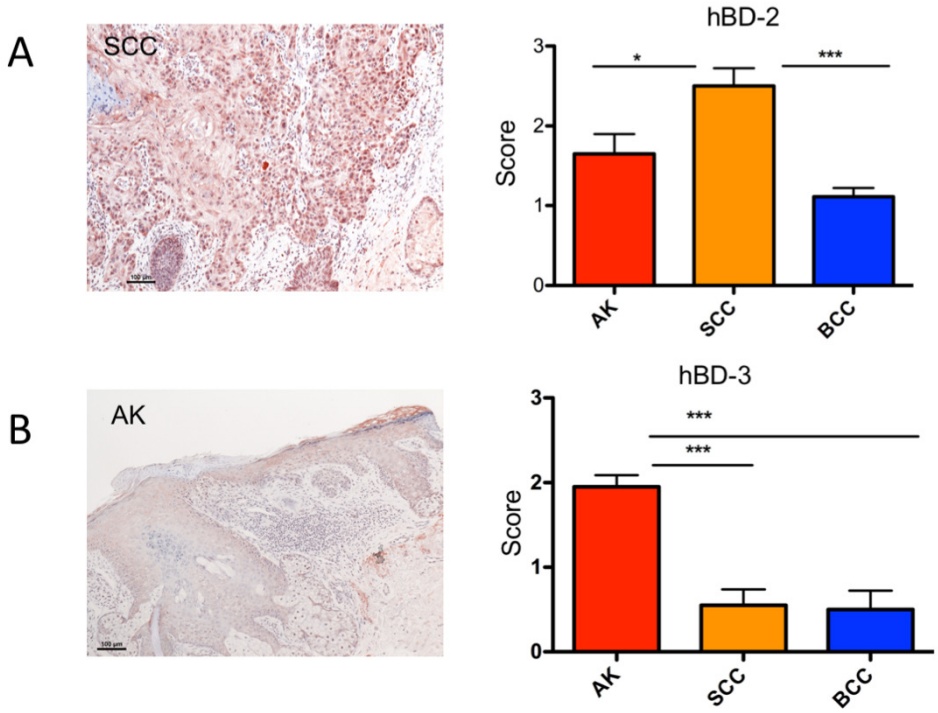

Figure 31. Protein expression of AMPs hBD-2 and -3 in human skin tumors assessed by immunohistochemistry. Immunohistochemical scoring of hBD-2 (A) and hBD-3 (B) protein expression in tumor samples. Representative images showing the staining pattern are shown on the left (AK, n=5; SCC, n=5; BCC, n=5; *p< 0.05; ***p< 0.005, one-way ANOVA, Tukey's multiple comparison test).

Together, these findings show that AMPs are differently expressed in keratinocytic skin tumors, wherein hBD-2 and hBD-3 show a stronger expression in AK and SCC.

1.6. Pearson correlation matrix of assessed features in AK, SCC and BCC shows a significant positive correlation of hBD-2 expression with *S. aureus* in SCC.

Broad correlation analysis of assessed parameters which includes AMP expression, bacterial, *Staphylococcus and S. aureus* loads, histologically scored levels of hyper-/parakeratosis, inflammatory infiltrate and neutrophilic granulocytes as a known predictor of skin tumor progression (90) were performed. Several significant correlations were observed as seen in the correlation matrices (Figure 32). Most pertinent to our study was the significant positive correlation of hBD-2 expression with *Staphylococcus* and *S. aureus* loads in SCCs. Other significantly positive but differing correlations within AMP mRNA levels were apparent in the entities. Also, only hBD-3 showed a significant positive correlation with psoriasin and hBD-2 expression in all of the tumor entities. Correlations between hyper- and parakeratosis, inflammation, and neutrophilic granulocytes were not evident. Only in BCCs, hyper-/parakeratosis and neutrophils were associated with increased AMP expressions. Two significant negative correlations were found: inflammation with hBD-1 expression in BCCs and inflammation with bacterial load in SCCs (Figure 32). Collectively, this analysis proposes a possible connection between the type of microbial colonization and AMP expressions with particular prominence on *S. aureus* overabundance and hBD-2 expression in SCCs. Broadly, our analysis proposes that an altered microbial colonization in keratinocyte skin tumors could influence AMP expression with probable down-stream effects on tumor biology (1).

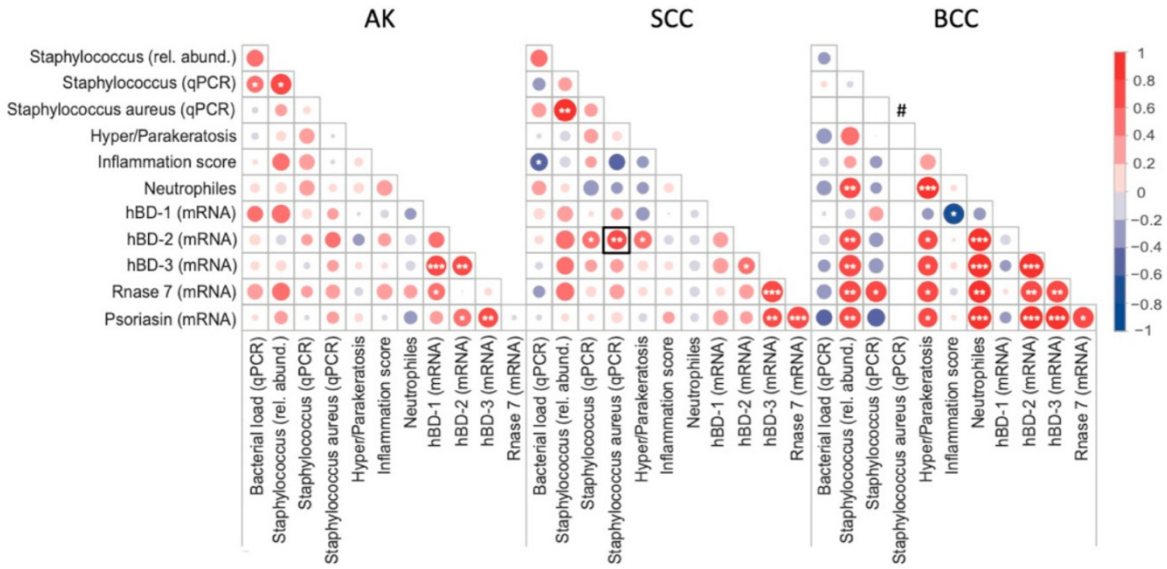

Figure 32. Pearson correlation matrix of assessed features in AK, SCC and BCC. Strong correlations are specified by large circles, while weak correlations are shown by small circles. The color of the scale bar signifies the kind of correlation with 1 indicating a strong positive correlation (dark red) and -1 demonstrating a strong negative correlation (dark blue). t-tests were applied for significance testing to the individual correlations, and significant correlations were indicated with * $p < 0.05$, ** $p < 0.05$, *** $p < 0.005$; specified as stars in the respective circles. The significant correlation of *S. aureus* loads with *hBD-2* mRNA expression in SCC is highlighted (box); # implies that no *S. aureus* signals were detected in BCC with qPCR. Adopted from (1)

1.7. *S. aureus* challenge of cutaneous SCC cells stimulates hBD-2 expression and confers a proliferative stimulus on tumor cells.

It has been shown that *S. aureus* induces expression of *hbd-2* and *-3* in differentiated primary keratinocytes (74). However, no such studies have been performed with cutaneous squamous cell carcinoma cells challenged with *S. aureus*. Hence, to assess whether *S. aureus* leads to induction of hBDs in SCC (HSC-1 and SCL-1) and in HaCaT cells (resembling non–tumorous keratinocytes), we performed co-culture experiments. Two strains of *S. aureus* DSM799 and DSM11823 were used for this assay with increasing MOIs of 2, 20 and 100, respectively. Of note, these strains are devoid of classical secreted toxin genes, which was necessary for employing co-culture experiments since toxin producing strains (e.g. DSM 1104 harboring enterotoxin G and I) immediately overgrew and induced pronounced cell death in preliminary experiments (Figure 35). Bacterial growth was assessed simultaneously by CFU plating before and after infection (Figure 33). After 24 hours of challenge, hBD-1, -2 & -3 mRNA expression was measured by qRT-PCR (1).

Prior to the bacterial infection, both the strains of *S. aureus* were assessed for their growth kinetics to determine their density during the exponential growth phase. This was then used to calculate input multiplicity of infection (MOIs) for the co-culture experiments. Both the strains reached the exponential phase with a similar density between 12-14 hours and 14-hour time point was used for infection experiments (Figure 34).

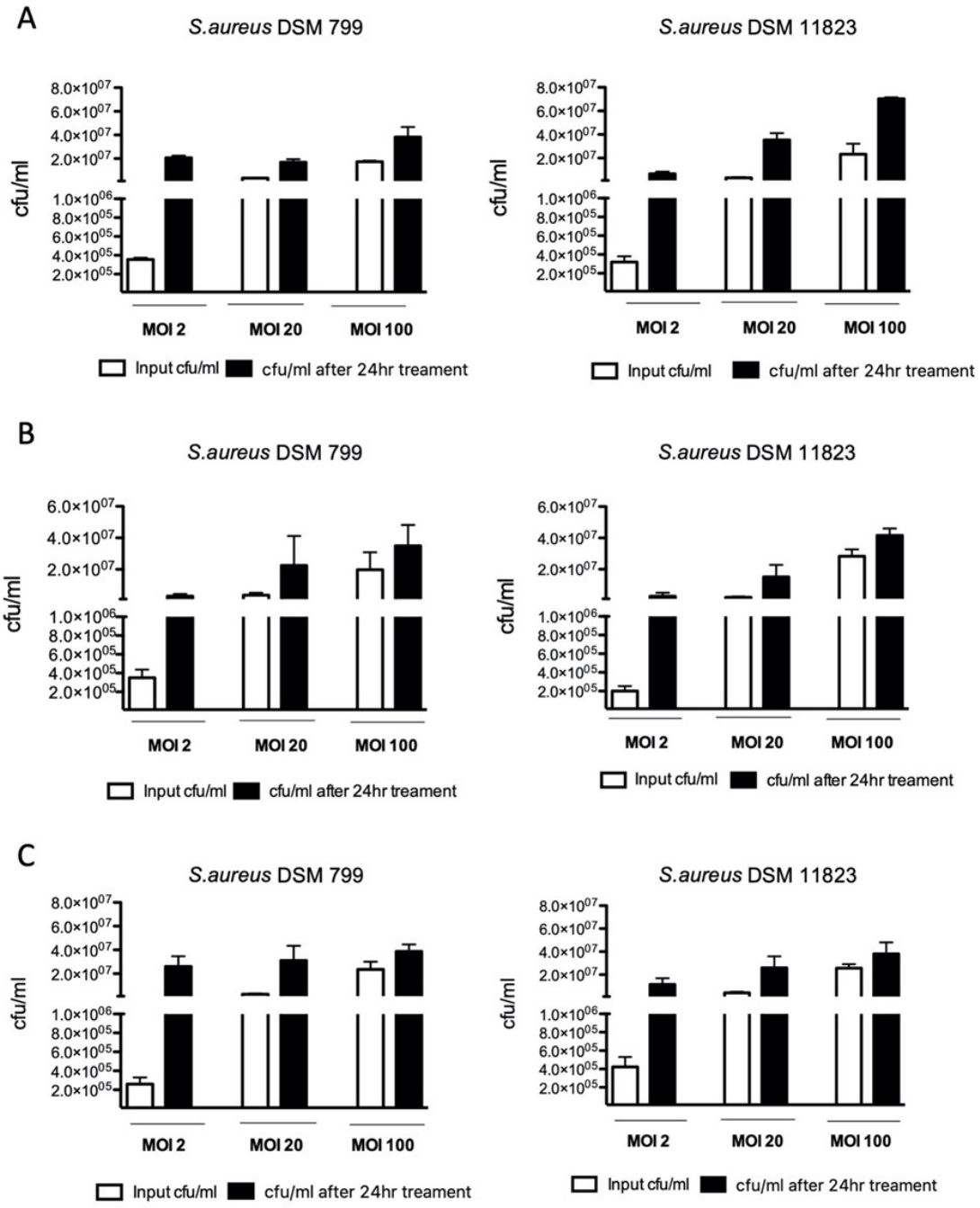

Figure 33. CFU plating of *S. aureus* strains DSM 799 and DSM11823 before (input) and after 24 hrs. of challenge of (A) HSC-1, (B) SCL-1 and (C) HaCaT cells. Adopted from (1).

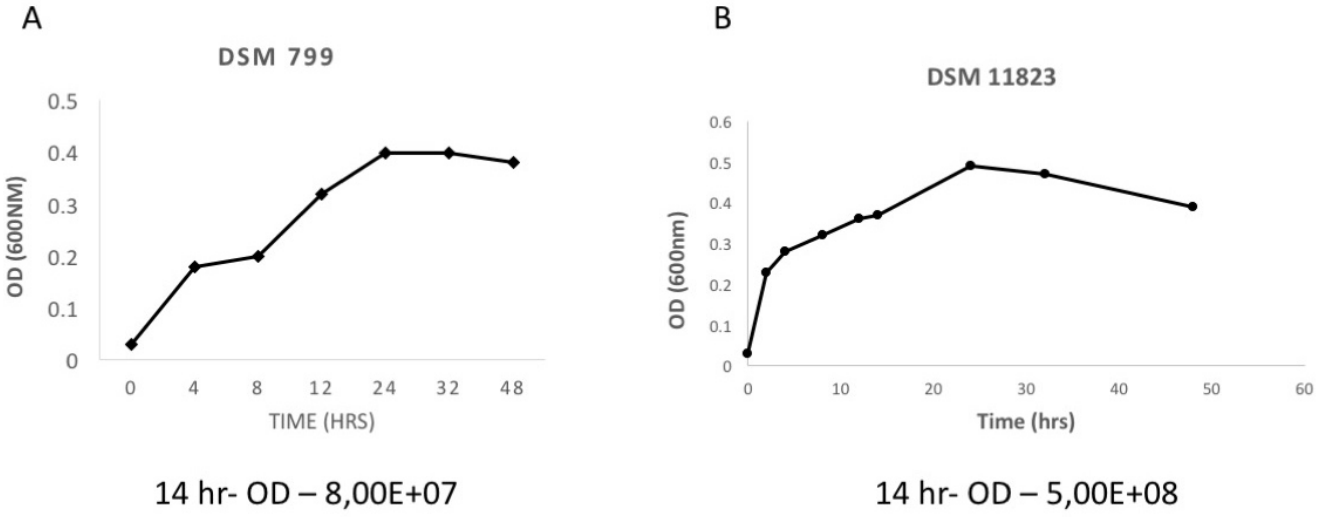

Figure 34. *S. aureus* growth curve assessment of strains (A) DSM799 and (B) DSM11823 to determine their density in the exponential phase. 14-hour time point for both the strains was used for co-culture experiments.

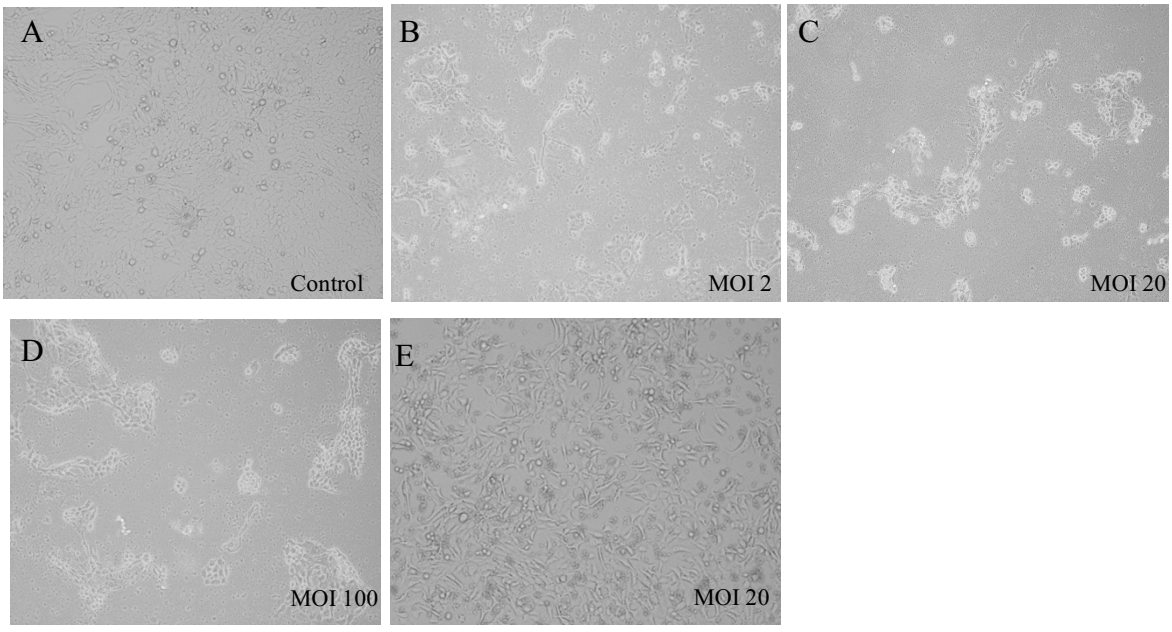

Figure 35. Microscopic images of SCC cells (HSC-1) treated with *Staphylococcus aureus* strain DSM1104 at MOI 2, 20 & 100 (B-D) in comparison to untreated control cells (A) and cells treated with strain DSM11823 at MOI 20 (E) for 24 hours. SCC cells treated with strain

DSM1104 (harboring enterotoxin) led to cell death as visible from apoptotic cells/cell debris at MOI 2 (B) and cell debris at MOI 20 and 100 (C-D). Treatment with DSM 11823 shows no cell debris or apoptotic cells at MOI 20 (E).

hBD-1, -2 and *-3* expression levels were assessed by qRT-PCR after 24 hours of challenge. Both strains of *S. aureus* when co-cultivated with HSC-1 and SCL-1 significantly increased the expression of *hBD-2* mRNA levels compared to *hBD-1* and *-3* in a dose-dependent manner at MOI 2, 20 & 100, whereas HaCaT showed no or only a minor increase of both *hBD-2* and *-3* mRNA expression compared to *hBD-1* (Figure 36). Notably, a significant increase in the number of viable cells were observed when cSCC cells were treated with *S. aureus* strains (DSM799 and DSM11823) in a dose-dependent manner as measured by flow-cytometry (Figure 37 A) or the cck-8 assay (Figure 37 B). Of note, the growth-promoting effect leveled off to some extent at higher MOIs. No increase in the percentage of viable cells were observed when HaCaT cells were co-cultured with *S. aureus* (Figure 37 A-B) (1).

Notably, co-culture with either of the strains did not show any visible changes in cell morphology of cutaneous SCC cells or HaCaT cells (Figure 38 & 39), necrosis and apoptosis as measured by flow cytometry (Figure 40) (1).

To summarize, *S. aureus* specifically induces *hBD-2* mRNA expression in cutaneous SCC cells and induces tumor cell growth which could hypothetically promote tumor progression.

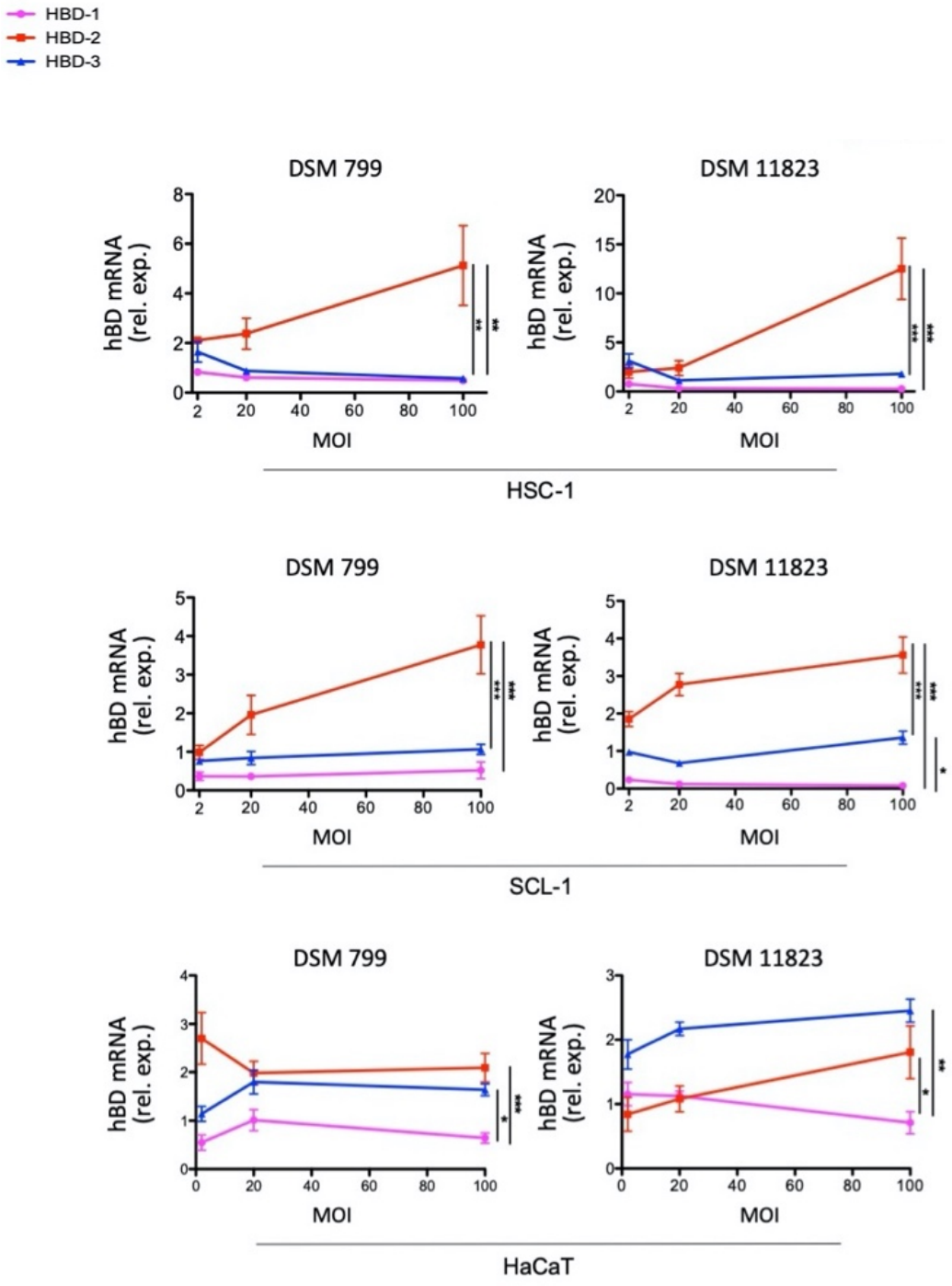

Figure 36. *S. aureus* challenge of cSCC cells stimulates hBD-2 expression. hBD2 mRNA expression measured by qPCR is dose-dependently and dominantly increased in SCC cells with increasing MOIs of *S. aureus* strains DSM799 and DSM11823 (**p<0.01, ***p< 0.005, one-way ANOVA, Bonferroni correction). Adopted from (1).

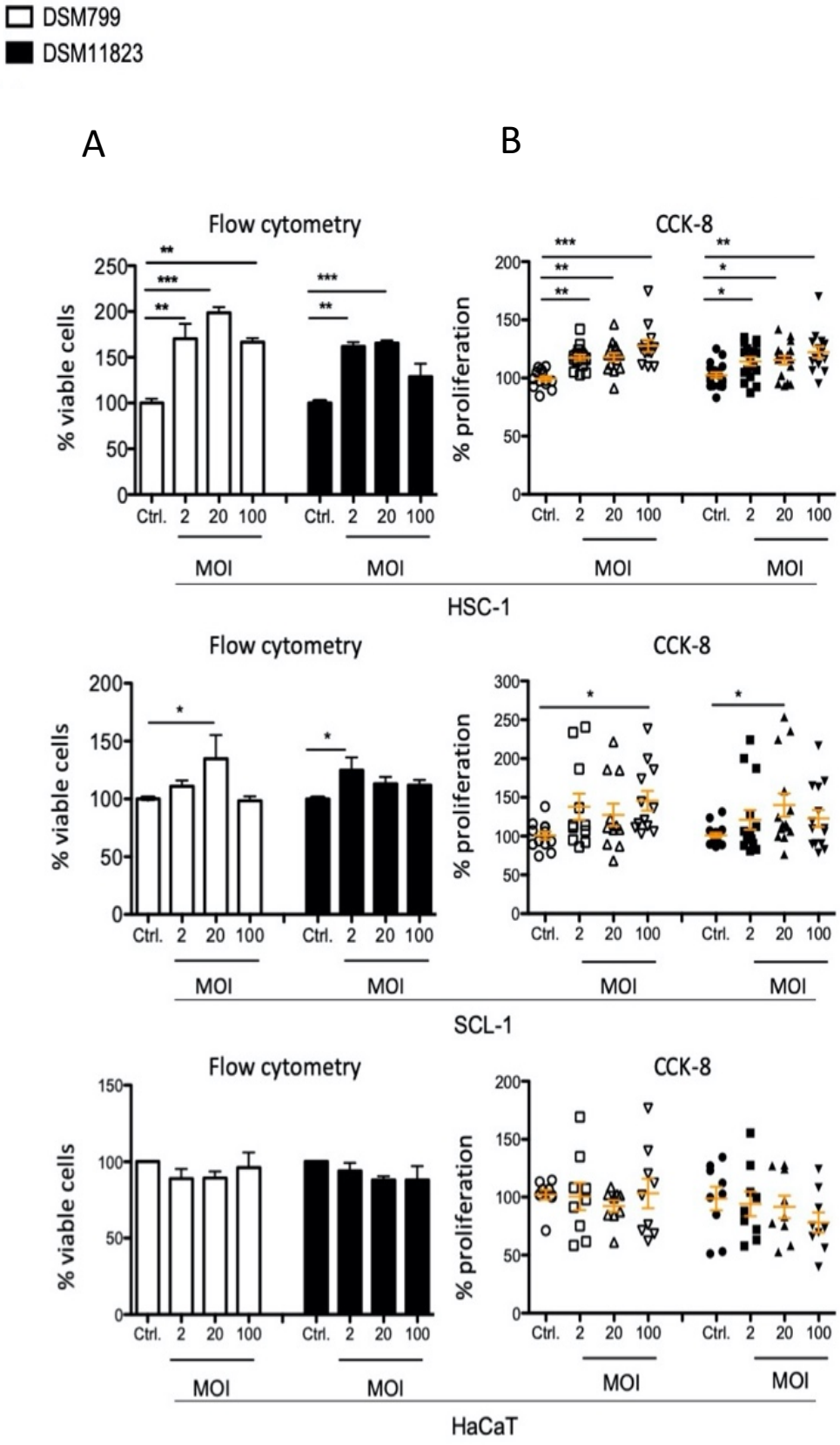
DSM799
DSM11823
A
B
Flow cytometry
CCK-8
% viable cells
% proliferation
Ctrl. 2 20 100 Ctrl. 2 20 100
MOI MOI
HSC-1
SCL-1
HaCaT

Figure 37. *S. aureus* challenge of cSCC cells shows a significant increase in viable cells (A) A significant increase in the number of viable cells was observed when SCC cells were treated with *S. aureus* strains of DSM799 and DSM11823 at MOI 2, 20 & 100 as measured by the average number of viable cells per second using Flow cytometry (bar chart represents the mean value of percentage of viable cells normalized to control $\pm$ standard error from three independent experiments (**p< 0.01; ***p< 0.005, one-way ANOVA; Dunnett's multiple comparison test) and by (B) CCK-8 assay (* p < 0.05; ** p < 0.01; *** p < 0.005, Kruskal–Wallis, Dunn's multiple comparison test). HaCaT showed no increase in cell number. Adopted from (1).

A

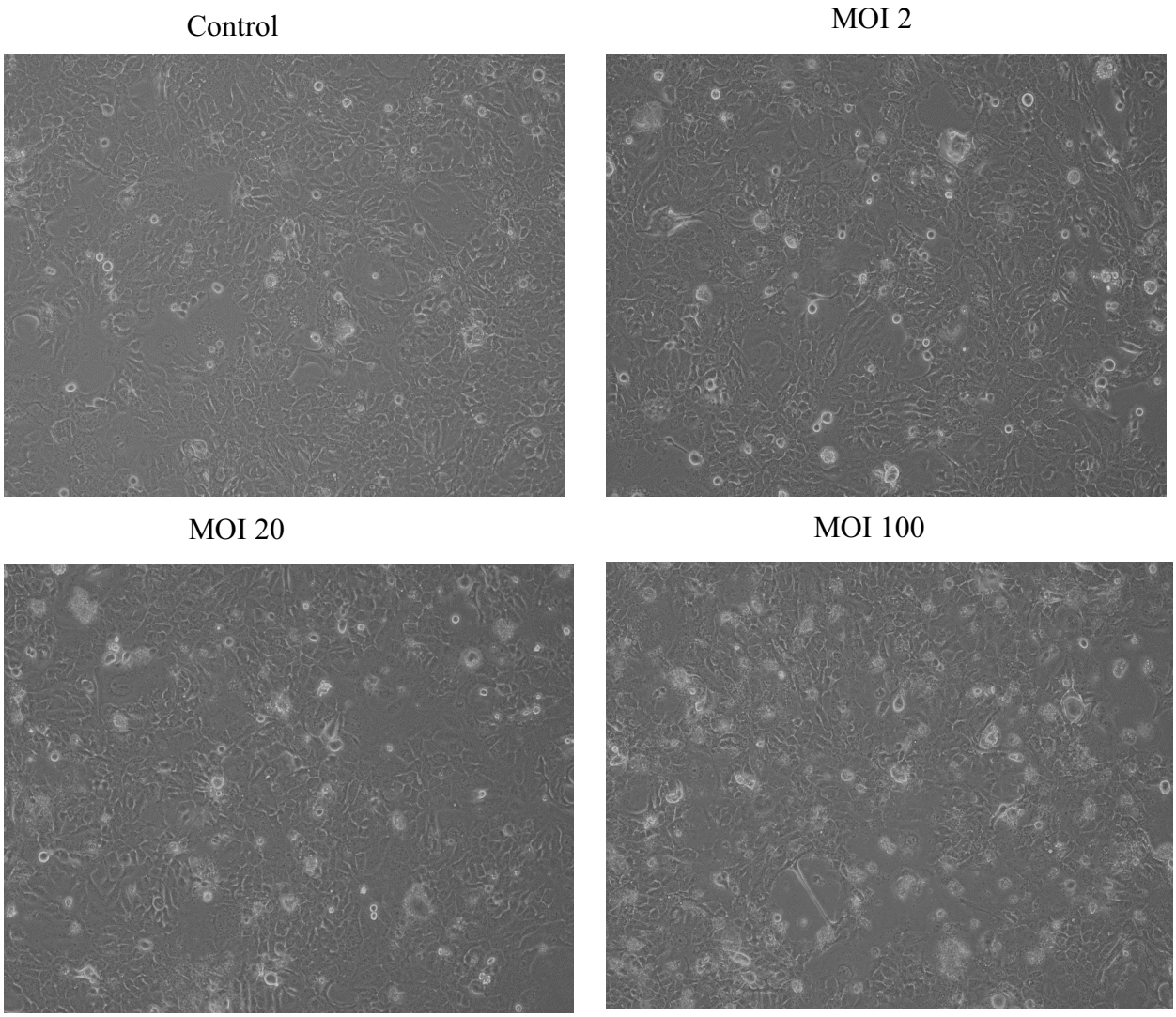

B

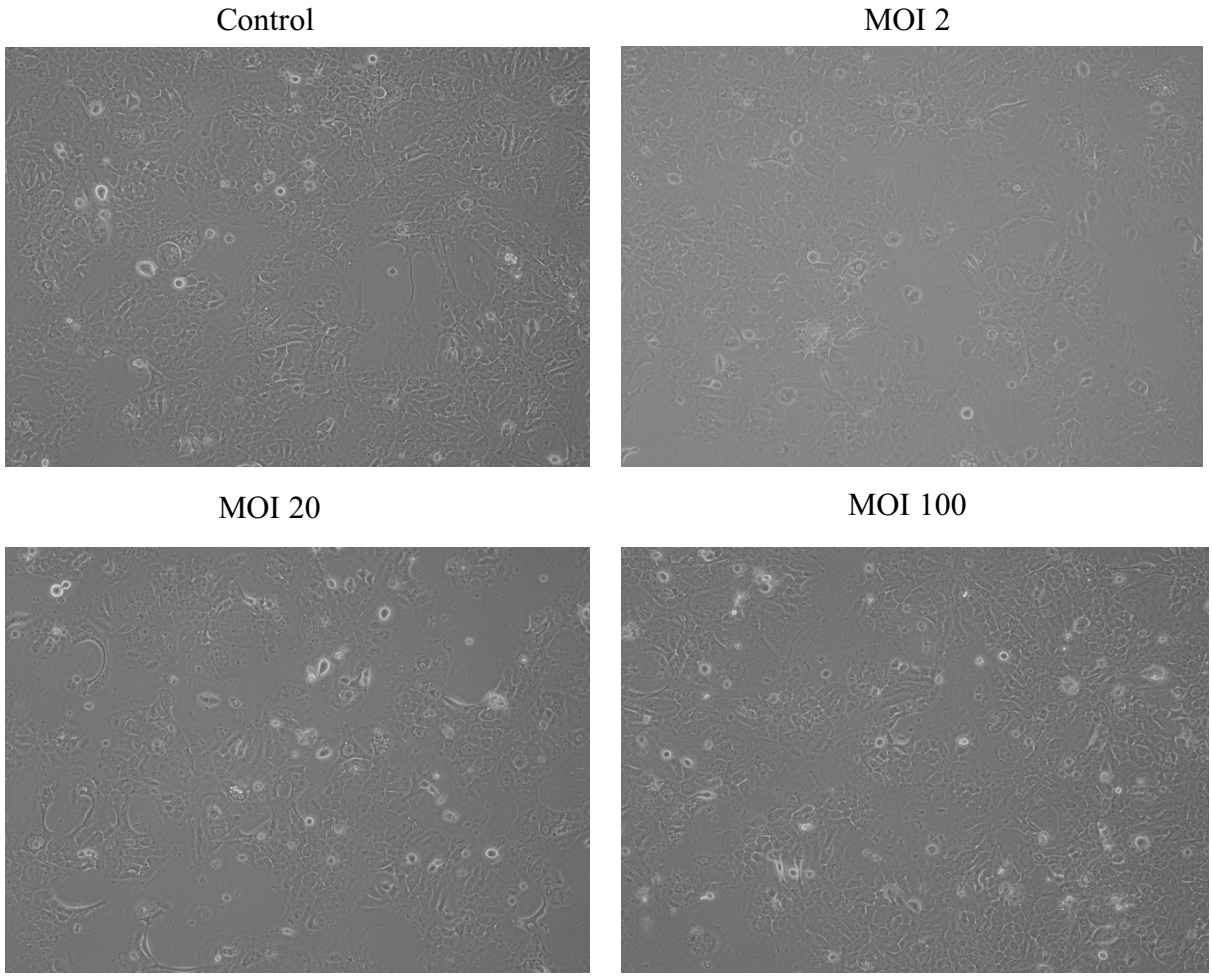

Figure 38. Microscopic images of HSC-1 cells treated with *Staphylococcus aureus* strains DSM799 (A) and DSM 11823 (B) at MOI 2, 20 & 100 for 24 hours. No significant change in cell morphology was observed in any of the treated cells compared to untreated control.

A

Control

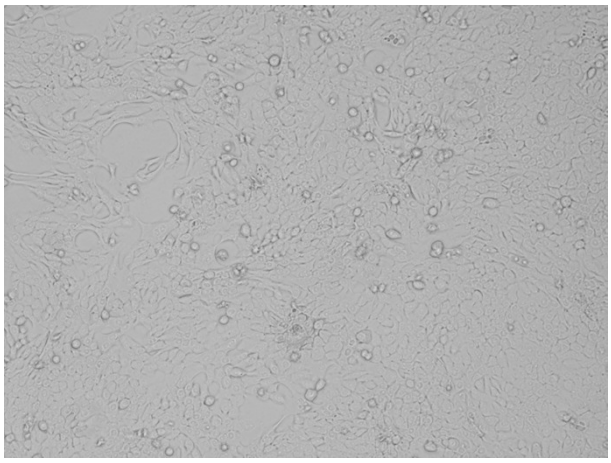

MOI 2

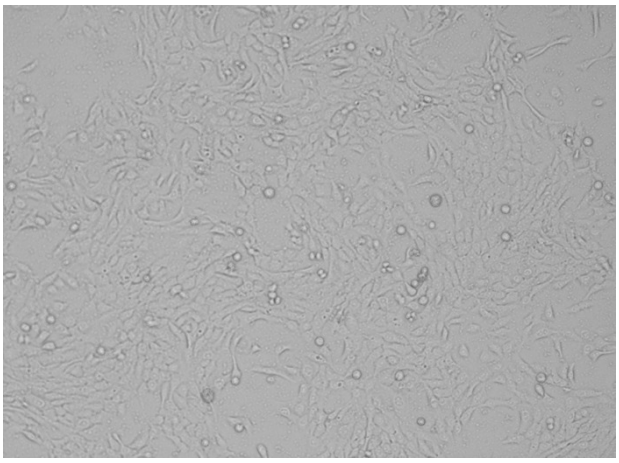

MOI 20

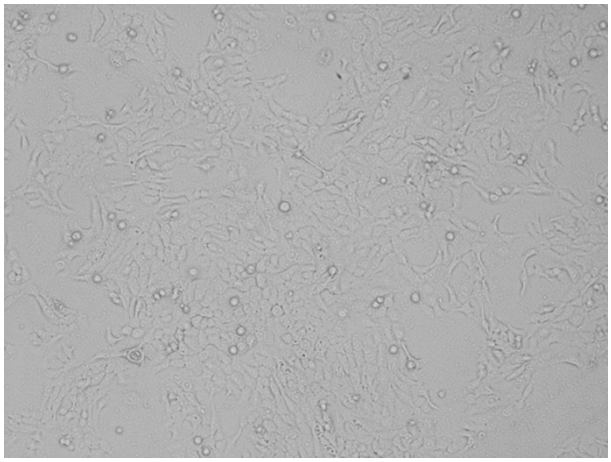

MOI 100

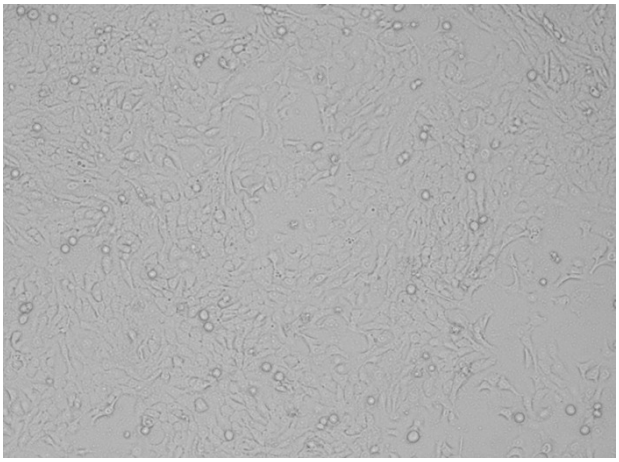

B

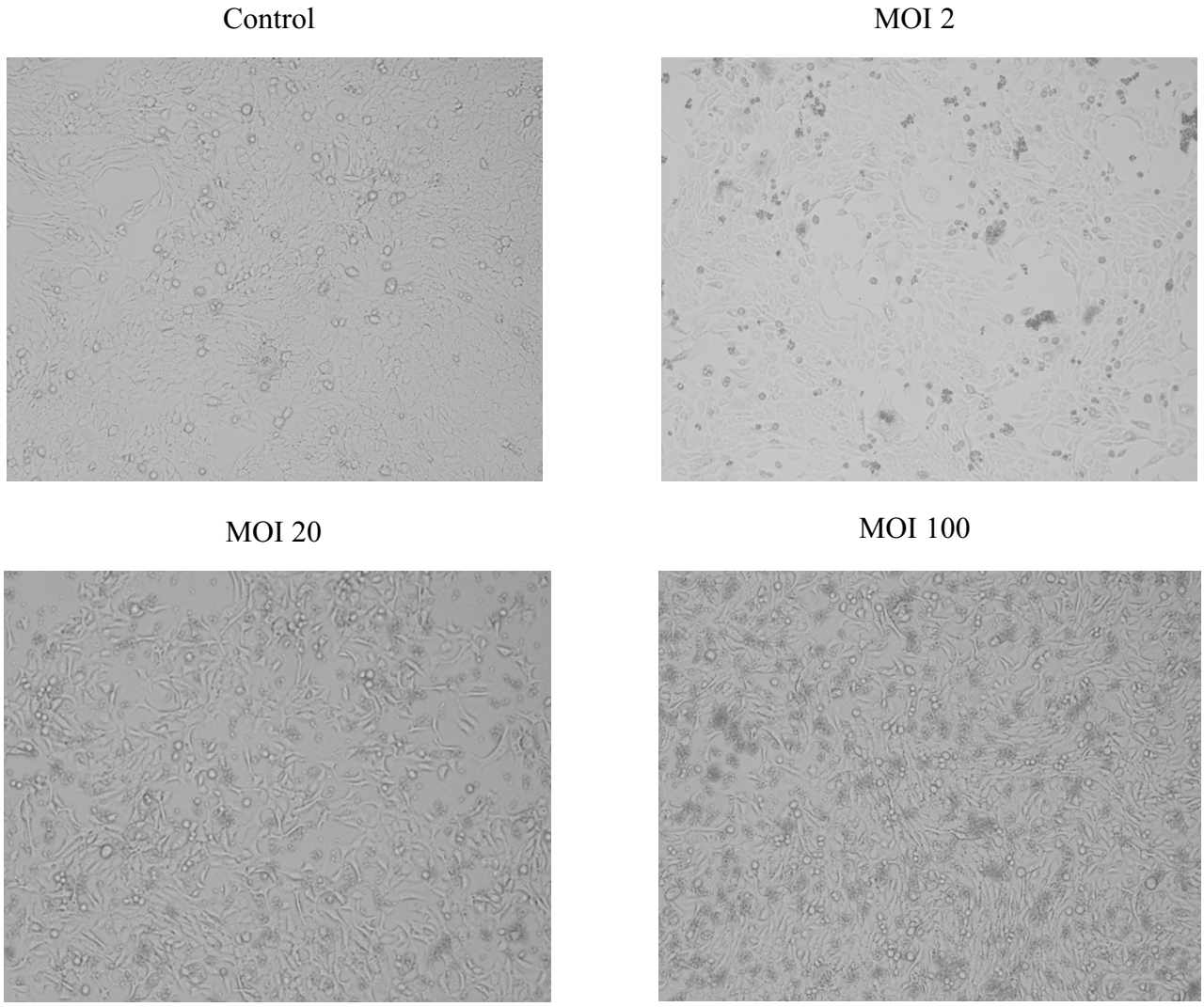

Figure 39. Microscopic images of HaCaT cells treated with *Staphylococcus aureus* strains DSM799 (A) and DSM 11823 (B) at MOI 2, 20 & 100 for 24 hours. No significant change in cell morphology was observed in any of the treated cells compared to untreated control.

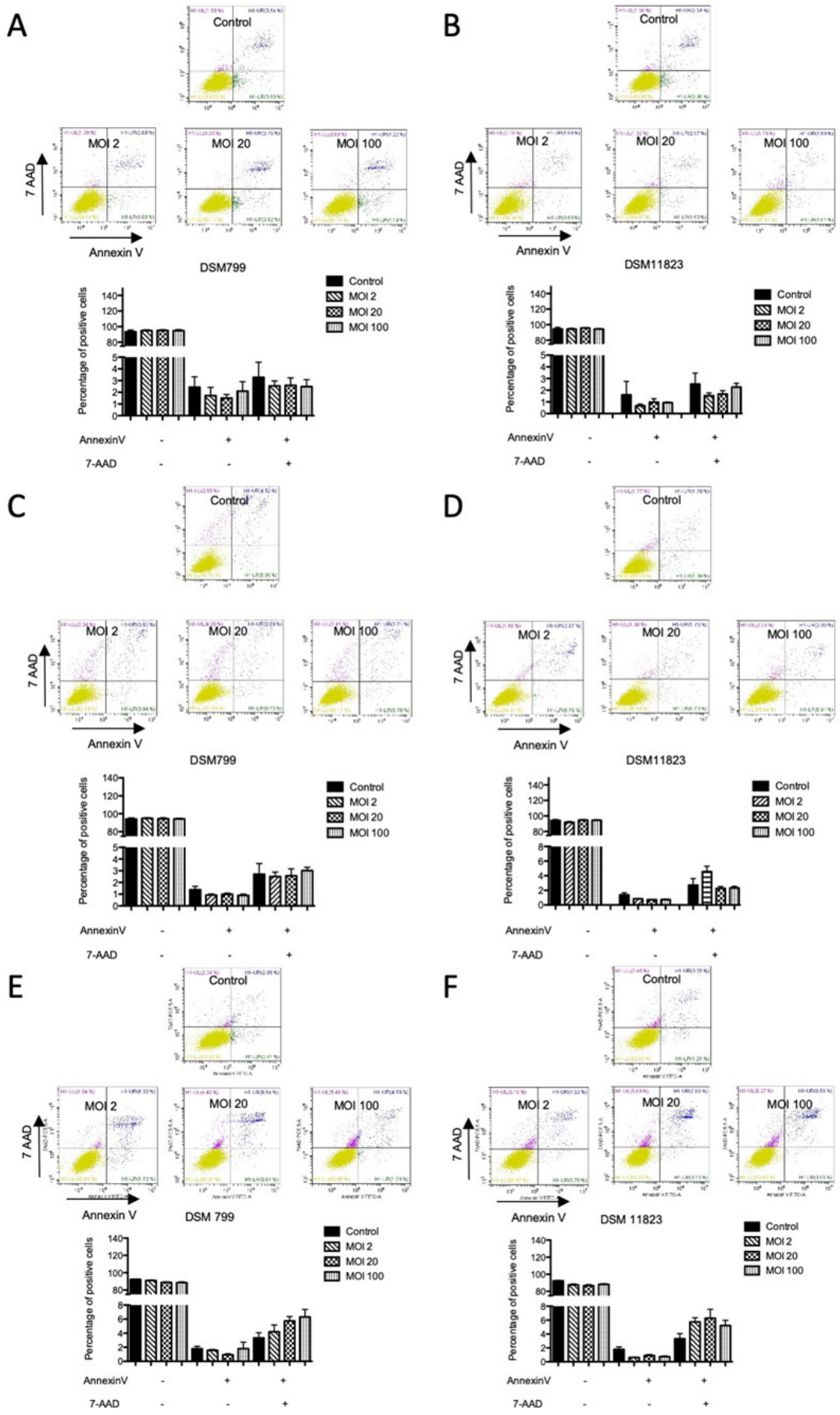
A
Control
MOI 2
MOI 20
MOI 100
7 AAD
Annexin V
DSM799
Percentage of positive cells
Control
MOI 2
MOI 20
MOI 100
AnnexinV - + +
7-AAD - - +
B
Control
MOI 2
MOI 20
MOI 100
7 AAD
Annexin V
DSM11823
Percentage of positive cells
Control
MOI 2
MOI 20
MOI 100
AnnexinV - + +
7-AAD - - +
C
Control
MOI 2
MOI 20
MOI 100
7 AAD
Annexin V
DSM799
Percentage of positive cells
Control
MOI 2
MOI 20
MOI 100
AnnexinV - + +
7-AAD - - +
D
Control
MOI 2
MOI 20
MOI 100
7 AAD
Annexin V
DSM11823
Percentage of positive cells
Control
MOI 2
MOI 20
MOI 100
AnnexinV - + +
7-AAD - - +
E
Control
MOI 2
MOI 20
MOI 100
7 AAD
Annexin V
DSM 799
Percentage of positive cells
Control
MOI 2
MOI 20
MOI 100
AnnexinV - + +
7-AAD - - +
F
Control
MOI 2
MOI 20
MOI 100
7 AAD
Annexin V
DSM 11823
Percentage of positive cells
Control
MOI 2
MOI 20
MOI 100
AnnexinV - + +
7-AAD - - +

Figure 40. Apoptosis and live/dead assay of SCC and HaCaT cells. HSC-1 (A, B), SCL-1 (C, D) and HaCaT (E, F) cells challenged with S. aureus DSM799 and DSM11823 assessed by Annexin V/7-AAD staining and flow cytometry. No significant difference in apoptotic and necrotic cells were evident compared to controls. Bar chart representation of three independent Annexin V/7-AAD assays showing the percentage of viable (Annexin 7-AAD-), apoptotic (Annexin V+/7-AAD-) and dead (Annexin V+/7-AAD+) cells, respectively. Bars show the mean ±SD. *p<0.05, **p<0.01, ***p<0.001, by one-way ANOVA and post-hoc Dunnett's test. Adopted from (1).

1.8. Human ß-defensins (hBD) differentially regulate the cell proliferation of cSCC cells.

hBDs are known to mediate cell proliferation of various tumor cell lines like oral and head and neck squamous cell carcinoma.(121, 133, 190) and are also the major AMPs produced by human skin (49, 115). hBD-2, -3 and -4 have also been implicated to stimulate epidermal keratinocyte migration and proliferation (115). To assess whether hBDs directly induce cell growth of SCC cells, we incubated cells with 20 µg/ml hBD-1, -2 and -3, a concentration found on human skin (115) and monitored cell proliferation with a live-cell monitoring system (xCelligence^{TM}) as well as by a standard cell counting assay (CCK-8). hBD-2 treatment significantly increased proliferation of HSC-1 cells (normalized cell index [nci] 3.147 ± 0.09 vs. 2.64 ± 0.05 at 16 h incubation) and SCL-1 cells (nci 6.28 ± 0.6 vs. 4.38 ± 0.3), whereas hBD-3 significantly impaired cell growth of both HSC-1 (nci 1.41 ± 0.15 vs. 2.64 ± 0.05) and SCL-1 cells (nci 2.96 ± 0.3 vs. 4.38 ± 0.3), respectively. hBD-1 showed no effect on cell growth (Figure 41 A). A similar pattern of proliferation was observed after 24 hrs when assessed using CCK-8 assay. HSC-1 cells treated with hBD-2 showed increased growth (0.91 ± 0.02% vs. 0.76 ± 0.05%) and when treated with hBD-3 showed reduced growth (0.36 ± 0.02% vs. 0.76 ± 0.05%) compared to controls; SCL-1 cells treated with hBD-2 also showed increased growth (0.89 ± 0.02% vs. 0.77 ± 0.01%) and when treated with hBD-3 showed reduced growth (0.55 ± 0.03% vs. 0.77 ± 0.01%) compared to controls (Figure 41 B) (1).

In summary, these data demonstrate that *S. aureus* particularly stimulated *hBD-2* expression in both cutaneous SCC cell lines HSC-1 and SCL-1, which also led to increased tumor cell growth. Such effects were not observed by infecting the non-tumorous HaCaT cell line. In particular, hBD-2 and hBD-3 have opposing effects on SCC cell growth, wherein the former

induces, and the latter inhibits proliferation. Since *S. aureus* mainly induces hBD-2 expression in SCC cells, it is intriguing to speculate that *S. aureus* overabundance prevalent in SCC might favor increased tumor cell proliferation which might impact its growth and disease progression (1).

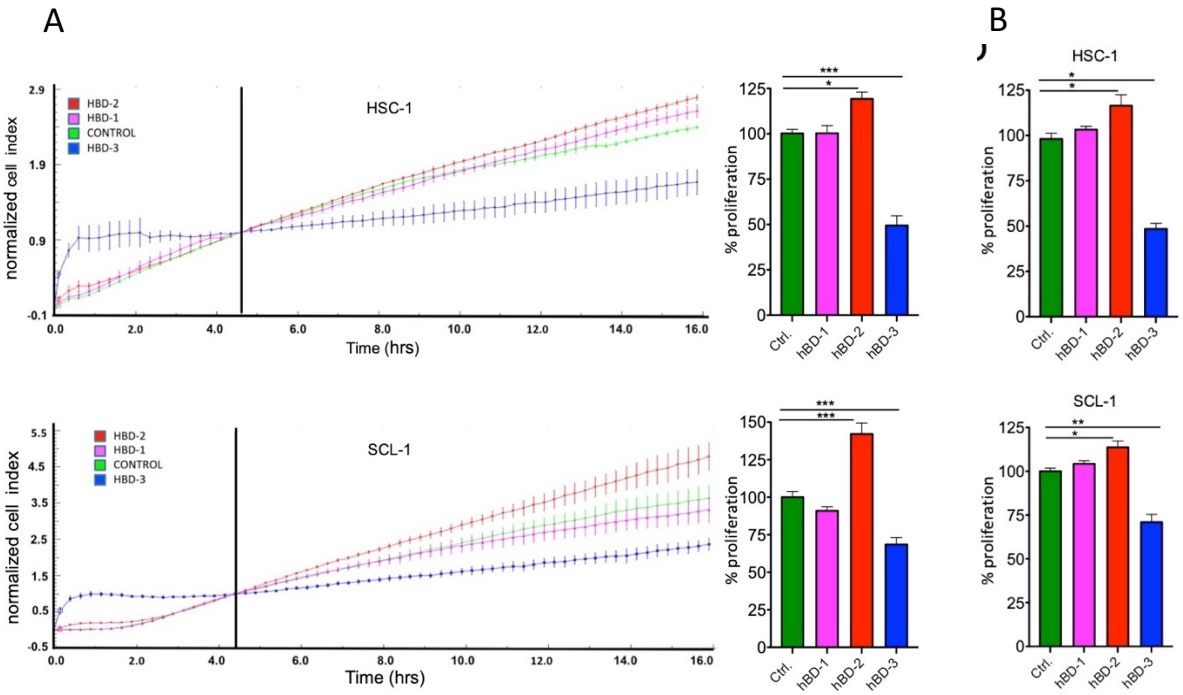

Figure 41. hBD-2 expression leads to increased cell proliferation: (A) Real-time monitoring of HSC-1 growth with the xCelligenceTM system during challenge with 20 µg/ml hBD-1, -2 and -3, respectively. A significantly increased cell proliferation indicated by the normalized cell index during hBD-2 challenge and a significantly decreased proliferation during hBD-3 challenge was detected after 16 hrs (*p<0.05; ***p<0.005, one-way ANOVA, Turkey's multiple comparison test). (B) Relative (%) cell proliferation compared to controls (untreated cells) after 16 hrs using the xCelligenceTM system (*p<0.05; ***p<0.005, one-way ANOVA, Turkey's multiple comparison test). (C) Increased (hBD-2) and decreased (hBD-1) cell proliferation of HSC-1 cells treated with 20 µg/ml hBD-1, -2 and -3 for 24 hrs measured by the CCK-8 assay (*p< 0.05, Kruskal-Wallis, Dunn's multiple comparison test). Adopted from (1).

Part 2:

2. *Fusobacterium* and *F. nucleatum* are increased in adenomatous polyps and colorectal carcinoma

Another well-characterized microbial habitat is the gastrointestinal tract, which is home to trillions of microbes. These microbiota, along with their metabolic byproducts and host interactions, directly influence both normal physiology and disease processes. Fusobacterium species, specifically *F. nucleatum* has been associated with tumorigenesis of epithelial tumors of the GI tract (89, 96, 97). In this regard, the Fusobacterium-specific adhesin FadA has shown to drive tumorigenesis. Quantitative real-time PCR was performed using *Fusobacterium* genus-specific and *Fusobacterium nucleatum* specific primers. Normal colon tissue, colon adenomatous polyps (i.e. the non-invasive precursor) and invasive colon carcinoma (CRC) specimens served as input for qPCR. A gradual increase in the abundance of *Fusobacterium* and *F. nucleatum* was measured from normal colon to adenoma and colorectal carcinoma. Interestingly, a decrease in *FadA* levels was observed from adenoma to carcinoma suggesting a down-regulation of this virulence factor during neoplasia progression (figure 42A). A similar pattern of expression was observed in paired adenoma and carcinoma samples as well (figure 42 B).

A

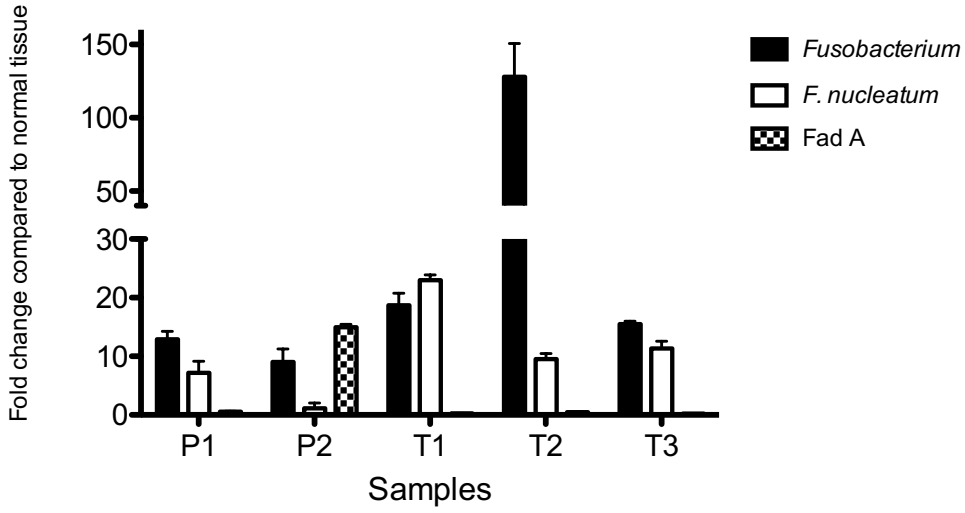

B

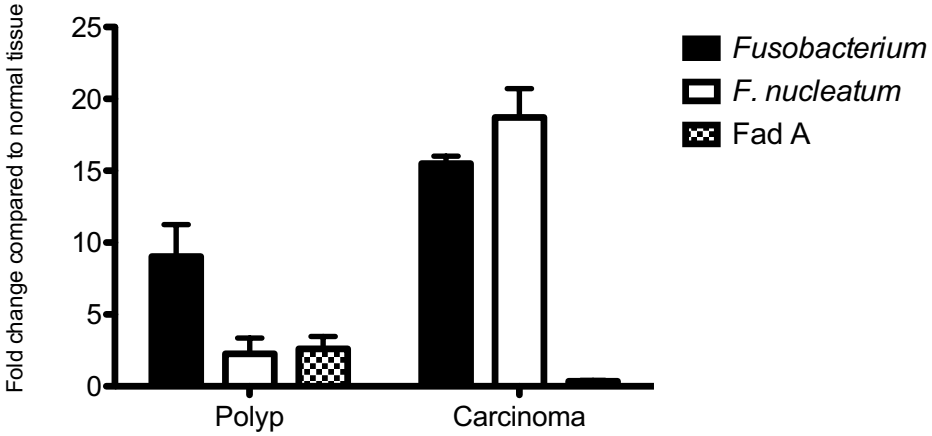

Figure 42. *Fusobacterium* and *F. nucleatum* abundance increase in polyps and colorectal carcinoma. Quantitative real-time PCR for the detection of *Fusobacterium*, *F. nucleatum* and FadA in A: polyps (P) and carcinoma (T) B: In a paired sample of polyp and carcinoma.

Part 3:

Published in https://doi.org/10.3389/fmicb.2017.00180

3. Optimization of fungal DNA isolation and amplification from skin FFPE samples

We compared fungal DNA yield and amplification of skin FFPE samples extracted from Qiagen FFPE kit with modifications. Mechanical disruption using bead-beating was added to the extraction procedure since this step was shown to be crucial for complete lysis of microbial cells in specimens, significantly influencing correct community representation (191, 192). Interestingly, bead-beating significantly led to lower DNA yields (Table 7) in comparison to extraction without bead-beating (Figure 43 A), and a significantly decreased signal-to-noise ratio in ITS PCR, impairing efficient fungal PCR amplification (Figure 43 B). Thus, mechanical lysis of specimens could also prevent reliable mycobiota analysis especially if low-biomass samples like skin are used (2).

Next, in an attempt to use the most appropriate primers to retrieve much of the fungal community present in skin FFPE samples, we used ITS1F and ITS2 R to amplify the ITS1 region and ITS3F and ITS4R to amplify the ITS2 region (193, 194). We observed increased PCR performance using ITS2 primers in human skin FFPE sample's DNA isolated without bead-beating. Table 8 summarizes commonly used ITS1 and ITS2 oligonucleotide primers. Thus, these results indicate that the choice of the DNA isolation method and the use of ideal ITS region for fungal amplification needs to be adapted depending on the requirements of the study (Eg: type of tissue material and site of investigation) (2).

Sample ID	Diagnosis	DNA (ng) with bead beating	DNA (ng) without bead beating
S1	Healthy skin	22,7	43,8
S2	Keratocanthoma	14,24	67,73
S3	Healthy skin	16,54	52,07
S4	Basal cell carcinoma	8,19	47,25
S5	Squamous cell carcinoma	3,56	157
S6	Basal cell carcinoma	72,66	151,49
S7	Healthy skin	40,16	76,67
S8	Healthy skin	37,56	63,98
S9	Healthy skin	1,2	23,14
S10	Skin diagnosed with fungal infection	18,14	57,73

Table 7. Samples used in the study and assessment of DNA extraction protocol with and without bead beating. Adopted from (2).

Region	Name	Sequence (Forward)	Name	Sequence (Reverse)	Length (bp)	Tm (°C)	References
ITS1	ITS1	TCCGTAGGTGAACCTGCGG	ITS2	GCTGCGTTCTTCATCGATGC	~290	65	White et al., 1990; Muñoz-Cadavid et al., 2010; Schoch et al., 2012
	ITS5	GGAAGTAAAAGTCGTAACAAGG	ITS2	GCTGCGTTCTTCATCGATGC	~315	63	White et al., 1990
	ITS1F	CTTGGTCATTTAGAGGAAGTAA	ITS2	GCTGCGTTCTTCATCGATGC	~350	51	Mello et al., 2011
	ITS1-F_KYO2	TAGAGGAAGTAAAAGTCGTAA	ITS2_KYO2	TTYRCTRCGTTCTTCATC	~300–400	47	Toju et al., 2012
	18S-F	GTAAAAGTCGTAACAAGGTTTC	5.8S-1R	GTTCAAAGAYTCGATGATTCAC	~300–400	*ns	Findley et al., 2013
ITS2	ITS3	GCATCGATGAAGAACGCAGC	ITS4	TCCTCCGCTTATTGATATGC	~330	62	White et al., 1990, Muñoz-Cadavid et al., 2010; Mello et al., 2011; Flury et al., 2014
	ITS3_KYO2	GATGAAGAACGYAGYRAA	ITS4	TCCTCCGCTTATTGATATGC	~400	47	Toju et al., 2012
	fITS9	GAACGCAGCRAAIIGYGA	ITS4	TCCTCCGCTTATTGATATGC	~390	55	Ihrmark et al., 2012
	fITS7	GTGAR TC ATC GAATC TTTG	ITS4	TCCTCCGCTTATTGATATGC	~340	57	Ihrmark et al., 2012
	gITS7	GTGARTCATCGARTCTTTG	ITS4	TCCTCCGCTTATTGATATGC	~340	56	Ihrmark et al., 2012
	5.8S-F	GTGAATCATCGARTCTTTGAAC	28S1-R	ATGCTTAAGTTCAGCGGGTA	~300	*ns	Findley et al., 2013
ITS1-2 incl. 5.8S rRNA gene	ITS5	GGAAGTAAAAGTCGTAACAAGG	ITS4	TCCTCCGCTTATTGATATGC	~641	58	White et al., 1990; Muñoz-Cadavid et al., 2010; Flury et al., 2014
	ITS1F	CTTGGTCATTTAGAGGAAGTAA	ITS4-B	CAGGAGACTTGTACACGGTCCAG	~600	55	Gardes and Bruns, 1993
	ITS1-F_KYO2	TAGAGGAAGTAAAAGTCGTAA	ITS4	TCCTCCGCTTATTGATATGC	~700	47	Toju et al., 2012

ns, not specified.

Table 8. Overview of commonly used ITS1 and ITS2 primer pair. Adopted from (2).

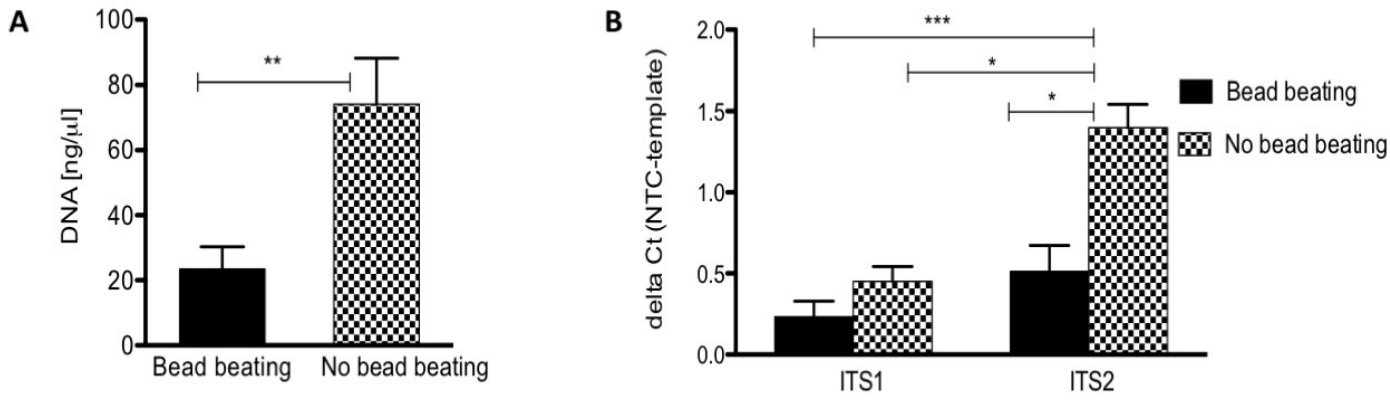

Figure 43. Fungal DNA isolation and ITS amplification (A) Significant difference in the concentration of isolated DNA with and without bead beating (**p<0.005 by Mann Whitney test; n=10; data are mean±SEM). (B) Significantly higher detection of fungal abundance using

ITS2 primers from DNA isolated without bead beating, (*p< 0.05, ***p<0.005; n=10 by Kruskal-Wallis; data are mean±SEM). Adopted from (2).

VI. Discussion

Malignant tumors are intricate gathering of transformed cells harboring genetic aberrations associated with non-neoplastic cells which include immune and stromal cells as well as microbes. Notably, the development of cancer affects the normal microbiome and vice versa. Depending on the type of microbes present, the lesion could either progress or regress to cancer. Indeed, the homeostatic balance between host and microbiome is either disturbed or restored and the mechanism by which this dysbiosis or eubiosis impacts progression or regression to cancer includes pro-inflammatory or anti-inflammatory response. Skin and colon both represent organs, which harbor considerable bacterial microbiome. Also, apart from bacteria, fungi constitute an important part of the human microbiota. In this regard, we demonstrate 3 aspects in this thesis. Our first findings indicate that changes in the skin microbiota emerging during carcinogenesis of epithelial skin tumors could promote tumor growth via modulation of AMP expression. We further show in the second part, the abundance of *Fusobacterium* species in adenomatous polyps and CRC in comparison to normal tissue. Finally, the third part demonstrates an optimal method to extract DNA from skin FFPE samples and the use of ideal ITS region for fungal amplification.

Skin being the largest organ of the human body, represents the first line of defense against foreign microbes (33). DNA sequencing studies have aided in identification of skin disorder associated microbes such as *S. aureus* with atopic dermatitis and *P. acnes* with acne vulgaris (19). However, the role of skin microbiome in carcinogenesis is not well studied. Since skin FFPE samples were used for the study, optimization of an ideal DNA isolation method was essential to isolate maximum microbial DNA present in our skin sample entities. From our analysis, Maxwell 16 FFPE Plus LEV DNA purification kit demonstrated to be better than the QIAamp DNA FFPE tissue kit. Additional sequential bead-beating and enzymatic steps aided in better isolation of microbial DNA by effective cell lysis. This process aided in better homogenization of skin tissue samples which is difficult to lyse given their structure. Also, since skin harbors a significant number of gram-positive bacteria, using lytic enzymes (mutanolysin and lysostaphin) led to better isolation of microbial DNA. For eg lysostaphin, a glycylglycine endopeptidase is known to specifically cleave the cross-linking pentaglycine bridges in the cell wall of *staphylococci* (149, 195). Similarly, Mutanolysin also has lytic activity against some species of *Streptococcus* and *Lactobacillus* (149, 196). Finally, Maxwell

16 FFPE Plus LEV DNA purification kit being semi-automated eased the DNA isolation procedure for a large sample set.

We next assessed the microbiota of main keratinocyte skin tumors- AK, SCC & BCC. Histology revealed significant microbial colonization mainly in AKs and SCCs. Microbiota profiling of these keratinocyte skin tumors showed significantly different microbial community compositions in comparison to normal skin, and also in between tumor entities. Our analysis showed that AK and SCC have a significantly higher microbial richness but lower evenness and diversity as compared to BCC. These results suggest the presence of certain dominant (driver) bacteria in AK and SCC. PCoA showed a significant difference in the microbial community between AK and SCC compared to BCC, but no difference between AK and SCC. Given that each entity is signified by a specific histoarchitecture (microanatomy), representing different microbial habitats, it is reasonable to hypothesize that these specific niches might select for a certain microbiota composition. This notion is also supported by the fact that AK, the precursor lesion, and SCC, the advanced (invasive) tumor, represent rather similar microbiota compositions differing from BCC. One hallmark feature of AK and SCC is hyper- and parakeratosis, which represents abundant layered keratin on the lesional surface. Microscopy revealed abundant microbial structures resembling cocci in regions of hyper and/or parakeratosis. Bacterial load assessed by qPCR showed no change in AKs and SCCs compared to normal skin but a reduction in BCC. Taxonomic analysis showed increased *Staphylococcus* in AKs and SCCs and an overabundance of the species *S. aureus* in SCCs as a prominent feature which was also confirmed by qPCR. However, the cause for increased S. *aureus* in relation to the resident microbiota in cSCCs is so far not known, but the reasons could be several. In our study, *S. aureus* loads as determined by qPCR and the hyper-/parakeratosis as measured using microscopy did not significantly correlate. Viewing this from the perspective of host-microbiota interdependence, it could be hypothesized that a changed microbial habitat (eg: hyperkeratosis) could change the ability of certain microbes to colonize (1). Also, other studies support the fact that hyperkeratosis does not seem to favor *S. aureus* growth. For example, a study by Kullander *et al* investigating the benign skin lesion seborrheic keratosis, also characterized by hyperkeratosis, found no *S. aureus* overabundance (169). Additional assessment of psoriasis samples in our study (also hyper- and parakeratotic) did not show an overabundance of *Staphylococcus aureus* (Figure 24). Notably, current knowledge suggests that psoriasis is dominated by bacterial taxa like *Streptococcus*, *Corynebacterium* or the fungi *Malassezia* and *Candida* (197-202) but the association of *S. aureus* with psoriasis is

not clear so far (203). Also, other factors such as tumor-specific metabolites could play an important role in promoting colonization with *S. aureus.* Interestingly the skin of immunocompetent individuals is typically not infected with *S. aureus* unless the barrier is injured or broken (204). Thus, the ulcerating nature of SCC might also favor *S. aureus* colonization. Importantly, *S. aureus* was also found in the infiltrative neoplastic epithelium in SCCs, which could be of pertinence to the progression of the disease. Drawing parallels to what is known with *F. nucleatum* and colorectal cancer, its shown that *F. nucleatum* migrate with invasive and metastatic tumor tissue, in turn having a direct influence on cancer cell proliferation and growth (205). Lastly, *S. aureus* growth could also be influenced by the changed metabolism of neoplastic cells. Both AKs and SCCs are known to have impaired production of sebum (206) which could inhibit commensals like *Propionibacterium* (dependent on lipids derived from sebum), in turn opening niches for proliferation of *S. aureus* (16, 207). Another skin commensal, which is a known competitor of *S. aureus* is *S. epidermidis*. Notably, we found that abundance of *S. epidermidis* as measured by qPCR was reduced in tumors in comparison to normal skin, supporting the notion that increased pathogenic *S. aureus* colonization might lead to decreased commensal abundance. Also, *S. epidermidis* was recently shown to protect against skin cancer (1, 10, 17, 48).

Approximately 15 % of the human cancers are attributed to infectious sources (208) wherein the concomitant type and the severity of inflammation is often a predictor of tumor progression (209). Consequently, certain microbiome-types likely show a stronger capacity to drive tumorigenesis. One such example is *Helicobacter pyroli* inducing chronic gastritis and stomach cancer (210). *Staphylococcus aureus* is an important human pathogen which is known to be responsible for a vast majority of bacterial skin infections in humans (49). It is known to be associated with flares of atopic dermatitis (43, 46) and could also be often isolated from chronic wounds and burn scars (211). However, *S. aureus* is also known to asymptomatically colonize 30% of the healthy individuals but it is generally considered pathogenic if present on the skin and is known to drive inflammation (46, 56, 117). We, therefore, graded the level of inflammation in our keratinocyte skin tumor samples and assessed whether the microbial community types are different. Higher inflammation levels significantly correlated with increased species richness, a different microbial community type and increased abundance of *Staphylococcus* in only AK but not in SCC or BCC, suggesting the involvement of *Staphylococcus* in skin tumor development. We also observed increased abundance of *S. aureus* correlating with higher inflammation levels in AK. Interestingly, the common skin

commensal *S. epidermidis* is known to dampen inflammation (212) and enhances the expression of the AMPs in keratinocytes to increase skin defense against infection (213), which correlates to less or no detection of *S. epidermidis* in our tumor entities.

Keratinocytes actively participate in the innate immune response of the skin by the production of various cytokines, chemokines and AMPs. AMPs are important in skin defense mechanisms and act against a broad spectrum of microbes (214). They are also known to be involved in tumor development and their altered expression in keratinocyte tumors are extensively studied (118, 141, 186, 189). The association of hBDs and *S. aureus* in each of the skin disorders are different indicating no general mechanism of this association. For example, in purulent skin infections, *S. aureus* severity is known to be associated with induction of hBD-3 but not hBD-2(214); in chronic venous ulcer, a significant induction of hBD-2 and psoriasin was observed but no significant association between bacterial colonization and AMP expression were observed (215); several studies in AD have shown increased as well as impaired hBD expression depending on the severity of infection and inflammation (216). Also, specific *Staphylococcal* enterotoxin A producing *S. aureus* strain isolated from AD induced upregulation of hBD-2 expression in HaCaT which could result in the induction of persistent eczematous skin lesion indicating strain-specific effects (217). Contrasting to these findings, nasal carriers of *S. aureus* showed a down regulation of hBD-2 and -3 retaining an advantage of epithelial colonization and infection (218). It has been shown that infection of human primary epidermal keratinocytes or HaCaT with *S. aureus* leads to upregulation of hBD-2, hBD-3 and RNase 7 (118, 186). However, the differentiation state of the keratinocyte is a major factor contributing to the expression pattern of hBDs (74). In particular, hBD-2 and the constitutively expressed hBD-1 exerts only weak activity against *S. aureus* unlike hBD-3 and RNase7 which are highly active against *S. aureus* (187). Importantly, *S. aureus* seem to have developed strategies to repress AMP action. For example, IsdA (surface protein iron surface determinant A) of *S. aureus* is known to decrease bacterial cellular hydrophobicity making the bacteria resistant against hBD-2 (1, 219).

Interestingly, studies show that skin keratinocytes discriminate the commensal *S. epidermidis* from pathogenic *S. aureus* by differentially inducing AMPs and activating distinct signaling pathways which in turn induce an adaptive and innate immune response accordingly (74). Also, both the mechanisms induced by commensal and pathogen are known to act in a synergetic manner to amplify the immune response in human skin (74). Of note, hBD-3 is known to be

highly active against *S. aureus* (187) and, according to our study, exerts a suppressive growth of the cSCC cells. Also, *S. epidermidis* is known to inhibit both nares colonization and biofilm formation by *S. aureus* (220) (213). Further, *S. aureus* colonization has shown to reduce the abundance of *S. epidermidis.* Hence, from our findings, it could be claimed that due to high abundance of *S. aureus* colonization in our tumor entities AK & SCC, *S. epidermidis* abundance is inhibited which in turn explains the low or nil induction of hBD-3 expression when challenged with *S. aureus.*

Our experiments investigating SCC cells originating from cutaneous tumor were reported for the first time to the best of our knowledge. We noted significant induction of only hBD-2 after *S. aureus* challenge, whereas hBD-1 and hBD-3 were not induced. Interestingly, hBDs are known to be involved in neoplasia progression (221). Several studies have reported dysregulation of hBDs in various cancers cells like oral, esophageal, kidney, liver and others (221). Depending on the anatomical locations and cancer type, hBDs seem to be differentially regulated (221). Hence, the induction of just hBD-2 in cSCC after *S. aureus* challenge that we observed seems to be specific to keratinocyte skin cancer cells. Also, each AMP affects the growth promotion and migratory behavior of keratinocytes which seem to be largely dependent on the origin of the cell (221). For example, hBD-1 has shown to inhibit migration and proliferation of oral, prostrate, renal and bladder tumor cells (222-224) whereas hBD-2 has shown to inhibit the proliferation of oral cancer cells and promote the proliferation of esophageal, lung and cervical cancer cells (134, 135, 190, 225). Meanwhile, hBD-3 promoted the proliferation and migration of cervical cancer cells and inhibited colon cancer cell migration (226, 227). Therefore, it has been claimed that a specific ß-defensin may promote or inhibit cancer cell proliferation/migration depending on the origin of the cancer cell, and the consequence is known to be associated with whether the defensin is increased or decreased in the tumor from which the cells originate (1, 221).

In our study, only hBD-2 challenge promoted an increased cSCC cell proliferation, suggesting a self-perpetuating circulus-vitiosus for *S. aureus* and keratinocyte skin cancer. In contrast, hBD-3, which was not induced by *S. aureus* challenge, had an inhibitory effect on the cSCC cells suggesting that a change in the expression pattern of hBD-2 and hBD-3 in cutaneous SCC might be the basis of growth promotion induced by *S. aureus* colonization. However, none of these effects were seen in non-tumorous keratinocytes i.e., HaCaT. Notably, differential expression of AMPs in our tumor tissue samples such as increased hBD-3 mRNA expression

in AK and SCC as measured by qPCR but no significant increase of hBD-3 mRNA in cSCC cells when treated by *S. aureus* could also be attributed to other factors like UV which are known to modulate skin AMPs vastly (228).

Another important factor for consideration is the microbiota composition of the skin that varies greatly from oral or GI mucosa, implying that the cutaneous and mucosal development of SCC and involvement of resident microbiota might differ greatly (229). For example, oropharyngeal mucosa is colonized by a completely different microbiota than the skin and also tumors arising at this site are primarily caused by smoking and HPV, thus representing a differing SCC etiology compared to human skin. Interestingly, in a non-neoplastic disease like atopic dermatitis, induction of skin keratinocyte proliferation by *S. aureus* was recently shown (48). A lowered hBD-2, -3 and LL-37 expression in AD which are driven by skewed cytokine signaling appear to influence *S. aureus* colonization (230-232). Other factors like the severity of inflammation and infection in AD also influence AMP expression levels (216). Therefore, molecular factors of *S. aureus* which are involved in driving skin pathogenesis and tumorigenesis depends on the context and would need to be elucidated by further research (1).

In summary, these results show an increased *Staphylococcus aureus* abundance in AK and SCC, dominating the hyperkeratotic region, significantly inducing hBD-2 expression which in turn leads to hyperproliferation of squamous epithelia. These results are specific to cSCC as is observed in two cSCC cell lines with two different strains of *S. aureus*. Collectively, this knowledge might aid in the development of biotherapeutics for out-competition of skin pathogens such as *S. aureus*. Since *S. aureus* is also genetically diverse and expresses a varying repertoire of virulence factors, it could be that only certain strains of *S. aureus* are involved in SCC pathogenesis. Therefore, cultivation studies enabling genomic investigations of *S. aureus* strains derived from AK and SCC samples are important for future research aims. Such knowledge might also allow the development of (bacterial) biomarkers for risk assessment of AK to SCC progression (1).

Colorectal carcinoma (CRC) similar to cSCC, is also a malignant tumor known to develop from specific precursor lesions, i.e. adenomatous polyp. Kostic et al (2012) characterized the microbial composition of CRC and found that *Fusobacterium nucleatum* was enriched in carcinomas (89). Later McCoy et al (2013) showed that the *Fusobacterium* is enriched in adenomas in comparison to normal tissues (97). We validated these results and observed a

subsequent increase in the abundance of *Fusobacterium* and *F. nucleatum* in adenoma and carcinoma in comparison to healthy tissue and also from polyp to carcinoma in paired samples. A decrease in the adhesion molecule FadA from adenoma to carcinoma which is required by the *F. nucleatum* for attachment and invasion into epithelial cells was observed suggesting a downregulation in the advanced entity. Multiple potential mechanisms have been studied so far by which *F. nucleatum* promotes CRC. Interestingly, *Fusobacterium* overabundance is also positively correlated with IBD (102). IBD is associated with an increased risk for the development of CRC. Hence, it would be noteworthy to explore the link between the role of *Fusobacterium* spp. in colorectal carcinoma pathogenesis and its associated IBD cases.

Lastly, we also addressed some of the critical issues in mycobiota analysis in our study. Fungi are prevalent in all microbial colonized body sites such as skin, gastrointestinal, respiratory and genital tract (2). Fungal cell abundance varies from <0.1% of microorganisms in the GI tract to up to 10% on the skin, depending on the habitat (31). However, microbiota investigations have mainly focused on bacteria and measures to culture and characterize fungi are not well established. A variety of clinical specimens like whole blood, plasma, serum, fresh tissues, biopsies, cells in culture, and paraffin-embedded tissue specimens are used for detection and identification of fungal pathogens. A number of methods and kits are available for isolation and purification of fungal DNA (12) (233-236) though they all follow similar basic processes. However, formalin-fixed paraffin-embedded (FFPE) specimens represent an important source of archived and morphologically defined material when fresh clinical tissue is unavailable or difficult to obtain (237, 238). Nucleic acid isolation from FFPE tissues are known to be quite challenging in comparison to fresh tissue. This could be due to cross-linking of biomolecules, fragmentation of nucleic acids and also the period from the time of fixation. Many other factors, such as the pH value of the fixative, storage conditions, and particularly the extraction methodology, are known to influence the obtained nucleic acid quality greatly (238, 239). Also, the isolated DNA may contain remnants of substances that might inhibit the amplification reaction and chemicals such as formalin may inhibit the proteinase K used in DNA extraction (194, 240). In short, obtaining high-quality fungal DNA from FFPE is difficult, as only minimal quantities of intact DNA may be present in the sample (194). Therefore, finding the most suitable method of nucleic acid isolation from clinical samples, especially from FFPE yielding maximum coverage of the fungi present is an indispensable factor. Several protocols and kits have been described for isolation and purification of fungal nucleic acids from environmental samples and FFPE so far. The protocol generally involves

mechanical tissue disruption, enzymatic cell membrane lysis; especially addition of lyticase to break down the rigid fungi cell wall followed by column or automated isolation (233, 241). A total of 69 commercially available kits are known to be reported for manual and automated extraction of nucleic acids from FFPE material (238). However, Cadavid et al., 2010 have shown that two kits- TaKaRa (Takara Bio Inc, Shiga, Japan) and QiaAmp kit (Qiagen, Chatsworth, CA) to be efficient in fungal DNA isolation from FFPE with slight modifications from the suggested kit's protocol (194). In our study, we used the Qiagen FFPE kit with modifications suggested by Cadavid et al., 2010, both with and without bead beating. Interestingly, we observed that bead-beating significantly lead to lower DNA yields and a significantly decreased signal-to-noise ratio in ITS PCR, impairing efficient fungal PCR amplification. Though, we observed from our studies on skin FFPE samples that using bead beating in the isolation procedure led to a reduction in fungal detection, other factors such as the fungal abundance, type of sample and difference in the body site such as skin, lung, gut, scalp etc influence detection to a great extent. Therefore, it is important to take into account the above factors while choosing the right method for isolation (2).

Once the DNA is extracted, in order to amplify the fungal DNA, a multitude of primers have been designed so far (233). The internal transcribed region (ITS) was proposed as the formal barcode for fungal detection (233, 242). ITS1 and 2 regions of fungal ribosomal DNA are highly variable sequences and can be used to distinguish fungal species by PCR analysis (243). In general, ITS primers make use of the conserved regions, 18S, 5.8S, and 28S, of the rRNA gene to amplify the non-coding but transcribed regions between them (193). However, unlike for bacterial detection where 16S V1-V2 or V4 regions are known to be the most ideal marker with primers retrieving as many bacteria as possible, the primers available for fungal detection lack maximum coverage. In an attempt to use the most appropriate primers to retrieve much of the fungal community present in our FFPE sample sets, we used ITS1F and ITS2 R to amplify the ITS1 region and ITS3F and ITS4R to amplify the ITS2 region (193, 194). Two important factors that we considered while choosing primers for our study were the length of the amplified fragment (<300bp for qPCR) and to retrieve as many fungi as possible. Most of the literature known so far, claims that ITS2 region is better compared to ITS1 for fungal detection in FFPE samples (194, 244). We also observed increased PCR performance using ITS2 primers and human skin FFPE samples (Figure 41 B). However, other reports obtained similar amplification rates with ITS1 and ITS2 oligonucleotides(233, 245-247).

Also, though we observed increased PCR performance using the ITS2 primers for skin FFPE samples, several other reports have obtained similar amplification rates using both ITS1 and ITS2 primers but for different tissue material or from other body sites (233, 245, 246). Hence, it is important to take into account the type of tissue material available and the body site for fungal abundance, before finalizing on the method for DNA isolation and the ITS PCR amplification (2).

VII. Conclusions

1. Our study demonstrates the involvement of *S. aureus* in cutaneous neoplasia development and progression. Neoplastic transformation (e.g., via UV) leads to an altered microbial habitat (e.g., via increased keratin production leading to hyperkeratosis). This favors protumorigenic microbiota, specifically high loads of *S. aureus*, which modulates the expression of hBDs. Induced hBD-2 confers a protumorigenic growth stimulus on tumor cells, thereby promoting tumor growth (1). Analyzing the contribution of the skin microbiota to tumorigenesis will aid in better understanding of the complex interplay between the tumor microenvironment and tumor cells. This knowledge might open new avenues for innovative therapies modulating the microbiota in UV-damaged skin, thus counteracting SCC development and progression.

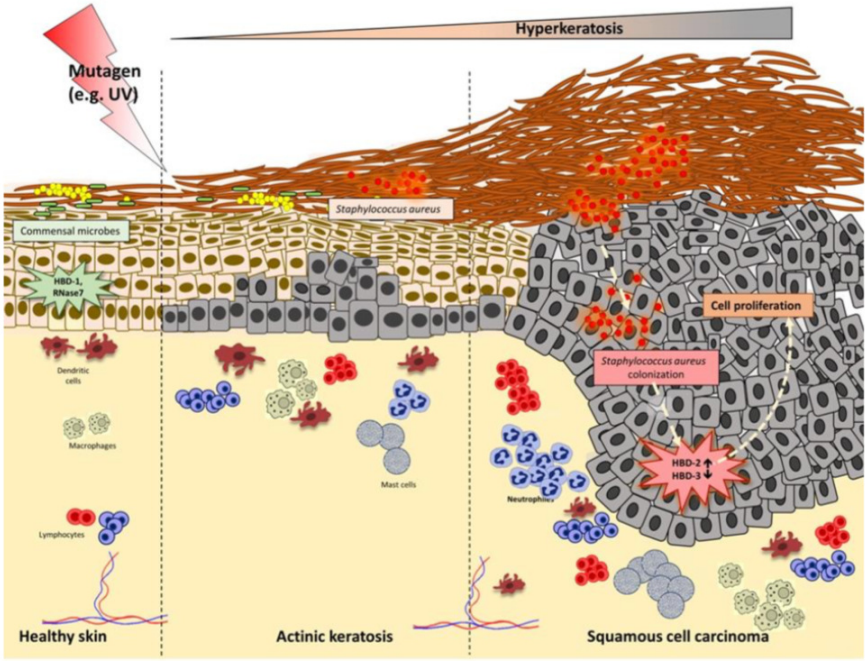

2. *F. nucleatum* is strongly associated with CRC progression from adenomatous polyps.

3. Fungal DNA isolation method and the ideal ITS region for detection of fungal abundance needs to be adapted depending on the needs of the study and also on the basis of the type of material, source and body site.

Taken together, establishing the contribution of microbiota to carcinogenesis will provide novel means for diagnostic and therapeutic interventions. Also, recognition of specific bacteria and fungi and the mechanisms by which they promote or regress carcinogenesis is necessary to advance specific therapeutic interventions.

VIII. Bibliography

1. Madhusudhan N, Pausan MR, Halwachs B, Durdevic M, Windisch M, Kehrmann J, et al. Molecular Profiling of Keratinocyte Skin Tumors Links Staphylococcus aureus Overabundance and Increased Human beta-Defensin-2 Expression to Growth Promotion of Squamous Cell Carcinoma. Cancers (Basel). 2020;12(3).
2. Halwachs B, Madhusudhan N, Krause R, Nilsson RH, Moissl-Eichinger C, Hogenauer C, et al. Critical Issues in Mycobiota Analysis. Front Microbiol. 2017;8:180.
3. Yousef H, Sharma S. Anatomy, Skin (Integument), Epidermis. StatPearls. Treasure Island (FL)2018.
4. Losquadro WD. Anatomy of the Skin and the Pathogenesis of Nonmelanoma Skin Cancer. Facial Plast Surg Clin North Am. 2017;25(3):283-9.
5. Slominski AT, Manna PR, Tuckey RC. On the role of skin in the regulation of local and systemic steroidogenic activities. Steroids. 2015;103:72-88.
6. OpenStax. Layers of the skin. 2013 June 27 2017. In: Anatomy and Physiology [Internet]. OpenStax , OpenStax Anatomy and Physiology. 6. Available from: http://cnx.org/contents/471cb008-6900-476c-8a65-539fdc592b75@6
.
7. Segre JA. Epidermal barrier formation and recovery in skin disorders. J Clin Invest. 2006;116(5):1150-8.
8. Nakatsuji T, Chiang HI, Jiang SB, Nagarajan H, Zengler K, Gallo RL. The microbiome extends to subepidermal compartments of normal skin. Nat Commun. 2013;4:1431.
9. Grice EA, Segre JA. The skin microbiome. Nat Rev Microbiol. 2011;9(4):244-53.
10. Byrd AL, Belkaid Y, Segre JA. The human skin microbiome. Nat Rev Microbiol. 2018;16(3):143-55.
11. Belkaid Y, Segre JA. Dialogue between skin microbiota and immunity. Science. 2014;346(6212):954-9.
12. Findley K, Oh J, Yang J, Conlan S, Deming C, Meyer JA, et al. Topographic diversity of fungal and bacterial communities in human skin. Nature. 2013;498(7454):367-70.
13. Gallo RL, Hooper LV. Epithelial antimicrobial defence of the skin and intestine. Nat Rev Immunol. 2012;12(7):503-16.
14. Naik S, Bouladoux N, Linehan JL, Han SJ, Harrison OJ, Wilhelm C, et al. Commensal-dendritic-cell interaction specifies a unique protective skin immune signature. Nature. 2015;520(7545):104-8.

15. Oh J, Byrd AL, Deming C, Conlan S, Program NCS, Kong HH, et al. Biogeography and individuality shape function in the human skin metagenome. Nature. 2014;514(7520):59-64.

16. Bouslimani A, Porto C, Rath CM, Wang M, Guo Y, Gonzalez A, et al. Molecular cartography of the human skin surface in 3D. Proc Natl Acad Sci U S A. 2015;112(17):E2120-9.

17. Nakatsuji T, Chen TH, Butcher AM, Trzoss LL, Nam SJ, Shirakawa KT, et al. A commensal strain of Staphylococcus epidermidis protects against skin neoplasia. Sci Adv. 2018;4(2):eaao4502.

18. Grice EA, Kong HH, Renaud G, Young AC, Program NCS, Bouffard GG, et al. A diversity profile of the human skin microbiota. Genome Res. 2008;18(7):1043-50.

19. Kong HH, Segre JA. Skin microbiome: looking back to move forward. J Invest Dermatol. 2012;132(3 Pt 2):933-9.

20. Scharschmidt TC, Fischbach MA. What Lives On Our Skin: Ecology, Genomics and Therapeutic Opportunities Of the Skin Microbiome. Drug Discov Today Dis Mech. 2013;10(3-4).

21. Grice EA. The intersection of microbiome and host at the skin interface: genomic- and metagenomic-based insights. Genome Res. 2015;25(10):1514-20.

22. Oh J, Byrd AL, Park M, Program NCS, Kong HH, Segre JA. Temporal Stability of the Human Skin Microbiome. Cell. 2016;165(4):854-66.

23. Weyrich LS, Dixit S, Farrer AG, Cooper AJ, Cooper AJ. The skin microbiome: Associations between altered microbial communities and disease. Australas J Dermatol. 2015;56(4):268-74.

24. Costello EK, Lauber CL, Hamady M, Fierer N, Gordon JI, Knight R. Bacterial community variation in human body habitats across space and time. Science. 2009;326(5960):1694-7.

25. Eckburg PB, Bik EM, Bernstein CN, Purdom E, Dethlefsen L, Sargent M, et al. Diversity of the human intestinal microbial flora. Science. 2005;308(5728):1635-8.

26. Dewhirst FE, Chen T, Izard J, Paster BJ, Tanner AC, Yu WH, et al. The human oral microbiome. J Bacteriol. 2010;192(19):5002-17.

27. Bik EM, Eckburg PB, Gill SR, Nelson KE, Purdom EA, Francois F, et al. Molecular analysis of the bacterial microbiota in the human stomach. Proc Natl Acad Sci U S A. 2006;103(3):732-7.

28. Pei Z, Bini EJ, Yang L, Zhou M, Francois F, Blaser MJ. Bacterial biota in the human distal esophagus. Proc Natl Acad Sci U S A. 2004;101(12):4250-5.
29. Gao Z, Tseng CH, Pei Z, Blaser MJ. Molecular analysis of human forearm superficial skin bacterial biota. Proc Natl Acad Sci U S A. 2007;104(8):2927-32.
30. Grice EA, Kong HH, Conlan S, Deming CB, Davis J, Young AC, et al. Topographical and temporal diversity of the human skin microbiome. Science. 2009;324(5931):1190-2.
31. Belkaid Y, Naik S. Compartmentalized and systemic control of tissue immunity by commensals. Nat Immunol. 2013;14(7):646-53.
32. Underhill DM, Iliev ID. The mycobiota: interactions between commensal fungi and the host immune system. Nat Rev Immunol. 2014;14(6):405-16.
33. Findley K, Grice EA. The skin microbiome: a focus on pathogens and their association with skin disease. PLoS Pathog. 2014;10(10):e1004436.
34. Hannigan GD, Meisel JS, Tyldsley AS, Zheng Q, Hodkinson BP, SanMiguel AJ, et al. The human skin double-stranded DNA virome: topographical and temporal diversity, genetic enrichment, and dynamic associations with the host microbiome. MBio. 2015;6(5):e01578-15.
35. Chen AC, McMillan NAJ, Antonsson A. Human papillomavirus type spectrum in normal skin of individuals with or without a history of frequent sun exposure. J Gen Virol. 2008;89(Pt 11):2891-7.
36. Antonsson A, Erfurt C, Hazard K, Holmgren V, Simon M, Kataoka A, et al. Prevalence and type spectrum of human papillomaviruses in healthy skin samples collected in three continents. J Gen Virol. 2003;84(Pt 7):1881-6.
37. Foulongne V, Sauvage V, Hebert C, Dereure O, Cheval J, Gouilh MA, et al. Human skin microbiota: high diversity of DNA viruses identified on the human skin by high throughput sequencing. PLoS One. 2012;7(6):e38499.
38. Probst AJ, Auerbach AK, Moissl-Eichinger C. Archaea on human skin. PLoS One. 2013;8(6):e65388.
39. Moissl-Eichinger C, Probst AJ, Birarda G, Auerbach A, Koskinen K, Wolf P, et al. Human age and skin physiology shape diversity and abundance of Archaea on skin. Sci Rep. 2017;7(1):4039.
40. Koskinen K, Pausan MR, Perras AK, Beck M, Bang C, Mora M, et al. First Insights into the Diverse Human Archaeome: Specific Detection of Archaea in the Gastrointestinal Tract, Lung, and Nose and on Skin. mBio. 2017;8(6).
41. Iebba V, Totino V, Gagliardi A, Santangelo F, Cacciotti F, Trancassini M, et al. Eubiosis and dysbiosis: the two sides of the microbiota. New Microbiol. 2016;39(1):1-12.

42. Leyden JJ, McGinley KJ, Mills OH, Kligman AM. Propionibacterium levels in patients with and without acne vulgaris. J Invest Dermatol. 1975;65(4):382-4.
43. Kong HH, Oh J, Deming C, Conlan S, Grice EA, Beatson MA, et al. Temporal shifts in the skin microbiome associated with disease flares and treatment in children with atopic dermatitis. Genome Res. 2012;22(5):850-9.
44. Leyden JJ, Marples RR, Kligman AM. Staphylococcus aureus in the lesions of atopic dermatitis. Br J Dermatol. 1974;90(5):525-30.
45. Huang JT, Abrams M, Tlougan B, Rademaker A, Paller AS. Treatment of Staphylococcus aureus colonization in atopic dermatitis decreases disease severity. Pediatrics. 2009;123(5):e808-14.
46. Kobayashi T, Glatz M, Horiuchi K, Kawasaki H, Akiyama H, Kaplan DH, et al. Dysbiosis and Staphylococcus aureus Colonization Drives Inflammation in Atopic Dermatitis. Immunity. 2015;42(4):756-66.
47. Conti F, Ceccarelli F, Iaiani G, Perricone C, Giordano A, Amori L, et al. Association between Staphylococcus aureus nasal carriage and disease phenotype in patients affected by systemic lupus erythematosus. Arthritis Res Ther. 2016;18:177.
48. Byrd AL, Deming C, Cassidy SKB, Harrison OJ, Ng WI, Conlan S, et al. Staphylococcus aureus and Staphylococcus epidermidis strain diversity underlying pediatric atopic dermatitis. Sci Transl Med. 2017;9(397).
49. Krishna S, Miller LS. Innate and adaptive immune responses against Staphylococcus aureus skin infections. Semin Immunopathol. 2012;34(2):261-80.
50. McCaig LF, McDonald LC, Mandal S, Jernigan DB. Staphylococcus aureus-associated skin and soft tissue infections in ambulatory care. Emerg Infect Dis. 2006;12(11):1715-23.
51. Moran GJ, Krishnadasan A, Gorwitz RJ, Fosheim GE, McDougal LK, Carey RB, et al. Methicillin-resistant S. aureus infections among patients in the emergency department. N Engl J Med. 2006;355(7):666-74.
52. Leyden JJ, McGinley KJ, Vowels B. Propionibacterium acnes colonization in acne and nonacne. Dermatology. 1998;196(1):55-8.
53. Clavaud C, Jourdain R, Bar-Hen A, Tichit M, Bouchier C, Pouradier F, et al. Dandruff is associated with disequilibrium in the proportion of the major bacterial and fungal populations colonizing the scalp. PLoS One. 2013;8(3):e58203.
54. Alekseyenko AV, Perez-Perez GI, De Souza A, Strober B, Gao Z, Bihan M, et al. Community differentiation of the cutaneous microbiota in psoriasis. Microbiome. 2013;1(1):31.

55. Kang D, Shi B, Erfe MC, Craft N, Li H. Vitamin B12 modulates the transcriptome of the skin microbiota in acne pathogenesis. Sci Transl Med. 2015;7(293):293ra103.
56. Chen YE, Fischbach MA, Belkaid Y. Skin microbiota-host interactions. Nature. 2018;553(7689):427-36.
57. Wentworth AB, Drage LA, Wengenack NL, Wilson JW, Lohse CM. Increased incidence of cutaneous nontuberculous mycobacterial infection, 1980 to 2009: a population-based study. Mayo Clin Proc. 2013;88(1):38-45.
58. Merritt RW, Walker ED, Small PL, Wallace JR, Johnson PD, Benbow ME, et al. Ecology and transmission of Buruli ulcer disease: a systematic review. PLoS Negl Trop Dis. 2010;4(12):e911.
59. Nakabayashi A, Sei Y, Guillot J. Identification of Malassezia species isolated from patients with seborrhoeic dermatitis, atopic dermatitis, pityriasis versicolor and normal subjects. Med Mycol. 2000;38(5):337-41.
60. Dawson TL, Jr. Malassezia globosa and restricta: breakthrough understanding of the etiology and treatment of dandruff and seborrheic dermatitis through whole-genome analysis. J Investig Dermatol Symp Proc. 2007;12(2):15-9.
61. Saunders CW, Scheynius A, Heitman J. Malassezia fungi are specialized to live on skin and associated with dandruff, eczema, and other skin diseases. PLoS Pathog. 2012;8(6):e1002701.
62. Casas C, Paul C, Lahfa M, Livideanu B, Lejeune O, Alvarez-Georges S, et al. Quantification of Demodex folliculorum by PCR in rosacea and its relationship to skin innate immune activation. Exp Dermatol. 2012;21(12):906-10.
63. Totte JE, van der Feltz WT, Hennekam M, van Belkum A, van Zuuren EJ, Pasmans SG. Prevalence and odds of Staphylococcus aureus carriage in atopic dermatitis: a systematic review and meta-analysis. Br J Dermatol. 2016;175(4):687-95.
64. Graether SP. Biochemistry and function of antifreeze proteins. xii, 221 pages p.
65. Liu H, Archer NK, Dillen CA, Wang Y, Ashbaugh AG, Ortines RV, et al. Staphylococcus aureus Epicutaneous Exposure Drives Skin Inflammation via IL-36-Mediated T Cell Responses. Cell Host Microbe. 2017;22(5):653-66 e5.
66. Nakamura Y, Oscherwitz J, Cease KB, Chan SM, Munoz-Planillo R, Hasegawa M, et al. Staphylococcus delta-toxin induces allergic skin disease by activating mast cells. Nature. 2013;503(7476):397-401.

67. Niebuhr M, Gathmann M, Scharonow H, Mamerow D, Mommert S, Balaji H, et al. Staphylococcal alpha-toxin is a strong inducer of interleukin-17 in humans. Infect Immun. 2011;79(4):1615-22.

68. Kaesler S, Skabytska Y, Chen KM, Kempf WE, Volz T, Koberle M, et al. Staphylococcus aureus-derived lipoteichoic acid induces temporary T-cell paralysis independent of Toll-like receptor 2. J Allergy Clin Immunol. 2016;138(3):780-90 e6.

69. Zhang LJ, Guerrero-Juarez CF, Hata T, Bapat SP, Ramos R, Plikus MV, et al. Innate immunity. Dermal adipocytes protect against invasive Staphylococcus aureus skin infection. Science. 2015;347(6217):67-71.

70. Nakatsuji T, Chen TH, Two AM, Chun KA, Narala S, Geha RS, et al. Staphylococcus aureus Exploits Epidermal Barrier Defects in Atopic Dermatitis to Trigger Cytokine Expression. J Invest Dermatol. 2016;136(11):2192-200.

71. Postma B, Poppelier MJ, van Galen JC, Prossnitz ER, van Strijp JA, de Haas CJ, et al. Chemotaxis inhibitory protein of Staphylococcus aureus binds specifically to the C5a and formylated peptide receptor. J Immunol. 2004;172(11):6994-7001.

72. Foster TJ. Immune evasion by staphylococci. Nat Rev Microbiol. 2005;3(12):948-58.

73. Rooijakkers SH, van Kessel KP, van Strijp JA. Staphylococcal innate immune evasion. Trends Microbiol. 2005;13(12):596-601.

74. Wanke I, Steffen H, Christ C, Krismer B, Gotz F, Peschel A, et al. Skin commensals amplify the innate immune response to pathogens by activation of distinct signaling pathways. J Invest Dermatol. 2011;131(2):382-90.

75. Boukamp P. Non-melanoma skin cancer: what drives tumor development and progression? Carcinogenesis. 2005;26(10):1657-67.

76. Brand D, Ackerman AB. Squamous cell carcinoma, not basal cell carcinoma, is the most common cancer in humans. J Am Acad Dermatol. 2000;42(3):523-6.

77. Organisation WH. Skin Cancers 2018 [Available from: www.who.int/uv/faq/skincancer/en/index1.html.

78. Wassberg C, Thorn M, Johansson AM, Bergstrom R, Berne B, Ringborg U. Increasing incidence rates of squamous cell carcinoma of the skin in Sweden. Acta Derm Venereol. 2001;81(4):268-72.

79. Grizzle WE, Srivastava S, Manne U. The biology of incipient, pre-invasive or intraepithelial neoplasia. Cancer Biomark. 2010;9(1-6):21-39.

80. Feldman SR, Fleischer AB, Jr. Progression of actinic keratosis to squamous cell carcinoma revisited: clinical and treatment implications. Cutis. 2011;87(4):201-7.

81. Berman B, Cockerell CJ. Pathobiology of actinic keratosis: ultraviolet-dependent keratinocyte proliferation. J Am Acad Dermatol. 2013;68(1 Suppl 1):S10-9.
82. Marks R. Nonmelanotic skin cancer and solar keratoses. The quiet 20th century epidemic. Int J Dermatol. 1987;26(4):201-5.
83. Marks R, Foley P, Goodman G, Hage BH, Selwood TS. Spontaneous remission of solar keratoses: the case for conservative management. Br J Dermatol. 1986;115(6):649-55.
84. Frost CA, Green AC. Epidemiology of solar keratoses. Br J Dermatol. 1994;131(4):455-64.
85. Anwar J, Wrone DA, Kimyai-Asadi A, Alam M. The development of actinic keratosis into invasive squamous cell carcinoma: evidence and evolving classification schemes. Clin Dermatol. 2004;22(3):189-96.
86. Fukamizu H, Inoue K, Matsumoto K, Okayama H, Moriguchi T. Metastatic squamous-cell carcinomas derived from solar keratosis. J Dermatol Surg Oncol. 1985;11(5):518-22.
87. Forslund O, Iftner T, Andersson K, Lindelof B, Hradil E, Nordin P, et al. Cutaneous human papillomaviruses found in sun-exposed skin: Beta-papillomavirus species 2 predominates in squamous cell carcinoma. J Infect Dis. 2007;196(6):876-83.
88. Asgari MM, Kiviat NB, Critchlow CW, Stern JE, Argenyi ZB, Raugi GJ, et al. Detection of human papillomavirus DNA in cutaneous squamous cell carcinoma among immunocompetent individuals. J Invest Dermatol. 2008;128(6):1409-17.
89. Kostic AD, Gevers D, Pedamallu CS, Michaud M, Duke F, Earl AM, et al. Genomic analysis identifies association of Fusobacterium with colorectal carcinoma. Genome Res. 2012;22(2):292-8.
90. Becker JC, Andersen MH, Schrama D, Thor Straten P. Immune-suppressive properties of the tumor microenvironment. Cancer Immunol Immunother. 2013;62(7):1137-48.
91. Grivennikov SI, Wang K, Mucida D, Stewart CA, Schnabl B, Jauch D, et al. Adenoma-linked barrier defects and microbial products drive IL-23/IL-17-mediated tumour growth. Nature. 2012;491(7423):254-8.
92. Khan AA, Shrivastava A, Khurshid M. Normal to cancer microbiome transformation and its implication in cancer diagnosis. Biochim Biophys Acta. 2012;1826(2):331-7.
93. Abed J, Emgard JE, Zamir G, Faroja M, Almogy G, Grenov A, et al. Fap2 Mediates Fusobacterium nucleatum Colorectal Adenocarcinoma Enrichment by Binding to Tumor-Expressed Gal-GalNAc. Cell Host Microbe. 2016;20(2):215-25.
94. Schwabe RF, Jobin C. The microbiome and cancer. Nat Rev Cancer. 2013;13(11):800-12.

95. Tudek B, Speina E. Oxidatively damaged DNA and its repair in colon carcinogenesis. Mutat Res. 2012;736(1-2):82-92.
96. Allen-Vercoe E, Strauss J, Chadee K. Fusobacterium nucleatum: an emerging gut pathogen? Gut Microbes. 2011;2(5):294-8.
97. McCoy AN, Araujo-Perez F, Azcarate-Peril A, Yeh JJ, Sandler RS, Keku TO. Fusobacterium is associated with colorectal adenomas. PLoS One. 2013;8(1):e53653.
98. Rubinstein MR, Wang X, Liu W, Hao Y, Cai G, Han YW. Fusobacterium nucleatum promotes colorectal carcinogenesis by modulating E-cadherin/beta-catenin signaling via its FadA adhesin. Cell Host Microbe. 2013;14(2):195-206.
99. Kostic AD, Chun E, Robertson L, Glickman JN, Gallini CA, Michaud M, et al. Fusobacterium nucleatum potentiates intestinal tumorigenesis and modulates the tumor-immune microenvironment. Cell Host Microbe. 2013;14(2):207-15.
100. Shang FM, Liu HL. Fusobacterium nucleatum and colorectal cancer: A review. World J Gastrointest Oncol. 2018;10(3):71-81.
101. Lukas M. Inflammatory bowel disease as a risk factor for colorectal cancer. Dig Dis. 2010;28(4-5):619-24.
102. Strauss J, Kaplan GG, Beck PL, Rioux K, Panaccione R, Devinney R, et al. Invasive potential of gut mucosa-derived Fusobacterium nucleatum positively correlates with IBD status of the host. Inflamm Bowel Dis. 2011;17(9):1971-8.
103. Gevers D, Kugathasan S, Denson LA, Vazquez-Baeza Y, Van Treuren W, Ren B, et al. The treatment-naive microbiome in new-onset Crohn's disease. Cell Host Microbe. 2014;15(3):382-92.
104. Thrumurthy SG, Thrumurthy SS, Gilbert CE, Ross P, Haji A. Colorectal adenocarcinoma: risks, prevention and diagnosis. BMJ. 2016;354:i3590.
105. Compare D, Nardone G. Contribution of gut microbiota to colonic and extracolonic cancer development. Dig Dis. 2011;29(6):554-61.
106. Karin M, Greten FR. NF-kappaB: linking inflammation and immunity to cancer development and progression. Nat Rev Immunol. 2005;5(10):749-59.
107. Fukata M, Chen A, Vamadevan AS, Cohen J, Breglio K, Krishnareddy S, et al. Toll-like receptor-4 promotes the development of colitis-associated colorectal tumors. Gastroenterology. 2007;133(6):1869-81.
108. Moresco EM, LaVine D, Beutler B. Toll-like receptors. Curr Biol. 2011;21(13):R488-93.

109. Tye H, Kennedy CL, Najdovska M, McLeod L, McCormack W, Hughes N, et al. STAT3-driven upregulation of TLR2 promotes gastric tumorigenesis independent of tumor inflammation. Cancer Cell. 2012;22(4):466-78.
110. Nesic D, Hsu Y, Stebbins CE. Assembly and function of a bacterial genotoxin. Nature. 2004;429(6990):429-33.
111. Travaglione S, Fabbri A, Fiorentini C. The Rho-activating CNF1 toxin from pathogenic E. coli: a risk factor for human cancer development? Infect Agent Cancer. 2008;3:4.
112. Cuevas-Ramos G, Petit CR, Marcq I, Boury M, Oswald E, Nougayrede JP. Escherichia coli induces DNA damage in vivo and triggers genomic instability in mammalian cells. Proc Natl Acad Sci U S A. 2010;107(25):11537-42.
113. Bottomley MJ, Thomson J, Harwood C, Leigh I. The Role of the Immune System in Cutaneous Squamous Cell Carcinoma. Int J Mol Sci. 2019;20(8).
114. Zhang LJ, Gallo RL. Antimicrobial peptides. Curr Biol. 2016;26(1):R14-9.
115. Niyonsaba F, Ushio H, Nakano N, Ng W, Sayama K, Hashimoto K, et al. Antimicrobial peptides human beta-defensins stimulate epidermal keratinocyte migration, proliferation and production of proinflammatory cytokines and chemokines. J Invest Dermatol. 2007;127(3):594-604.
116. Brogden KA. Antimicrobial peptides: pore formers or metabolic inhibitors in bacteria? Nat Rev Microbiol. 2005;3(3):238-50.
117. Cogen AL, Nizet V, Gallo RL. Skin microbiota: a source of disease or defence? Br J Dermatol. 2008;158(3):442-55.
118. Schauber J, Gallo RL. Expanding the roles of antimicrobial peptides in skin: alarming and arming keratinocytes. J Invest Dermatol. 2007;127(3):510-2.
119. Miller LS, Sorensen OE, Liu PT, Jalian HR, Eshtiaghpour D, Behmanesh BE, et al. TGF-alpha regulates TLR expression and function on epidermal keratinocytes. J Immunol. 2005;174(10):6137-43.
120. Sorensen OE, Thapa DR, Roupe KM, Valore EV, Sjobring U, Roberts AA, et al. Injury-induced innate immune response in human skin mediated by transactivation of the epidermal growth factor receptor. J Clin Invest. 2006;116(7):1878-85.
121. Mburu YK, Abe K, Ferris LK, Sarkar SN, Ferris RL. Human beta-defensin 3 promotes NF-kappaB-mediated CCR7 expression and anti-apoptotic signals in squamous cell carcinoma of the head and neck. Carcinogenesis. 2011;32(2):168-74.

122. Niyonsaba F, Ushio H, Nagaoka I, Okumura K, Ogawa H. The human beta-defensins (-1, -2, -3, -4) and cathelicidin LL-37 induce IL-18 secretion through p38 and ERK MAPK activation in primary human keratinocytes. J Immunol. 2005;175(3):1776-84.

123. Zasloff M. Antimicrobial peptides and suppression of apoptosis in human skin. J Invest Dermatol. 2009;129(4):824-6.

124. Fulton C, Anderson GM, Zasloff M, Bull R, Quinn AG. Expression of natural peptide antibiotics in human skin. The Lancet. 1997;350(9093):1750-1.

125. Ali RS, Falconer A, Ikram M, Bissett CE, Cerio R, Quinn AG. Expression of the peptide antibiotics human beta defensin-1 and human beta defensin-2 in normal human skin. J Invest Dermatol. 2001;117(1):106-11.

126. Harder J, Bartels J, Christophers E, Schroder JM. A peptide antibiotic from human skin. Nature. 1997;387(6636):861.

127. Schroder JM, Harder J. Antimicrobial skin peptides and proteins. Cell Mol Life Sci. 2006;63(4):469-86.

128. Midorikawa K, Ouhara K, Komatsuzawa H, Kawai T, Yamada S, Fujiwara T, et al. Staphylococcus aureus susceptibility to innate antimicrobial peptides, beta-defensins and CAP18, expressed by human keratinocytes. Infect Immun. 2003;71(7):3730-9.

129. Wenghoefer M, Pantelis A, Dommisch H, Reich R, Martini M, Allam JP, et al. Decreased gene expression of human beta-defensin-1 in the development of squamous cell carcinoma of the oral cavity. Int J Oral Maxillofac Surg. 2008;37(7):660-3.

130. Kesting MR, Loeffelbein DJ, Hasler RJ, Wolff KD, Rittig A, Schulte M, et al. Expression profile of human beta-defensin 3 in oral squamous cell carcinoma. Cancer Invest. 2009;27(5):575-81.

131. Mizukawa N, Sawaki K, Yamachika E, Fukunaga J, Ueno T, Takagi S, et al. Presence of human beta-defensin-2 in oral squamous cell carcinoma. Anticancer Res. 2000;20(3B):2005-7.

132. Sawaki K, Mizukawa N, Yamaai T, Yoshimoto T, Nakano M, Sugahara T. High concentration of beta-defensin-2 in oral squamous cell carcinoma. Anticancer Res. 2002;22(4):2103-7.

133. Winter J, Pantelis A, Reich R, Martini M, Kraus D, Jepsen S, et al. Human beta-defensin-1, -2, and -3 exhibit opposite effects on oral squamous cell carcinoma cell proliferation. Cancer Invest. 2011;29(3):196-201.

134. Gao C, Yue WM, Tian H, Li L, Li SH, Si LB. Human beta-defensin 2 promotes the proliferation of lung cancer cells through ATP-binding cassette transporter G2. Int J Clin Exp Patho. 2016;9(6):5944-9.

135. Markeeva N, Lysovskiy I, Zhuravel E, Soldatkina M, Lyzogubov V, Usenko V, et al. Involvement of human beta-defensin-2 in proliferation of transformed cells of human cervix. Exp Oncol. 2005;27(4):308-13.

136. Braff MH, Hawkins MA, Di Nardo A, Lopez-Garcia B, Howell MD, Wong C, et al. Structure-function relationships among human cathelicidin peptides: dissociation of antimicrobial properties from host immunostimulatory activities. J Immunol. 2005;174(7):4271-8.

137. Katz E, Demain AL. The peptide antibiotics of Bacillus: chemistry, biogenesis, and possible functions. Bacteriol Rev. 1977;41(2):449-74.

138. Jeong H, Sim YM, Kim HJ, Lee DW, Lim SK, Lee SJ. Genome Sequence of the Vancomycin-Producing Amycolatopsis orientalis subsp. orientalis Strain KCTC 9412T. Genome Announc. 2013;1(3).

139. Schauber J, Gallo RL. Antimicrobial peptides and the skin immune defense system. J Allergy Clin Immunol. 2009;124(3 Suppl 2):R13-8.

140. Otto M. Staphylococcus colonization of the skin and antimicrobial peptides. Expert Rev Dermatol. 2010;5(2):183-95.

141. Bardan A, Nizet V, Gallo RL. Antimicrobial peptides and the skin. Expert Opin Biol Ther. 2004;4(4):543-9.

142. Ganz T. Defensins: antimicrobial peptides of innate immunity. Nat Rev Immunol. 2003;3(9):710-20.

143. Pazgier M, Hoover DM, Yang D, Lu W, Lubkowski J. Human beta-defensins. Cell Mol Life Sci. 2006;63(11):1294-313.

144. Kosciuczuk EM, Lisowski P, Jarczak J, Strzalkowska N, Jozwik A, Horbanczuk J, et al. Cathelicidins: family of antimicrobial peptides. A review. Mol Biol Rep. 2012;39(12):10957-70.

145. Braff MH, Zaiou M, Fierer J, Nizet V, Gallo RL. Keratinocyte production of cathelicidin provides direct activity against bacterial skin pathogens. Infect Immun. 2005;73(10):6771-81.

146. Jann NJ, Schmaler M, Kristian SA, Radek KA, Gallo RL, Nizet V, et al. Neutrophil antimicrobial defense against Staphylococcus aureus is mediated by phagolysosomal but not extracellular trap-associated cathelicidin. J Leukoc Biol. 2009;86(5):1159-69.

147. Bals R, Wang X, Zasloff M, Wilson JM. The peptide antibiotic LL-37/hCAP-18 is expressed in epithelia of the human lung where it has broad antimicrobial activity at the airway surface. Proc Natl Acad Sci U S A. 1998;95(16):9541-6.

148. Frohm M, Agerberth B, Ahangari G, Stahle-Backdahl M, Liden S, Wigzell H, et al. The expression of the gene coding for the antibacterial peptide LL-37 is induced in human keratinocytes during inflammatory disorders. J Biol Chem. 1997;272(24):15258-63.

149. Yuan S, Cohen DB, Ravel J, Abdo Z, Forney LJ. Evaluation of methods for the extraction and purification of DNA from the human microbiome. PLoS One. 2012;7(3):e33865.

150. Baker GC, Smith JJ, Cowan DA. Review and re-analysis of domain-specific 16S primers. Journal of Microbiological Methods. 2003;55(3):541-55.

151. Klymiuk I, Bambach I, Patra V, Trajanoski S, Wolf P. 16S Based Microbiome Analysis from Healthy Subjects' Skin Swabs Stored for Different Storage Periods Reveal Phylum to Genus Level Changes. Front Microbiol. 2016;7:2012.

152. Kozich JJ, Westcott SL, Baxter NT, Highlander SK, Schloss PD. Development of a dual-index sequencing strategy and curation pipeline for analyzing amplicon sequence data on the MiSeq Illumina sequencing platform. Appl Environ Microbiol. 2013;79(17):5112-20.

153. Schloss PD, Gevers D, Westcott SL. Reducing the effects of PCR amplification and sequencing artifacts on 16S rRNA-based studies. PLoS One. 2011;6(12):e27310.

154. Huse SM, Welch DM, Morrison HG, Sogin ML. Ironing out the wrinkles in the rare biosphere through improved OTU clustering. Environ Microbiol. 2010;12(7):1889-98.

155. Edgar RC, Haas BJ, Clemente JC, Quince C, Knight R. UCHIME improves sensitivity and speed of chimera detection. Bioinformatics. 2011;27(16):2194-200.

156. Wang Q, Garrity GM, Tiedje JM, Cole JR. Naive Bayesian classifier for rapid assignment of rRNA sequences into the new bacterial taxonomy. Applied and Environmental Microbiology. 2007;73(16):5261-7.

157. Quast C, Pruesse E, Yilmaz P, Gerken J, Schweer T, Yarza P, et al. The SILVA ribosomal RNA gene database project: improved data processing and web-based tools. Nucleic Acids Res. 2013;41(Database issue):D590-6.

158. Pruesse E, Quast C, Knittel K, Fuchs BM, Ludwig W, Peplies J, et al. SILVA: a comprehensive online resource for quality checked and aligned ribosomal RNA sequence data compatible with ARB. Nucleic Acids Res. 2007;35(21):7188-96.

159. Caporaso JG, Kuczynski J, Stombaugh J, Bittinger K, Bushman FD, Costello EK, et al. QIIME allows analysis of high-throughput community sequencing data. Nat Methods. 2010;7(5):335-6.

160. Edgar RC. Search and clustering orders of magnitude faster than BLAST. Bioinformatics. 2010;26(19):2460-1.

161. Lozupone C, Lladser ME, Knights D, Stombaugh J, Knight R. UniFrac: an effective distance metric for microbial community comparison. ISME J. 2011;5(2):169-72.

162. Yoon SH, Ha SM, Kwon S, Lim J, Kim Y, Seo H, et al. Introducing EzBioCloud: a taxonomically united database of 16S rRNA gene sequences and whole-genome assemblies. Int J Syst Evol Microbiol. 2017;67(5):1613-7.

163. Roshan Moniri M, Young A, Reinheimer K, Rayat J, Dai LJ, Warnock GL. Dynamic assessment of cell viability, proliferation and migration using real time cell analyzer system (RTCA). Cytotechnology. 2015;67(2):379-86.

164. psych : Procedures for Personality and Psychological Research. [Internet]. 2017.

165. Furet JP, Firmesse O, Gourmelon M, Bridonneau C, Tap J, Mondot S, et al. Comparative assessment of human and farm animal faecal microbiota using real-time quantitative PCR. FEMS Microbiol Ecol. 2009;68(3):351-62.

166. Li W, Han L, Yu P, Ma C, Wu X, Moore JE, et al. Molecular characterization of skin microbiota between cancer cachexia patients and healthy volunteers. Microb Ecol. 2014;67(3):679-89.

167. Chakravorty S, Helb D, Burday M, Connell N, Alland D. A detailed analysis of 16S ribosomal RNA gene segments for the diagnosis of pathogenic bacteria. J Microbiol Methods. 2007;69(2):330-9.

168. Brakstad OG, Aasbakk K, Maeland JA. Detection of Staphylococcus aureus by polymerase chain reaction amplification of the nuc gene. J Clin Microbiol. 1992;30(7):1654-60.

169. Kullander J, Forslund O, Dillner J. Staphylococcus aureus and squamous cell carcinoma of the skin. Cancer Epidemiol Biomarkers Prev. 2009;18(2):472-8.

170. Hohnadel M, Felden L, Fijuljanin D, Jouette S, Chollet R. A new ultrasonic high-throughput instrument for rapid DNA release from microorganisms. J Microbiol Methods. 2014;99:71-80.

171. Byrne FJ, Waters SM, Waters PS, Curtin W, Kerin M. Development of a molecular methodology to quantify Staphylococcus epidermidis in surgical wash-out samples from prosthetic joint replacement surgery. Eur J Orthop Surg Traumatol. 2007.

172. Picard FJ, Ke D, Boudreau DK, Boissinot M, Huletsky A, Richard D, et al. Use of tuf sequences for genus-specific PCR detection and phylogenetic analysis of 28 streptococcal species. J Clin Microbiol. 2004;42(8):3686-95.

173. Vordenbaumen S, Pilic D, Otte JM, Schmitz F, Schmidt-Choudhury A. Defensin-mRNA expression in the upper gastrointestinal tract is modulated in children with celiac disease and Helicobacter pylori-positive gastritis. J Pediatr Gastroenterol Nutr. 2010;50(6):596-600.

174. Alp S, Skrygan M, Schlottmann R, Kreuter A, Otte JM, Schmidt WE, et al. Expression of beta-defensin 1 and 2 in nasal epithelial cells and alveolar macrophages from HIV-infected patients. Eur J Med Res. 2005;10(1):1-6.

175. Hegyi Z, Zwicker S, Bureik D, Peric M, Koglin S, Batycka-Baran A, et al. Vitamin D analog calcipotriol suppresses the Th17 cytokine-induced proinflammatory S100 "alarmins" psoriasin (S100A7) and koebnerisin (S100A15) in psoriasis. J Invest Dermatol. 2012;132(5):1416-24.

176. Garreis F, Gottschalt M, Schlorf T, Glaser R, Harder J, Worlitzsch D, et al. Expression and regulation of antimicrobial peptide psoriasin (S100A7) at the ocular surface and in the lacrimal apparatus. Invest Ophthalmol Vis Sci. 2011;52(7):4914-22.

177. Schmittgen TD, Livak KJ. Analyzing real-time PCR data by the comparative C(T) method. Nat Protoc. 2008;3(6):1101-8.

178. Moissl C, Rudolph C, Huber R. Natural Communities of Novel Archaea and Bacteria with a String-of-Pearls-Like Morphology: Molecular Analysis of the Bacterial Partners. Applied and Environmental Microbiology. 2002;68(2):933-7.

179. Wagner M, Amann R, Kampfer P, Assmus B, Hartmann A, Hutzler P, et al. Identification and in-Situ Detection of Gram-Negative Filamentous Bacteria in Activated-Sludge. Syst Appl Microbiol. 1994;17(3):405-17.

180. Lawson TS, Connally RE, Iredell JR, Vemulpad S, Piper JA. Detection of Staphylococcus aureus with a fluorescence in situ hybridization that does not require lysostaphin. J Clin Lab Anal. 2011;25(2):142-7.

181. Kempf VA, Trebesius K, Autenrieth IB. Fluorescent In situ hybridization allows rapid identification of microorganisms in blood cultures. J Clin Microbiol. 2000;38(2):830-8.

182. Kondo S, Aso K. Establishment of a cell line of human skin squamous cell carcinoma in vitro. Br J Dermatol. 1981;105(2):125-32.

183. Boukamp P, Petrussevska RT, Breitkreutz D, Hornung J, Markham A, Fusenig NE. Normal keratinization in a spontaneously immortalized aneuploid human keratinocyte cell line. J Cell Biol. 1988;106(3):761-71.

184. Montalban-Arques A, Wurm P, Trajanoski S, Schauer S, Kienesberger S, Halwachs B, et al. Propionibacterium acnes overabundance and natural killer group 2 member D system activation in corpus-dominant lymphocytic gastritis. J Pathol. 2016;240(4):425-36.

185. Moniri MR, Young A, Reinheimer K, Rayat J, Dai LJ, Warnock GL. Dynamic assessment of cell viability, proliferation and migration using real time cell analyzer system (RTCA). Cytotechnology. 2015;67(2):379-86.

186. Braff MH, Gallo RL. Antimicrobial peptides: an essential component of the skin defensive barrier. Curr Top Microbiol Immunol. 2006;306:91-110.

187. Brandwein M, Bentwich Z, Steinberg D. Endogenous Antimicrobial Peptide Expression in Response to Bacterial Epidermal Colonization. Front Immunol. 2017;8:1637.

188. Dinulos JG, Mentele L, Fredericks LP, Dale BA, Darmstadt GL. Keratinocyte expression of human beta defensin 2 following bacterial infection: role in cutaneous host defense. Clin Diagn Lab Immunol. 2003;10(1):161-6.

189. Scola N, Gambichler T, Saklaoui H, Bechara FG, Georgas D, Stucker M, et al. The expression of antimicrobial peptides is significantly altered in cutaneous squamous cell carcinoma and precursor lesions. Br J Dermatol. 2012;167(3):591-7.

190. Shi N, Jin F, Zhang X, Clinton SK, Pan Z, Chen T. Overexpression of human beta-defensin 2 promotes growth and invasion during esophageal carcinogenesis. Oncotarget. 2014;5(22):11333-44.

191. de Boer R, Peters R, Gierveld S, Schuurman T, Kooistra-Smid M, Savelkoul P. Improved detection of microbial DNA after bead-beating before DNA isolation. J Microbiol Methods. 2010;80(2):209-11.

192. Reck M, Tomasch J, Deng Z, Jarek M, Husemann P, Wagner-Dobler I, et al. Stool metatranscriptomics: A technical guideline for mRNA stabilisation and isolation. BMC Genomics. 2015;16:494.

193. White T, Bruns, T., Lee, S., and Taylor, J. . Amplification and direct sequencing of fungal ribosomal RNA genes for phylogenetics: Academic Press, Inc.; 1990.

194. Munoz-Cadavid C, Rudd S, Zaki SR, Patel M, Moser SA, Brandt ME, et al. Improving molecular detection of fungal DNA in formalin-fixed paraffin-embedded tissues: comparison of five tissue DNA extraction methods using panfungal PCR. J Clin Microbiol. 2010;48(6):2147-53.

195. Schindler CA, Schuhardt VT. Lysostaphin: A New Bacteriolytic Agent for the Staphylococcus. Proc Natl Acad Sci U S A. 1964;51:414-21.
196. Yokogawa K, Kawata S, Nishimura S, Ikeda Y, Yoshimura Y. Mutanolysin, bacteriolytic agent for cariogenic Streptococci: partial purification and properties. Antimicrob Agents Chemother. 1974;6(2):156-65.
197. Fahlen A, Engstrand L, Baker BS, Powles A, Fry L. Comparison of bacterial microbiota in skin biopsies from normal and psoriatic skin. Arch Dermatol Res. 2012;304(1):15-22.
198. Thio HB. The Microbiome in Psoriasis and Psoriatic Arthritis: The Skin Perspective. J Rheumatol Suppl. 2018;94:30-1.
199. Gao Z, Tseng CH, Strober BE, Pei Z, Blaser MJ. Substantial alterations of the cutaneous bacterial biota in psoriatic lesions. PLoS One. 2008;3(7):e2719.
200. Prohic A. Identification of Malassezia species isolated from scalp skin of patients with psoriasis and healthy subjects. Acta Dermatovenerol Croat. 2003;11(1):10-6.
201. Ayala-Fontanez N, Soler DC, McCormick TS. Current knowledge on psoriasis and autoimmune diseases. Psoriasis (Auckl). 2016;6:7-32.
202. Benhadou F, Mintoff D, Schnebert B, Thio HB. Psoriasis and Microbiota: A Systematic Review. Diseases. 2018;6(2).
203. Chang HW, Yan D, Singh R, Liu J, Lu X, Ucmak D, et al. Alteration of the cutaneous microbiome in psoriasis and potential role in Th17 polarization. Microbiome. 2018;6(1):154.
204. Todd JK. Staphylococcal infections. Pediatr Rev. 2005;26(12):444-50.
205. Bullman S, Pedamallu CS, Sicinska E, Clancy TE, Zhang X, Cai D, et al. Analysis of Fusobacterium persistence and antibiotic response in colorectal cancer. Science. 2017;358(6369):1443-8.
206. Wood DLA, Lachner N, Tan JM, Tang S, Angel N, Laino A, et al. A Natural History of Actinic Keratosis and Cutaneous Squamous Cell Carcinoma Microbiomes. MBio. 2018;9(5).
207. Gribbon EM, Cunliffe WJ, Holland KT. Interaction of Propionibacterium acnes with skin lipids in vitro. J Gen Microbiol. 1993;139(8):1745-51.
208. Kuper H, Adami HO, Trichopoulos D. Infections as a major preventable cause of human cancer. J Intern Med. 2000;248(3):171-83.
209. Chang AH, Parsonnet J. Role of bacteria in oncogenesis. Clin Microbiol Rev. 2010;23(4):837-57.

210. Uemura N, Okamoto S, Yamamoto S, Matsumura N, Yamaguchi S, Yamakido M, et al. Helicobacter pylori infection and the development of gastric cancer. N Engl J Med. 2001;345(11):784-9.

211. Kooistra-Smid M, Nieuwenhuis M, van Belkum A, Verbrugh H. The role of nasal carriage in Staphylococcus aureus burn wound colonization. FEMS Immunol Med Microbiol. 2009;57(1):1-13.

212. Naik S, Bouladoux N, Wilhelm C, Molloy MJ, Salcedo R, Kastenmuller W, et al. Compartmentalized control of skin immunity by resident commensals. Science. 2012;337(6098):1115-9.

213. Lai Y, Cogen AL, Radek KA, Park HJ, Macleod DT, Leichtle A, et al. Activation of TLR2 by a small molecule produced by Staphylococcus epidermidis increases antimicrobial defense against bacterial skin infections. J Invest Dermatol. 2010;130(9):2211-21.

214. Zanger P, Holzer J, Schleucher R, Scherbaum H, Schittek B, Gabrysch S. Severity of Staphylococcus aureus infection of the skin is associated with inducibility of human beta-defensin 3 but not human beta-defensin 2. Infect Immun. 2010;78(7):3112-7.

215. Dressel S, Harder J, Cordes J, Wittersheim M, Meyer-Hoffert U, Sunderkotter C, et al. Differential expression of antimicrobial peptides in margins of chronic wounds. Exp Dermatol. 2010;19(7):628-32.

216. Chieosilapatham P, Ogawa H, Niyonsaba F. Current insights into the role of human beta-defensins in atopic dermatitis. Clin Exp Immunol. 2017;190(2):155-66.

217. Cho JW, Cho SY, Lee KS. Roles of SEA-expressing Staphylococcus aureus, isolated from an atopic dermatitis patient, on expressions of human beta-defensin-2 and inflammatory cytokines in HaCaT cells. Int J Mol Med. 2009;23(3):331-5.

218. Quinn GA, Cole AM. Suppression of innate immunity by a nasal carriage strain of Staphylococcus aureus increases its colonization on nasal epithelium. Immunology. 2007;122(1):80-9.

219. Clarke SR, Mohamed R, Bian L, Routh AF, Kokai-Kun JF, Mond JJ, et al. The Staphylococcus aureus surface protein IsdA mediates resistance to innate defenses of human skin. Cell Host Microbe. 2007;1(3):199-212.

220. Iwase T, Uehara Y, Shinji H, Tajima A, Seo H, Takada K, et al. Staphylococcus epidermidis Esp inhibits Staphylococcus aureus biofilm formation and nasal colonization. Nature. 2010;465(7296):346-9.

221. Ghosh SK, McCormick TS, Weinberg A. Human Beta Defensins and Cancer: Contradictions and Common Ground. Front Oncol. 2019;9:341.

222. Joly S, Compton LM, Pujol C, Kurago ZB, Guthmiller JM. Loss of human beta-defensin 1, 2, and 3 expression in oral squamous cell carcinoma. Oral Microbiol Immunol. 2009;24(5):353-60.
223. Donald CD, Sun CQ, Lim SD, Macoska J, Cohen C, Amin MB, et al. Cancer-specific loss of beta-defensin 1 in renal and prostatic carcinomas. Lab Invest. 2003;83(4):501-5.
224. Sun CQ, Arnold R, Fernandez-Golarz C, Parrish AB, Almekinder T, He J, et al. Human beta-defensin-1, a potential chromosome 8p tumor suppressor: control of transcription and induction of apoptosis in renal cell carcinoma. Cancer Res. 2006;66(17):8542-9.
225. Kamino Y, Kurashige Y, Uehara O, Sato J, Nishimura M, Yoshida K, et al. HBD-2 is downregulated in oral carcinoma cells by DNA hypermethylation, and increased expression of hBD-2 by DNA demethylation and gene transfection inhibits cell proliferation and invasion. Oncol Rep. 2014;32(2):462-8.
226. Xu D, Zhang B, Liao C, Zhang W, Wang W, Chang Y, et al. Human beta-defensin 3 contributes to the carcinogenesis of cervical cancer via activation of NF-kappaB signaling. Oncotarget. 2016;7(46):75902-13.
227. Uraki S, Sugimoto K, Shiraki K, Tameda M, Inagaki Y, Ogura S, et al. Human beta-defensin-3 inhibits migration of colon cancer cells via downregulation of metastasis-associated 1 family, member 2 expression. Int J Oncol. 2014;45(3):1059-64.
228. Glaser R, Navid F, Schuller W, Jantschitsch C, Harder J, Schroder JM, et al. UV-B radiation induces the expression of antimicrobial peptides in human keratinocytes in vitro and in vivo. J Allergy Clin Immunol. 2009;123(5):1117-23.
229. Segata N, Haake SK, Mannon P, Lemon KP, Waldron L, Gevers D, et al. Composition of the adult digestive tract bacterial microbiome based on seven mouth surfaces, tonsils, throat and stool samples. Genome Biol. 2012;13(6):R42.
230. Nomura I, Goleva E, Howell MD, Hamid QA, Ong PY, Hall CF, et al. Cytokine milieu of atopic dermatitis, as compared to psoriasis, skin prevents induction of innate immune response genes. J Immunol. 2003;171(6):3262-9.
231. Marcinkiewicz M, Majewski S. The role of antimicrobial peptides in chronic inflammatory skin diseases. Postepy Dermatol Alergol. 2016;33(1):6-12.
232. Glaser R, Meyer-Hoffert U, Harder J, Cordes J, Wittersheim M, Kobliakova J, et al. The antimicrobial protein psoriasin (S100A7) is upregulated in atopic dermatitis and after experimental skin barrier disruption. J Invest Dermatol. 2009;129(3):641-9.

233. Lindahl BD, Nilsson RH, Tedersoo L, Abarenkov K, Carlsen T, Kjoller R, et al. Fungal community analysis by high-throughput sequencing of amplified markers--a user's guide. New Phytol. 2013;199(1):288-99.

234. Gosiewski T, Salamon D, Szopa M, Sroka A, Malecki MT, Bulanda M. Quantitative evaluation of fungi of the genus Candida in the feces of adult patients with type 1 and 2 diabetes - a pilot study. Gut Pathog. 2014;6(1):43.

235. Ghannoum MA, Jurevic RJ, Mukherjee PK, Cui F, Sikaroodi M, Naqvi A, et al. Characterization of the oral fungal microbiome (mycobiome) in healthy individuals. PLoS Pathog. 2010;6(1):e1000713.

236. Paulino LC, Tseng CH, Strober BE, Blaser MJ. Molecular analysis of fungal microbiota in samples from healthy human skin and psoriatic lesions. J Clin Microbiol. 2006;44(8):2933-41.

237. Sangoi AR, Rogers WM, Longacre TA, Montoya JG, Baron EJ, Banaei N. Challenges and pitfalls of morphologic identification of fungal infections in histologic and cytologic specimens: a ten-year retrospective review at a single institution. Am J Clin Pathol. 2009;131(3):364-75.

238. Kocjan BJ, Hosnjak L, Poljak M. Commercially available kits for manual and automatic extraction of nucleic acids from formalin-fixed, paraffin-embedded (FFPE) tissues. Acta Dermatovenerol Alp Pannonica Adriat. 2015;24(3):47-53.

239. Bonin S, Stanta G. Nucleic acid extraction methods from fixed and paraffin-embedded tissues in cancer diagnostics. Expert Rev Mol Diagn. 2013;13(3):271-82.

240. Coura R, Prolla JC, Meurer L, Ashton-Prolla P. An alternative protocol for DNA extraction from formalin fixed and paraffin wax embedded tissue. J Clin Pathol. 2005;58(8):894-5.

241. van Burik JA, Schreckhise RW, White TC, Bowden RA, Myerson D. Comparison of six extraction techniques for isolation of DNA from filamentous fungi. Med Mycol. 1998;36(5):299-303.

242. Schoch CL, Seifert KA, Huhndorf S, Robert V, Spouge JL, Levesque CA, et al. Nuclear ribosomal internal transcribed spacer (ITS) region as a universal DNA barcode marker for Fungi. Proc Natl Acad Sci U S A. 2012;109(16):6241-6.

243. Martin KJ, Rygiewicz PT. Fungal-specific PCR primers developed for analysis of the ITS region of environmental DNA extracts. BMC Microbiol. 2005;5:28.

244. Babouee Flury B, Weisser M, Prince SS, Bubendorf L, Battegay M, Frei R, et al. Performances of two different panfungal PCRs to detect mould DNA in formalin-fixed paraffin-embedded tissue: what are the limiting factors? BMC Infect Dis. 2014;14:692.
245. Mello A, Napoli C, Murat C, Morin E, Marceddu G, Bonfante P. ITS-1 versus ITS-2 pyrosequencing: a comparison of fungal populations in truffle grounds. Mycologia. 2011;103(6):1184-93.
246. ImkeSchmittac ALBM. Comparison of ITS1 and ITS2 rDNA in 454 sequencing of hyperdiverse fungal communities. Fungal ecology. 2013;6(1):102-9.
247. Blaalid R, Kumar S, Nilsson RH, Abarenkov K, Kirk PM, Kauserud H. ITS1 versus ITS2 as DNA metabarcodes for fungi. Mol Ecol Resour. 2013;13(2):218-24.

IX. Appendix

Appendix 1. Human skin samples used in this study

Sample ID	Age	Sex	Condition	Tumor region	Exact location (if available)	Specimen type	Microbiota analysis	Bacterial load (microscopy	Fungal load (microscopy)	AMP qPCR	16S qPCR	*aphylococcus* qP	*S. aureus* qPCR	*S. epidermidis*	FISH	er/Parakeratammation Sc	Inflammatio	Neutrophiles
1	76	Male	AK	Head	Frontal	Total excision	X	X	X	X	X	X	X	X	X	X	X	X
2	68	Male	AK	Ear	Ear helix, left	Punch biopsy	X	X	X	X						X	X	X
3	74	Male	AK	Cheek	Cheek left	Total excision	X	X	X	X		X	X	X		X	X	X
4	60	Male	AK	Nose	Nose bridge middle	Punch biopsy	X	X	X	X	X	X	X	X	X	X	X	X
5	60	Male	AK	Head	Parietal, middle	Punch biopsy	X	X	X	X	X	X	X	X		X	X	X
6	74	Male	AK	Upper arm	Left	Punch biopsy	X	X	X		X	X				X	X	X
7	71	Male	AK	Ear	Preauricular left	Total excision	X	X	X		X	X	X	X		X	X	X
8	60	Female	AK	Nose	Glabella	Total excision	X	X	X	X	X	X		X		X	X	X
9	86	Female	AK	Upper lip	Right	Punch biopsy	X	X	X	X	X	X	X	X	X	X	X	X
10	67	Female	AK	Jaw	Right	Total excision	X	X	X	X	X	X	X	X	X	X	X	X
11	73	Male	AK	Eye	Orbita, right	Punch biopsy	X	X	X	X	X	X	X	X	X	X	X	X
12	94	Female	AK	Head	Frontolateral, left	Punch biopsy	X	X	X	X	X	X	X	X		X	X	X
13	77	Female	AK	Preauricular	Right	Total excision		X	X	X	X	X	X			X	X	X
14	75	Male	AK	Nose	Tip	Punch biopsy		X	X	X	X	X	X			X	X	X
15	75	Male	AK	Temple	Right	Total excision/shaving		X	X	X	X	X	X			X	X	X
16	72	Male	AK	Neck	Right	Total excision/shaving		X	X	X	X	X	X			X	X	X
17	90	Female	AK	Cheek	Right	Total excision/shaving		X	X		X	X	X			X	n.a.	n.a.
18	90	Female	AK	Cheek	Left	Total excision/shaving		X	X		X	X	X			X	X	X
19	75	Female	AK	Eyebrow	Left	Total excision/shaving		X	X	X	X	X	X			X	n.a.	n.a.
20	75	Female	AK	Cheek	Right	Total excision/shaving		X	X	X	X	X	X			X	X	X
21	75	Female	AK	Nose	Bridge	Total excision/shaving		X	X	X	X	X	X			X	n.a.	n.a.
22	82	Male	AK	Parietal		Total excision/shaving		X	X	X	X	X	X			X	X	X
23	48	Male	AK	Scalp	Parietal	Total excision		X	X	X	X	X	X			X	n.a.	n.a.
24	77	Female	AK	Cheek	Left	Total excision		X	X	X		X				X	X	X
25	75	Male	AK	Ear	Ear helix, left	Total excision/shaving		X	X	X						X	n.a.	n.a.
26	87	Male	SCC	Ear	Ear helix, right	Total excision	X	X	X	X	X	X		X		X	X	X
27	79	Female	SCC	Cheek	Right	Total excision	X	X	X	X	X	X	X	X		X	X	X
28	72	Male	SCC	Forehead	Parietal,left	Total excision	X	X	X	X	X	X	X	X	X	X	X	X
29	83	Male	SCC	Temple	Left	Punch biopsy	X	X	X	X						X	X	X
30	80	Female	SCC	Jaw	Angulus mandibularis, right	Punch biopsy	X	X	X	X	X	X	X	X	X	X	X	X
31	82	Female	SCC	Hand	Dorsum, right	Total excision	X	X	X	X	X	X	X	X		X	X	X
32	73	Female	SCC	Hand	Dorsum, left	Total excision	X	X	X	X	X	X	X	X		X	X	X
33	83	Female	SCC	Behind ear	Retroauricular, left	Total excision	X	X	X	X	X	X	X	X		X	X	X
34	84	Male	SCC	Wrist	Volar, right	Total excision	X	X	X	X	X	X	X	X	X	X	X	X
35	83	Male	SCC	Upper arm	Right	Punch biopsy	X	X	X	X	X	X				X	X	X
36	91	Male	SCC	Head	High frontal, middle	Punch biopsy	X	X	X	X	X	X		X	X	X	X	X
37	71	Male	SCC	Under the eye	Infraorbital, left	Total excision	X	X	X	X	X	X	X	X	X	X	X	X
38	72	Female	SCC	Forehead		Total excision		X	X	X	X	X	X			X	X	X
39	96	Female	SCC	Cheek	Left	Total excision/shaving		X	X	X	X	X	X			X	X	X
40	93	Female	SCC	Nose	Bridge, right	Total excision		X	X	X	X	X	X			X	X	X
41	88	Male	SCC	Scalp	Occipital	Total excision		X	X	X	X	X	X			X	X	X
42	84	Male	SCC	Cheek	Right	Total excision		X	X	X	X	X	X			X	X	X
43	84	Male	SCC	Forehead	Frontal, left	Punch biopsy		X	X	X	X	X	X			X	X	X
44	77	Male	SCC	Scalp	Temporal, left	Total excision		X	X	X	X	X	X			X	X	X
45	83	Female	SCC	Scalp	Parietal, left	Punch biopsy		X	X	X	X	X	X			X	X	X
46	88	Male	SCC	Scalp	Frontal	Total excision		X	X	X	X	X	X			X	X	X
47	88	Male	SCC	Ear	Ear helix, left	Total excision		X	X	X	X	X	X			X	X	X
48	82	Male	BCC	Head	Temporal, right	Total excision	X	X	X	X	X	X	X	X	X	X	X	X
49	90	Male	BCC	Shoulder	Left	Total excision	X	X	X	X	X	X	X	X	X	X	X	X
50	67	Female	BCC	Cheek	Left	Punch biopsy	X	X	X	X	X	X	X	X	X	X	X	X
51	69	Female	BCC	Eyebrow	Lateral, left	Punch biopsy	X	X	X		X					X	X	X
52	62	Female	BCC	Nose	Glabella	Punch biopsy	X	X	X	X	X	X	X	X		X	X	X
53	82	Female	BCC	Cheek	Right	Total excision	X	X	X	X	X	X	X	X		X	X	X
54	80	Male	BCC	Ear	Retroauricular, right	Total excision	X	X	X	X	X				X	X	X	X
55	81	Male	BCC	Cheek	Mandibular, left	Punch biopsy	X	X	X		X			X		X	X	X
56	70	Male	BCC	Forehead	Frontal	Total excision	X	X	X	X	X	X	X	X		X	X	X
57	81	Male	BCC	Neck	Left	Punch biopsy	X	X	X	X	X	X	X	X		X	X	X
58	58	Male	BCC	Shoulder	Right	Total excision	X	X	X	X	X	X	X	X	X	X	X	X
59	47	Female	BCC	Shoulder	Frontal, left	Total excision	X	X	X	X	X	X	X	X		X	X	X
60	83	Female	BCC	Temple	Right	Total excision	X	X	X	X	X	X	X			X	X	X
61	60	Male	NS	Forehead	Temporal, right	Total excision	X	X	X	X	X	X	X	X				
62	77	Male	NS (adjacent to sample 44)	Scalp	Temporal, left	Total excision	X	X	X	X	X	X	X	X				
63	83	Female	NS	Cheek	Reg. zygomatica, right	Total excision	X	X	X	X	X	X	X	X				
64	83	Female	NS (adjacent to sample 45)	Scalp	Temporal, left	Total excision	X	X	X	X	X	X	X	X				
65	77	Male	NS	Scalp	Parietal	Total excision	X	X	X	X	X	X	X					
66	44	Male	NS	Neck		Total excision	X	X	X	X	X	X	X	X				
67	71	Female	NS	Forehead		Total excision	X	X	X	X	X	X	X	X				
68	79	Male	NS	Forehead		Total excision	X	X	X	X	X	X	X	X				
69	88	Male	NS (adjacent to sample 47)	Ear		Total excision	X	X	X	X	X	X	X					
70	86	Male	NS	Cheek		Total excision	X	X	X	X	X	X	X					
71	54	Female	HS	Chest		Total excision	X	X	X	X			X	X				
72	60	Female	HS	Chest		Total excision	X	X	X	X			X	X				
73	60	Female	HS	Chest		Total excision	X	X	X	X	X	X	X	X				
74	46	Female	HS	Chest		Total excision	X	X	X	X	X	X	X	X				
75	52	Female	HS	Chest		Total excision	X	X	X	X	X	X	X	X				
76	63	Male	HS	Ear		Total excision	X							X				
77	22	Female	HS	Ear		Total excision	X											
78	22	Female	HS	Ear		Total excision	X											
79	58	Female	HS	Chin		Total excision	X							X				
80	48	Female	HS	Spine		Total excision	X											
81	78	Female	HS	Nose		Total excision	X											
82	57	Female	HS	Chest		Total excision	X											
83	22	Female	HS	Ear		Total excision	X											
84	62	Female	PS	Elbow	Left	Punch biopsy					X	X	X					
85	41	Female	PS	Foot	Media, left	Punch biopsy					X	X	X					
86	38	Female	PS	Foot	Lateral, right	Punch biopsy					X	X	X					
87	71	Female	PS	Back	Lateral, left	Punch biopsy					X	X	X					
88	31	Female	PS	Forehead	Right	Punch biopsy					X	X	X					

Note: AK, aktinic keratosis; SCC, squamous cell carcinoma; BCC, basal cell carcinoma; NS, normal skin (adjacent to tumor); HS, healthy skin; PS, psoriasis

Appendix 2. Human colon samples used in the study

Specimen	Diagnosis/Grade
Tumor	Adenocarcinoma; G2
Tumor	Adenocarcinoma; G2
paired normal colon	paired normal colon
paired normal colon (distal resection margin)	paired normal colon (distal resection margin)
Adenomatous polyp, Mucosa	Adenomatous polyp
Carcinoma, Mucosa	Adenocarcinoma; G2
Adenomatous polyp, Mucosa	Adenomatous polyp
Adenomatous polyp, Mucosa	Adenomatous polyp
Carcinoma, Mucosa	Adenocarcinoma; G2
Normal Mucosa	paired normal colon
Adenomatous polyp, Mucosa	Adenomatous polyp
Adenomatous polyp, Mucosa	Adenomatous polyp
Normal Mucosa	paired normal colon
Adenomatous polyp, Mucosa	Adenomatous polyp serrated (TSA)
Adenomatous polyp, Mucosa	Adenomatous polyp serrated (TSA)

Appendix 3. Microbiota Analysis Batch file

Batch file specifying parameters used for microbiota analyses. Parameters other than default settings are shown in parentheses

MOTHUR (v.1.23)
assemble.paired()
screen.seqs(criteria 97; optimize: minlength maxlength)
unique.seqs()
align.seqs(reference=silva.bacteria.fasta)
screen.seqs(maxhomop: 8; criteria: 97; optimize: start, end)
filter.seqs(vertical=T, trump=.)
unique.seqs()
pre.cluster()
chimera.uchime()
remove.seqs(dups=T)
classify.seqs(template=trainset9_032012.pds.fasta, taxonomy=trainset9_032012.pds.tax, cutoff=80)
remove.lineage(taxon=Mitochondria-Chloroplast-Archaea-Eukaryota-unknown)
deunique.seqs()
split.groups()

QIIME (v.1.8.0)
add_qiime_labels.py ()
pick_de_novo_otus.py ()
core_diversity_analyses.py (-e 42258)

LEfSe (v.1.0)
"(Kruskal-Wallis test: alpha=0.05; Wilcoxon test: alpha=0.05; LDA threshold=2.0)"
Three group comparison –one against all mode multi-class analysis

Appendix 4. Primers used in this study

TABLE S2. Primers used in this study

Gene symbol	Gene name	Primers	Sequence (5' to 3')	Reference
16S rRNA	16S ribosomal RNA	27F	AGAGTTTGATCCTGGCTCAG	Baker et al. 2003
		357R	CTGCTGCCTYCCGTA	
16S rRNA	16S ribosomal RNA (pan-bacterial)	F 1369	CGGTGAATACGTTCCCGG	Furet JP, et al; 2009
		R 1492	TACGGCTACCTTGTTACGACTT	
16S rRNA	16S ribosomal RNA (*P. acnes* specific)	PA74F	TTTTGTGGGGTGCTCGAG	Montalban-Arques A, et al., 2016
		PA216R	CCAACCGCCGAAACTTTC	
nuc A	Thermostable nuclease gene (*Staphylococcus aureus* specific)	F	GCGATTGATGGTGATACGGTT	Brakstad O, et al; 1992; Kullander J, et al; 2009
		R	AGCCAAGCCTTGACGAACTAAAGC	
GluSE	Glutamic acid-specific serine protease (*Staphylococcus epidermidis* specific)	F	GGCAAATTTGTGGGTCAAGA	Hohnadel M, et al., 2014, Byrne FJ, et al; 2014, Li W, et al; 2013
		R	TGGCTAATGGTTTGTCACCA	
tuf	Elongation factor Tu (*Streptococcus* specific)	F	GTACAGTTGCTTCAGGACGTATC	Picard FJ, et al., 2004
		R	TGGGTTGATTGAACCTGGTTTA	
16S rRNA	16S ribosomal RNA (*Staphylococcus* genus)	F	TGAGTGATGAAGGTCTTCGGATC	Li W, et al; 2013
		R	ATAACGCTTGCCACCTACGTATTAC	
hBD-1	Human beta defensin-1	F	AGATGGCCTCAGGTGGTAACTTT	Vordenbäumen S, et al., 2010
		R	GGGCAGGCAGAATAGAGACATT	
hBD-2	Human beta defensin-2	F	TGATGCCTCTTCCAGGTGTTT	Vordenbäumen S, et al., 2010
		R	GGATGACATATGGCTCCACTCTT	
hBD-3	Human beta defensin-3	F	TCCATTATCTTCTGTTTGCTTTGC	Vordenbäumen S, et al., 2010
		R	TTCTGTAATGTGTTTATGATTCCTCCAT	
Rnase7	Ribonuclease A family member 7	F	GAAGACCAAGCGCAAAGC	Zanger P, et al., 2009
		R	AGCAGAAGGGGGCAGAAT	
hs100A7	Psoriasin	F	CACACATCTCACTCATCCTTCTACTCG	Garreis F, et al., 2011
		R	GTTCTCCTTCATCATCGTCAGCAG	
actb	Human Beta actin	F	CGTGCTGCTGACCGAGG	Montalban-Arques A, et al., 2016
		R	ACAGCCTGGATAGCAACGTAC	

Appendix 5: LEfSe analysis output

LEfSe analysis output							
					Relative abundance (Mean +/- SD)		
Taxa	LOG	Category	LDA	P-value	AK	SCC	BCC
k__Bacteria	5,99979924	BCC	3,578977	0,035613158			
k__Bacteria.p__Firmicutes	5,73585245			-			
k__Bacteria.p__Firmicutes.c__Bacilli	5,71495893			-			
k__Bacteria.p__Firmicutes.c__Bacilli.o__Bacillales	5,67522886	SCC	5,231365	0,044817628	0.42123778 ± 0.1425	0.5287074 ± 0.1440	0.13771509 ± 0.0955
k__Bacteria.p__Firmicutes.c__Bacilli.o__Bacillales.f__Staphylococcaceae	5,64718814	SCC	5,262796	0,032681595	0.38648949 ± 0.1405	0.50702865 ± 0.14432	0.08181914 ± 0.07601
k__Bacteria.p__Firmicutes.c__Bacilli.o__Bacillales.f__Staphylococcaceae.g__Staphylococcus	5,64642601	SCC	5,262042	0,032681595	0.38618021 ± 0.1405	0.500662594 ± 0.14433	0.0816879 ± 0.0759
k__Bacteria.p__Actinobacteria	5,51188014			-			
k__Bacteria.p__Actinobacteria.c__Actinobacteria	5,50982455			-			
k__Bacteria.p__Actinobacteria.c__Actinobacteria.o__Actinomycetales	5,5097934			-			
k__Bacteria.p__Proteobacteria	5,36135611			-			
k__Bacteria.p__Actinobacteria.c__Actinobacteria.o__Actinomycetales.f__Corynebacteriaceae.g__Corynebacterium	5,30838996			-			
k__Bacteria.p__Actinobacteria.c__Actinobacteria.o__Actinomycetales.f__Corynebacteriaceae	5,30838996			-			
k__Bacteria.p__Actinobacteria.c__Actinobacteria.o__Actinomycetales.f__Propionibacteriaceae	5,24181871			-			
k__Bacteria.p__Actinobacteria.c__Actinobacteria.o__Actinomycetales.f__Propionibacteriaceae.g__Propionibacterium	5,24007879			-			
k__Bacteria.p__Firmicutes.c__Bacilli.o__Lactobacillales	5,10584208			-			
k__Bacteria.p__Proteobacteria.c__Betaproteobacteria	5,0709138	BCC	4,663697	0,005210471	0.05456506 ± 0.0655	0.01929579 ± 0.039	0.09904444 ± 0.0828
k__Bacteria.p__Bacteroidetes	5,02126527	BCC	4,310367	0,039418024	0.07302778 ± 0.0751	0.03803732 ± 0.05521	0.08393532 ± 0.0769
k__Bacteria.p__Proteobacteria.c__Betaproteobacteria.o__Burkholderiales	5,00485304			-			
k__Bacteria.p__Firmicutes.c__Bacilli.o__Lactobacillales.f__Streptococcaceae	4,97094955	BCC	4,667927	0,011173608	0.05303009 ± 0.0646	0.01208495 ± 0.03154	0.17836248 ±0.10617
k__Bacteria.p__Firmicutes.c__Bacilli.o__Lactobacillales.f__Streptococcaceae.g__Streptococcus	4,95012554	BCC	4,652343	0,010390857	0.04321807 ± 0.05870	0.01139704 ± 0.0306	0.17420746 ± 0.10519
k__Bacteria.p__Bacteroidetes.c__Bacteroidia.o__Bacteroidales	4,84209611			-			
k__Bacteria.p__Bacteroidetes.c__Bacteroidia	4,84209611			-			
k__Bacteria.p__Proteobacteria.c__Alphaproteobacteria	4,77924078			-			
k__Bacteria.p__Bacteroidetes.c__Bacteroidia.o__Bacteroidales.f__Bacteroidaceae	4,76160701			-			
k__Bacteria.p__Bacteroidetes.c__Bacteroidia.o__Bacteroidales.f__Bacteroidaceae.g__Bacteroides	4,76160701			-			
k__Bacteria.p__Firmicutes.c__Bacilli.o__Bacillales.f__OtherBacillales.g__OtherBacillales	4,72913143			-			
k__Bacteria.p__Firmicutes.c__Bacilli.o__Bacillales.f__OtherBacillales	4,72913143			-			
k__Bacteria.p__Proteobacteria.c__Betaproteobacteria.o__Burkholderiales.f__Comamonadaceae	4,65298929	BCC	4,241202	0,005622787	0.02208495 ± 0.0424	0.00446459 ± 0.0192	0.04009374 ± 0.05441
k__Bacteria.p__Actinobacteria.c__Actinobacteria.o__Actinomycetales.f__Micrococcaceae	4,64409262	BCC	4,293236	0,006812638	0.00856843 ± 0.026606	0.00887221 ± 0.02707	0.07625743 ± 0.073611
k__Bacteria.p__Proteobacteria.c__Gammaproteobacteria	4,62081795			-			
k__Bacteria.p__Proteobacteria.c__Betaproteobacteria.o__Burkholderiales.f__Comamonadaceae.g__unclassifiedComa	4,60159343	BCC	4,199414	0,005464178	0.01353481 ± 0.0333	0.00344813 ± 0.01692	0.03512845 ± 0.05106
k__Bacteria.p__Proteobacteria.c__Betaproteobacteria.o__Burkholderiales.f__Oxalobacteraceae	4,56881363			-			
k__Bacteria.p__Proteobacteria.c__Betaproteobacteria.o__Burkholderiales.f__Oxalobacteraceae.g__unclassifiedOxalob	4,46234698	BCC	3,980711	0,014832063	0.01556036 ± 0.03572	0.00648102 ± 0.02316	0.02264581 ± 0.0412618
k__Bacteria.p__Bacteroidetes.c__Flavobacteriia	4,42575628	BCC	3,997223	0,009895668	0.01689918 ± 0.0372	0.00397374 ± 0.018161	0.02509887 ± 0.04338
k__Bacteria.p__Bacteroidetes.c__Flavobacteriia.o__Flavobacteriales	4,42575628	BCC	3,997223	0,009895668	0.01689918 ± 0.03720	0.00397374 ± 0.0181	0.02509887 ± 0.0433
k__Bacteria.p__Actinobacteria.c__Actinobacteria.o__Actinomycetales.f__Microbacteriaceae	4,42303925	BCC	3,994863	0,014299395	0.01620178 ± 0.03644	0.00356243 ± 0.017195	0.02209157 ± 0.04076
k__Bacteria.p__Firmicutes.c__Clostridia.o__Clostridiales	4,40615493			-			
k__Bacteria.p__Firmicutes.c__Clostridia	4,40615493			-			
k__Bacteria.p__Bacteroidetes.c__Flavobacteriia.o__Flavobacteriales.f___Weeksellaceae_	4,40055447	BCC	3,982351	0,014684707	0.01475936 ± 0.0348	0.00346426 ± 0.01696	0.02336292 ± 0.04189
k__Bacteria.p__Proteobacteria.c__Gammaproteobacteria.o__Pseudomonadales	4,34983147			-			
k__Bacteria.p__Proteobacteria.c__Alphaproteobacteria.o__Rhodobacterales.f__Rhodobacteraceae	4,33802967			-			
k__Bacteria.p__Proteobacteria.c__Alphaproteobacteria.o__Rhodobacterales	4,33802967			-			
k__Bacteria.p__Actinobacteria.c__Actinobacteria.o__Actinomycetales.f__Micrococcaceae.g__Rothia	4,30752943			-			
k__Bacteria.p__Firmicutes.c__Clostridia.o__Clostridiales.f___Tissierellaceae_	4,30462806			-			
k__Bacteria.p__Proteobacteria.c__Alphaproteobacteria.o__Rhodobacterales.f__Rhodobacteraceae.g__unclassifiedRho	4,28158659	AK	3,958783	0,042157105	0.02155323 ± 0.0419	0.00093047 ± 0.0088	0.00438879 ± 0.01833
k__Bacteria.p__Bacteroidetes.c__Flavobacteriia.o__Flavobacteriales.f___Weeksellaceae_.g__Cloacibacterium	4,27320527	BCC	3,907204	0,002043536	0.01098896 ± 0.0300	0.001187 ± 0.0099	0.01771216 ± 0.03658
k__Bacteria.p__Proteobacteria.c__Alphaproteobacteria.o__Rhizobiales	4,25235302			-			
k__Bacteria.p__Proteobacteria.c__Betaproteobacteria.o__Burkholderiales.f__Alcaligenaceae	4,21798533			-			
k__Bacteria.p__Proteobacteria.c__Betaproteobacteria.o__Burkholderiales.f__Alcaligenaceae.g__Achromobacter	4,21782858			-			
k__Bacteria.p__Firmicutes.c__Clostridia.o__Clostridiales.f___Tissierellaceae_.g__Anaerococcus	4,20435153			-			
k__Bacteria.p__Proteobacteria.c__Alphaproteobacteria.o__Caulobacterales.f__Caulobacteraceae	4,17674363			-			
k__Bacteria.p__Proteobacteria.c__Alphaproteobacteria.o__Caulobacterales	4,17674363			-			

Appendix 5: LEfSe analysis output (continued)

k__Bacteria.p__Actinobacteria.c__Actinobacteria.o__Actinomycetales.f__Micrococcaceae.g__Micrococcus	4,1425893	BCC	3,728644	0,000612498	0.00333466 ± 0.01664	0.00080292 ± 0.00817€	0.01290447 ± 0.03130
k__Bacteria.p__Actinobacteria.c__Actinobacteria.o__Actinomycetales.f__Microbacteriaceae.g__Microbacterium	4,14025387			-			
k__Bacteria.p__Proteobacteria.c__Alphaproteobacteria.o__Caulobacterales.f__Caulobacteraceae.g__unclassifiedCaulc	4,13520198			-			
k__Bacteria.p__Proteobacteria.c__Gammaproteobacteria.o__Pseudomonadales.f__Pseudomonadaceae	4,13414499			-			
k__Bacteria.p__Firmicutes.c__Bacilli.o__Lactobacillales.f__Lactobacillaceae.g__Lactobacillus	4,108176			-			
k__Bacteria.p__Firmicutes.c__Bacilli.o__Lactobacillales.f__Lactobacillaceae	4,108176			-			
k__Bacteria.p__Proteobacteria.c__Gammaproteobacteria.o__Pseudomonadales.f__Pseudomonadaceae.g__Pseudomc	4,10474904			-			
k__Bacteria.p__Firmicutes.c__Bacilli.o__Gemellales	4,08321043			-			
k__Bacteria.p__Firmicutes.c__Bacilli.o__Gemellales.f__Gemellaceae	4,0832001			-			
k__Bacteria.p__Firmicutes.c__Bacilli.o__Gemellales.f__Gemellaceae.g__unclassifiedGemellaceae	4,07779904			-			
k__Bacteria.p__Proteobacteria.c__Betaproteobacteria.o__Burkholderiales.f__Comamonadaceae.g__OtherComamona	4,0431042			-			
k__Bacteria.p__Proteobacteria.c__Betaproteobacteria.o__Methylophilales	4,02356445	BCC	3,522511	0,042453557	0.0048963 ± 0.020150	0.00272906 ± 0.01505€	0.00783959 ± 0.02446
k__Bacteria.p__Proteobacteria.c__Betaproteobacteria.o__Methylophilales.f__Methylophilaceae	4,02356445	BCC	3,522511	0,042453557	0.0048963 ± 0.020150	0.00272906 ± 0.01505€	0.00783959 ± 0.024460
k__Bacteria.p__Proteobacteria.c__Betaproteobacteria.o__Methylophilales.f__Methylophilaceae.g__unclassifiedMethy	4,01617188			-			
k__Bacteria.p__Firmicutes.c__Bacilli.o__Lactobacillales.f__Aerococcaceae	4,01489034			-			
k__Bacteria.p__Firmicutes.c__Bacilli.o__Lactobacillales.f__Enterococcaceae	4,00828645			-			
k__Bacteria.p__Firmicutes.c__Bacilli.o__Lactobacillales.f__Enterococcaceae.g__Enterococcus	3,99323307			-			
k__Bacteria.p__Proteobacteria.c__Gammaproteobacteria.o__Enterobacteriales.f__Enterobacteriaceae	3,97957451			-			
k__Bacteria.p__Proteobacteria.c__Gammaproteobacteria.o__Enterobacteriales	3,97957451			-			
k__Bacteria.p__Proteobacteria.c__Gammaproteobacteria.o__Enterobacteriales.f__Enterobacteriaceae.g__unclassified	3,95439629			-			
k__Bacteria.p__Proteobacteria.c__Betaproteobacteria.o__Burkholderiales.f__Oxalobacteraceae.g__Janthinobacterium	3,93719408			-			
k__Bacteria.p__Proteobacteria.c__Gammaproteobacteria.o__Pseudomonadales.f__Moraxellaceae	3,9333045			-			
k__Bacteria.p__Proteobacteria.c__Deltaproteobacteria	3,91717908			-			
k__Bacteria.p__Proteobacteria.c__Deltaproteobacteria.o__Myxococcales	3,91717908			-			
k__Bacteria.p__Proteobacteria.c__Deltaproteobacteria.o__Myxococcales.f__0319_6G20	3,9123919			-			
k__Bacteria.p__Proteobacteria.c__Deltaproteobacteria.o__Myxococcales.f__0319_6G20.g__unclassified0319_6G20	3,9123919			-			
k__Bacteria.p__Bacteroidetes.c__Bacteroidia.o__Bacteroidales.f__Prevotellaceae	3,8957432			-			
k__Bacteria.p__Bacteroidetes.c__Bacteroidia.o__Bacteroidales.f__Prevotellaceae.g__Prevotella	3,8957432			-			
k__Bacteria.p__Firmicutes.c__Bacilli.o__Lactobacillales.f__Carnobacteriaceae	3,88513047			-			
k__Bacteria.p__Firmicutes.c__Bacilli.o__Lactobacillales.f__Carnobacteriaceae.g__Granulicatella	3,87820179			-			
k__Bacteria.p__Proteobacteria.c__Gammaproteobacteria.o__Pseudomonadales.f__Moraxellaceae.g__Enhydrobacter	3,83960511			-			
k__Bacteria.p__Actinobacteria.c__Actinobacteria.o__Actinomycetales.f__Microbacteriaceae.g__CandidatusAquiluna	3,82757892			-			
k__Bacteria.p__Fusobacteria	3,82707067			-			
k__Bacteria.p__Fusobacteria.c__Fusobacteriia	3,82707067			-			
k__Bacteria.p__Fusobacteria.c__Fusobacteriia.o__Fusobacteriales	3,82707067			-			
k__Bacteria.p__Proteobacteria.c__Alphaproteobacteria.o__Rhizobiales.f__Brucellaceae	3,81924303	BCC	3,390818	0,019510368	0.00165419 ± 0.01173	0.00125973 ± 0.01023€	0.00425169 ± 0.018046
k__Bacteria.p__Proteobacteria.c__Alphaproteobacteria.o__Rhizobiales.f__Brucellaceae.g__Ochrobactrum	3,81924303	BCC	3,391596	0,019428573	0.00165038 ± 0.01171	0.00123752 ± 0.01014	0.00425169 ± 0.0180461
k__Bacteria.p__Firmicutes.c__Bacilli.o__Lactobacillales.f__Streptococcaceae.g__Lactococcus	3,81575646			-			
k__Bacteria.p__Actinobacteria.c__Actinobacteria.o__Actinomycetales.f__Micrococcaceae.g__unclassifiedMicrococcac	3,80715066			-			
k__Bacteria.p__Actinobacteria.c__Actinobacteria.o__Actinomycetales.f__Actinomycetaceae	3,76338751			-			
k__Bacteria.p__Proteobacteria.c__Gammaproteobacteria.o__Xanthomonadales	3,76032106			-			
k__Bacteria.p__Proteobacteria.c__Gammaproteobacteria.o__Xanthomonadales.f__Xanthomonadaceae	3,75664644			-			
k__Bacteria.p__Proteobacteria.c__Alphaproteobacteria.o__Rickettsiales	3,7473058			-			
k__Bacteria.p__Proteobacteria.c__Alphaproteobacteria.o__Sphingomonadales	3,73900031			-			
k__Bacteria.p__Proteobacteria.c__Alphaproteobacteria.o__Rickettsiales.f__unclassifiedRickettsiales	3,73662601			-			
k__Bacteria.p__Proteobacteria.c__Alphaproteobacteria.o__Rickettsiales.f__unclassifiedRickettsiales.g__unclassifiedRi	3,73662601			-			
k__Bacteria.p__Proteobacteria.c__Betaproteobacteria.o__Neisseriales.f__Neisseriaceae	3,73387181	BCC	3,312422	0,036547513	0.0022 ± 0.01352	0.00125686 ± 0.01022	0.0068657 ± 0.02290
k__Bacteria.p__Proteobacteria.c__Betaproteobacteria.o__Neisseriales	3,73387181	BCC	3,312422	0,036547513	0.0022 ± 0.013525	0.00125686 ± 0.010227	0.0068657 ± 0.022902
k__Bacteria.p__Firmicutes.c__Bacilli.o__Lactobacillales.f__Aerococcaceae.g__Alkalibacterium	3,72700098			-			
k__Bacteria.p__Cyanobacteria	3,71064749			-			
k__Bacteria.p__Firmicutes.c__Clostridia.o__Clostridiales.f__Tissierellaceae_.g__Finegoldia	3,71001306			-			
k__Bacteria.p__Proteobacteria.c__Alphaproteobacteria.o__Sphingomonadales.f__Sphingomonadaceae	3,70572218			-			
k__Bacteria.p__Proteobacteria.c__Alphaproteobacteria.o__Rhizobiales.f__Rhizobiaceae	3,68528676			-			
k__Bacteria.p__Proteobacteria.c__Alphaproteobacteria.o__Rhizobiales.f__Rhizobiaceae.g__Agrobacterium	3,68473521			-			
k__Bacteria.p__Actinobacteria.c__Actinobacteria.o__Actinomycetales.f__Microbacteriaceae.g__Cryocola	3,63819712	AK	3,297696	0,007058176	0.00414824 ± 0.018554	0.00020171 ± 0.004095	0.00337229 ± 0.01607

Appendix 5: LEfSe analysis output (continued)

k__Bacteria.p__Firmicutes.c__Bacilli.o__Bacillales.f__Bacillaceae	3,63285436			-			
k__Bacteria.p__Cyanobacteria.c__4C0d_2	3,62502424			-			
k__Bacteria.p__Cyanobacteria.c__4C0d_2.o__MLE1_12.f__unclassifiedMLE1_12	3,62502424			-			
k__Bacteria.p__Cyanobacteria.c__4C0d_2.o__MLE1_12	3,62502424			-			
k__Bacteria.p__Cyanobacteria.c__4C0d_2.o__MLE1_12.f__unclassifiedMLE1_12.g__unclassifiedMLE1_12	3,62502424			-			
k__Bacteria.p__Fusobacteria.c__Fusobacteriia.o__Fusobacteriales.f__Fusobacteriaceae	3,59489881			-			
k__Bacteria.p__Fusobacteria.c__Fusobacteriia.o__Fusobacteriales.f__Fusobacteriaceae.g__Fusobacterium	3,59489881			-			
k__Bacteria.p__Bacteroidetes.c__Sphingobacteriia	3,5900082			-			
k__Bacteria.p__Bacteroidetes.c__Sphingobacteriia.o__Sphingobacteriales	3,5900082			-			
k__Bacteria.p__Firmicutes.c__Bacilli.o__Bacillales.f__Bacillaceae.g__Bacillus	3,58693146			-			
k__Bacteria.p__Actinobacteria.c__Actinobacteria.o__Actinomycetales.f__Nocardioidaceae	3,58095826			-			
k__Bacteria.p__Actinobacteria.c__Actinobacteria.o__Actinomycetales.f__Sporichthyaceae	3,57422394			-			
k__Bacteria.p__Actinobacteria.c__Actinobacteria.o__Actinomycetales.f__Sporichthyaceae.g__unclassifiedSporichthyac	3,57422394			-			
k__Bacteria.p__Proteobacteria.c__Gammaproteobacteria.o__Xanthomonadales.f__Xanthomonadaceae.g__Stenotropl	3,57259789			-			
k__Bacteria.p__Actinobacteria.c__Actinobacteria.o__Actinomycetales.f__unclassifiedActinomycetales	3,57169725			-			
k__Bacteria.p__Actinobacteria.c__Actinobacteria.o__Actinomycetales.f__unclassifiedActinomycetales.g__unclassifiedA	3,57169725			-			
k__Bacteria.p__Proteobacteria.c__Alphaproteobacteria.o__Rhodospirillales	3,55729808			-			
k__Bacteria.p__Firmicutes.c__Clostridia.o__Clostridiales.f__Veillonellaceae	3,55617042	AK	3,106559	0,046295316	0.00332895 ± 0.016627	0.00106948 ± 0.00943	0.00357266 ± 0.01654
k__Bacteria.p__Firmicutes.c__Bacilli.o__Bacillales.f__Exiguobacteraceae_	3,55477009			-			
k__Bacteria.p__Firmicutes.c__Bacilli.o__Bacillales.f__Exiguobacteraceae_.g__Exiguobacterium	3,55477009			-			
k__Bacteria.p__Fusobacteria.c__Fusobacteriia.o__Fusobacteriales.f__Leptotrichiaceae.g__Leptotrichia	3,54812235			-			
k__Bacteria.p__Fusobacteria.c__Fusobacteriia.o__Fusobacteriales.f__Leptotrichiaceae	3,54812235			-			
k__Bacteria.p__Bacteroidetes.c__Saprospirae_.o__Saprospirales_.f__Chitinophagaceae	3,53130131			-			
k__Bacteria.p__Bacteroidetes.c__Saprospirae_.o__Saprospirales_	3,53130131			-			
k__Bacteria.p__Bacteroidetes.c__Saprospirae_	3,53130131			-			
k__Bacteria.p__Firmicutes.c__Bacilli.o__Lactobacillales.f__Aerococcaceae.g__Facklamia	3,52953118			-			
k__Bacteria.p__Actinobacteria.c__Actinobacteria.o__Actinomycetales.f__Nocardioidaceae.g__unclassifiedNocardioida	3,52034102	BCC	3,213652	0,040045006	0.00171856 ± 0.01195	0.00016123 ± 0.003665	0.0027085 ± 0.01441
k__Bacteria.p__Actinobacteria.c__Actinobacteria.o__Actinomycetales.f__Actinomycetaceae.g__Actinomyces	3,5181185			-			
k__Bacteria.p__Proteobacteria.c__Alphaproteobacteria.o__Rhizobiales.f__unclassifiedRhizobiales	3,5162718			-			
k__Bacteria.p__Proteobacteria.c__Alphaproteobacteria.o__Rhizobiales.f__unclassifiedRhizobiales.g__unclassifiedRhizo	3,5162718			-			
k__Bacteria.p__Actinobacteria.c__Actinobacteria.o__Actinomycetales.f__Actinomycetaceae.g__Trueperella	3,50660013			-			
k__Bacteria.p__Proteobacteria.c__Betaproteobacteria.o__Neisseriales.f__Neisseriaceae.g__Neisseria	3,49403811			-			
k__Bacteria.p__Bacteroidetes.c__Flavobacteriia.o__Flavobacteriales.f__Weeksellaceae_.g__unclassified_Weeksellace	3,46746397	BCC	3,149524	0,009123855	0.00130187 ± 0.01040	0.000072373 ± 0.00245	0.00273779 ± 0.014492
k__Bacteria.p__Firmicutes.c__Bacilli.o__Lactobacillales.f__Aerococcaceae.g__Aerococcus	3,45098928			-			
k__Bacteria.p__Proteobacteria.c__Alphaproteobacteria.o__Rhizobiales.f__Methylobacteriaceae	3,44414616			-			
k__Bacteria.p__Proteobacteria.c__Alphaproteobacteria.o__Rhodospirillales.f__Rhodospirillaceae	3,44334184			-			
k__Bacteria.p__Proteobacteria.c__Gammaproteobacteria.o__Pasteurellales	3,44234154			-			
k__Bacteria.p__Proteobacteria.c__Gammaproteobacteria.o__Pasteurellales.f__Pasteurellaceae	3,44234154			-			
k__Bacteria.p__Proteobacteria.c__Gammaproteobacteria.o__Pasteurellales.f__Pasteurellaceae.g__Haemophilus	3,4416669			-			
k__Bacteria.p__Bacteroidetes.c__Bacteroidia.o__Bacteroidales.f__OtherBacteroidales.g__OtherBacteroidales	3,43257644			-			
k__Bacteria.p__Bacteroidetes.c__Bacteroidia.o__Bacteroidales.f__OtherBacteroidales	3,43257644			-			
k__Bacteria.p__Bacteroidetes.c__Saprospirae_.o__Saprospirales_.f__Chitinophagaceae.g__Sediminibacterium	3,42686011			-			
k__Bacteria.p__Bacteroidetes.c__Flavobacteriia.o__Flavobacteriales.f__Weeksellaceae_.g__Chryseobacterium	3,42312527			-			
k__Bacteria.p__Firmicutes.c__Clostridia.o__Clostridiales.f__Veillonellaceae.g__Veillonella	3,41929169			-			
k__Bacteria.p__Firmicutes.c__Clostridia.o__Clostridiales.f__Ruminococcaceae	3,41302627			-			
k__Bacteria.p__Proteobacteria.c__Alphaproteobacteria.o__Rhodospirillales.f__Acetobacteraceae	3,40505259			-			
k__Bacteria.p__Proteobacteria.c__Betaproteobacteria.o__Burkholderiales.f__Burkholderiaceae	3,37438791			-			
k__Bacteria.p__Proteobacteria.c__Gammaproteobacteria.o__Pseudomonadales.f__Moraxellaceae.g__Acinetobacter	3,36608002			-			
k__Bacteria.p__Firmicutes.c__Clostridia.o__Clostridiales.f__Ruminococcaceae.g__Ethanoligenens	3,34731078			-			
k__Bacteria.p__Bacteroidetes.c__Bacteroidia.o__Bacteroidales.f__Porphyromonadaceae	3,32983368			-			
k__Bacteria.p__Firmicutes.c__Bacilli.o__Lactobacillales.f__Aerococcaceae.g__Alloiococcus	3,32552268			-			
k__Bacteria.p__Bacteroidetes.c__Sphingobacteriia.o__Sphingobacteriales.f__unclassifiedSphingobacteriales.g__unclas	3,32547168			-			
k__Bacteria.p__Bacteroidetes.c__Sphingobacteriia.o__Sphingobacteriales.f__unclassifiedSphingobacteriales	3,32547168			-			
k__Bacteria.p__Actinobacteria.c__Actinobacteria.o__Actinomycetales.f__Micrococcaceae.g__Kocuria	3,3229957			-			
k__Bacteria.p__Thermi_	3,30791194			-			
k__Bacteria.p__Thermi_.c__Deinococci	3,30791194			-			
k__Bacteria.p__Proteobacteria.c__Alphaproteobacteria.o__Rhodospirillales.f__Rhodospirillaceae.g__unclassifiedRhod	3,30640026			-			
k__Bacteria.p__Bacteroidetes.c__Bacteroidia.o__Bacteroidales.f__Porphyromonadaceae.g__Porphyromonas	3,2961461			-			
k__Bacteria.p__Bacteroidetes.c__Cytophagia.o__Cytophagales.f__Cytophagaceae	3,28961447			-			
k__Bacteria.p__Bacteroidetes.c__Cytophagia	3,28961447			-			